UNIVERSITY OF CALIFORNIA, MERCED

Hydrological Connectivity of Vernal Pools

A Thesis submitted in partial satisfaction of the requirements
for the degree of Master of Science

in

Environmental Systems

by

Christina Tham

Committee in charge:

Professor Martha H. Conklin, Advisor
Professor Teamrat A. Ghezzehei
Dr. Niall F. McCarten
Professor Samuel J. Traina

2018

The Thesis of Christina Tham is approved, and is acceptable in quality and form for publication on microfilm and electronically:

Martha H. Conklin, Advisor

Teamrat A. Ghezzehei

Niall F. McCarten

Samuel J. Traina

University of California, Merced

2018

Table of Contents

List of Figures

List of Tables

List of Supplemental Materials

ABSTRACT

Hydrological Connectivity of Vernal Pools

by

Christina Tham

Master of Science in Environmental Systems

University of California, Merced, 2018

Vernal pools are shallow, short–lived, seasonal wetlands, underlined by an impermeable or slowly permeating layer, that form in depression pools. Vernal pools in California have been decimated by land developments, with only about 10 percent of their original land mass remaining. This has caused increased habitat fragmentation for invertebrates and plants, leaving many species vulnerable to endangerment and extinction. A thorough understanding of the hydrology of vernal pools is imperative to their continued survival, as they are important refugia for endangered, endemic species of plants and animals. The purpose of my research is to study the hydrological connectivity of two three–vernal pool series. My results show that vernal pools are not isolated wetlands; they are hydrologically connected to each other and to the landscape. There are several variables of my vernal pool system that determine the degree of hydrological connectivity– shallow subsurface confining layer, perched groundwater and surface water flow, inundation, and location. Understanding the hydrology of this unique, abiotic environment is imperative to the success of vernal pools and vernal pool species, as they undergo habitat loss and experience new selective pressures associated with climate change.

Chapter 1 Introduction

1.1 Introduction

The rapidly expanding population of California has led to the loss of approximately ninety–five percent of the state's original wetlands, with vernal pools suffering particularly extensive losses (Dahl, 1990). They were lost significantly to agriculture and urban development. The remaining vernal pools in California are among the most valuable and biologically productive ecosystems in the state. Many of the remaining vernal pools are at the edge of the Sierra Foothills, reserved in land that was not considered valuable agricultural land (Figure 1). Vernal pools serve as a habitat to a rich diversity of plants and invertebrates– many of which are designated by state and federal governments as rare, threated, or endangered.

Vernal pools are shallow, temporary wetlands that form in depression pools and are commonly found in Mediterranean climates with mild temperatures, cool, wet winters, and hot, dry summers. They form on many geological surfaces, such as alluvial terraces and basins, and volcanic mudflows. Most vernal pools in California are found in the older alluvial terraces along the east side of the Central Valley and in young terrace soils (Holland, 1978; Holland & Jain, 1977) (Figure 1). All vernal pools are underlined by an impermeable or slowly permeating layer, such as bedrock (Weitkamp et al., 1996), mudflows or lahars (Jokerst, 1990; Smith & Verrill, 1998), claypans or hardpans (Nikiforoff, 1941; Hobson & Dahlgren, 1998; Smith & Verrill, 1998; Rains et al., 2006), or clay–rich soils (Smith & Verrill, 1998). Those on clay–rich or hardpan soils are the most common types in Central Valley, California – covering over 4,100 km^2 (about 5%) of land surface area (Holland, 1998; Smith & Verrill, 1998) (Figure 1).

The life of a vernal pool can be broken down into four stages: wet, flood, flower, and dry (Keeley & Zedler, 1998). The wet phase begins with water saturation in early autumn, transitioning into the flood phase in late autumn or early winter as precipitation inundates the vernal pools. For the flood phase to occur, the rate of water input must exceed the rate of water output. In addition to water input from direct precipitation, water gets redistributed between vernal pools due to surface swales, or seasonal streams, and subsurface water movement. As the soil becomes saturated, water can move laterally above the impermeable layer. This can create a buffer pool, which will delay the start of the dry phase (Hanes & Stromberg, 1998). Vernal pools can fill and empty multiple times throughout the flood stage. The flower phase starts as vernal pools begin to dry out in spring, and vegetation begins to appear. As spring ends, the vernal pools enter their final stage, the dry phase, and become desiccated by late spring or summer.

Over the past couple of decades, there have been few attempts to examine the hydrology of vernal pools. For example, Rains et al. (2006, 2008) compared vernal pools on claypan with those on hardpan and looked at a series of vernal pools and identified a chemical evolution in perched groundwater within their vernal pool series. Other literature has examined species richness in relation to vernal pool inundation; but what about vernal pool hydrology with respect to their physical constraints?

The purpose of this study is to understand the hydrological connectivity of two three–vernal pool series. My aim is to examine variables that contribute to its hydrological connectivity. In this study, we used physical and chemical measurements gathered in water year (WY) 2016 to monitor water behaviors and characteristics in the Merced Vernal Pool and Grassland Reserve in Merced, California (Figure 1).

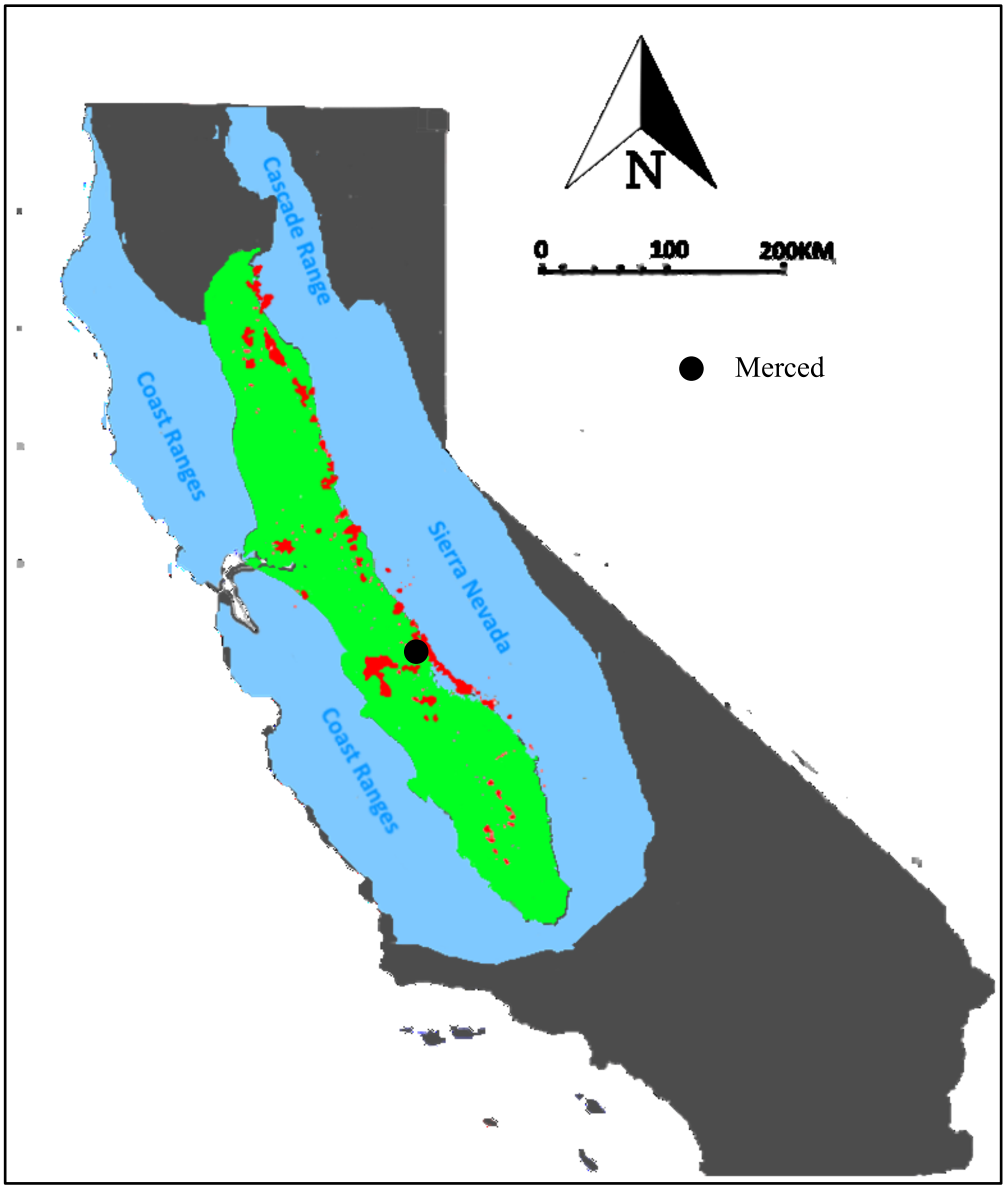

Figure 1 Composition map of existing vernal pools in Central Valley, CA as of 2012 are noted in red. Central Valley is noted in green. Source: Data Basin (https://databasin.org)

1.2 Vernal Pool Hydrology

Vernal pool hydrology can be summed by a simplified water balance equation, where the change in water volume is a function of water inputs from precipitation and perched groundwater and surface water sources, minus water output from evapotranspiration and perched groundwater and surface water sources (Leibowitz & Brooks, 2008) (Figure 2):

$$\Delta S = (P + Q_{in}) - (ET_o + Q_{out}) \qquad \textbf{Equation 1}$$

where

ΔS is change in water storage

P is direct precipitation

Q_{in} is perched groundwater and surface water into the vernal pool

Q_{out} is perched groundwater and surface water out of the vernal pool

ET_o is reference evapotranspiration

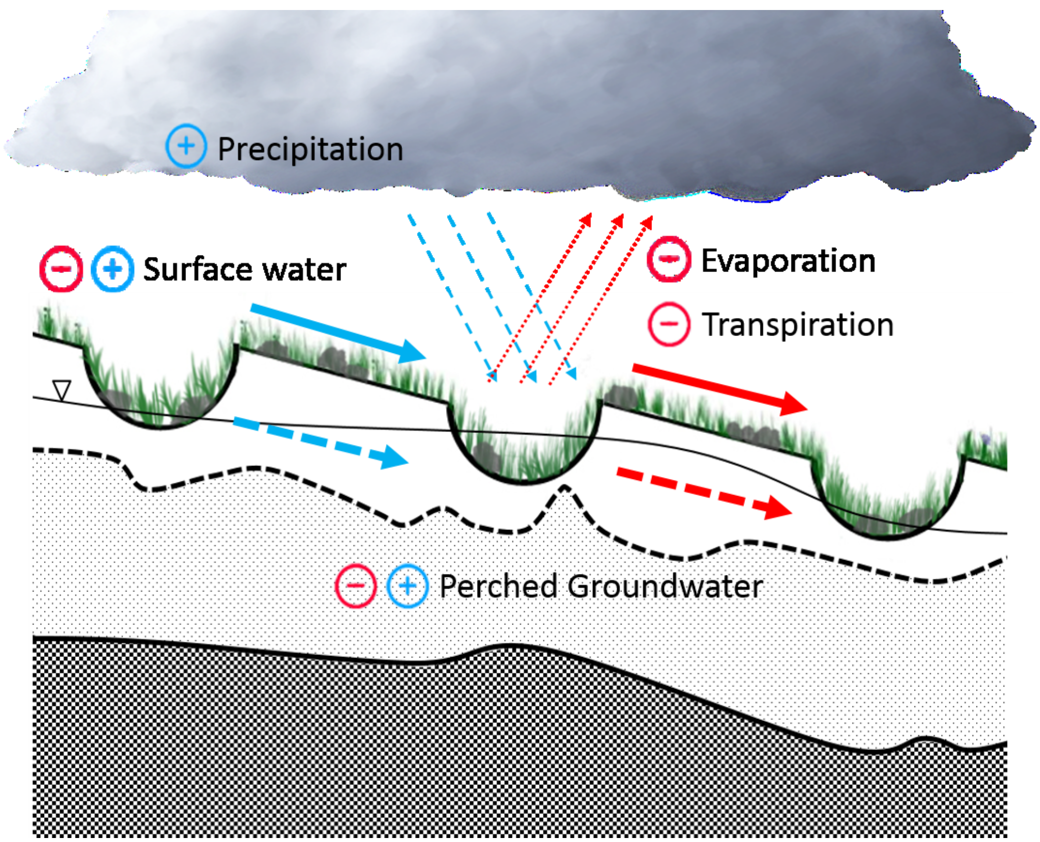

Figure 2 Schematic diagram of vernal pool transect and water input and outputs of my vernal pool system.

The hydrology of a vernal pool is composed of its hydrologic period and hydrologic regime. The hydrologic period is influenced by internal factors, and its hydrologic regime is influenced by external factors. Internal factors, such as the physical and biotic makeup of the vernal pool, influence only the environment of a single vernal pool or a closely grouped regional area, but will remain relatively stable over time. External characteristics, such as influences from the amount of precipitation, may affect an entire region of vernal pools, but can vary greatly over time.

1.2.1 Precipitation

Precipitation is the main source of water input for vernal pools. It can enter directly into the pool or indirectly as surface runoff.

1.2.2 Perched Groundwater

Precipitation infiltrates and perches on the confining layer. Perched groundwater–surface water interaction of vernal pools is influenced by elevation and flow of surrounding perched groundwater, geology of the area, edapholgy, and climate. Topographically high locations serve as recharge areas, while topographic lows serve as discharge areas. According to Rains et al. (2006), perched groundwater flow, hydrologic processes, and relative elevations may have greater influence and should not be overlooked.

1.2.3 Surface Water

Surface water can enter a pool through runoff or swales and exits through surface water outlets. To date, there is no published research regarding the flow of surface water into and out of vernal pools (Brooks, 2005), and it is believed that perched groundwater is the more significant contributor to the system. The surface water connection between vernal pools depends on the lateral and elevation distance between the vernal pools and the soil permeability of the flow path (Leibowitz & Vining, 2003). If surface water outflows are low, they will infiltrate into the ground before reaching nearby vernal pools.

1.2.4 Evapotranspiration

Evapotranspiration is another pathway of water loss in vernal pools. This is influenced by the temperature of the environment and increases as temperatures rise. Evapotranspiration of vernal pools represents the evaporation of water from the vernal pool's surface, along with water loss from vegetation. Vegetation is visible starting spring. Transpiration plays different roles in water loss throughout the water year, and it occurs within the vernal pool and in the uplands. There are plants living in the vernal pools and grasses growing in the uplands.

Chapter 2 Methods

For this study, a protocol was developed, in conjunction with compliance and review by the U.S. Fish and Wildlife Service, Sacramento Field Office, and the U.S. Fish and Wildlife Service, Carlsbad Field Office. It was also reviewed by the U.S. Environmental Protection Agency Region 9, San Francisco, the U.S. Army Corps of Engineers, Sacramento Office, and the California Department of Fish and Wildlife for California State regulations and permits.

2.1 Study Site

The Central Valley is a flat alluvial basin situated between the Sierra Nevada and Coast Ranges covering about 50,000 km^2 (Figure 1). It was formed from four million years of flood and eolian deposition and glacial outwash, 20 million years of volcanic eruptions, and 40 million years of coastal plain deposition. As a result, soil profile development in this area is very mature. My study site is situated on an extensive alluvial terrace landform with a Redding soil series (fine, mixed, active, thermic Abruptic Durixeralfs). Redding soil is composed of A1 (yellowish red gravelly loam), A2 (yellowish red gravelly loam), 2Bt (yellowish red clay), and 3Bqm (yellowish red duripan) soil layers (Figure 3). Redding soil is well or moderately well drained, 51–102 cm depth to duripan, and formed in alluvium derived from mixed sources. Vernal pools are common in areas with slopes of 0 to 3 percent.

Our study site (37.376105, –120.415150) was in the Merced Vernal Pools and Grassland Reserve (MVPGR) located in Merced, Central Valley, California. MVPGR – a 6,500–acre conservation preserve of vernal pools and grasslands – is part of the Virginia Smith Trust parcel and is one of 39 permanently–protected reserves of the University of California Natural Reserve System. Dairy cows seasonally graze in MVPGR as a way to manage non–native vegetation. My study site has an elevation range of 83–90 meters above sea level. It is composed of two catchments – Catchment 1 (C1) and Catchment 2 (C2) – each with three vernal pools of cascading elevations – upper pool (P1), middle pool (P2), and lower pool (P3); each series of vernal pools was connected to one another by swales. C1 has an area of 10,775 m^2 and C2 has an area of 15,059 m^2 (Figures 4, 5).

This region has a typical Mediterranean climate – cool, wet winters and hot, dry summers. In the past decade (WY 2007–2016), the study site had an annual average precipitation of 27.66 cm, minimum precipitation of 13.96 cm, and maximum precipitation of 49.18 cm, which typically fell between the months of November and April (Table 1).

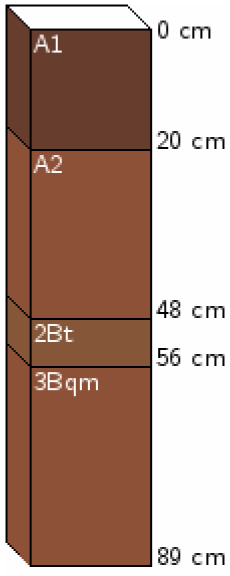

Figure 3 Redding soil profile. Source: SoilWeb – California Soil Resource Lab (https://casoilresource.lawr.ucdavis.edu/gmap/) See text for definition of soil layers.

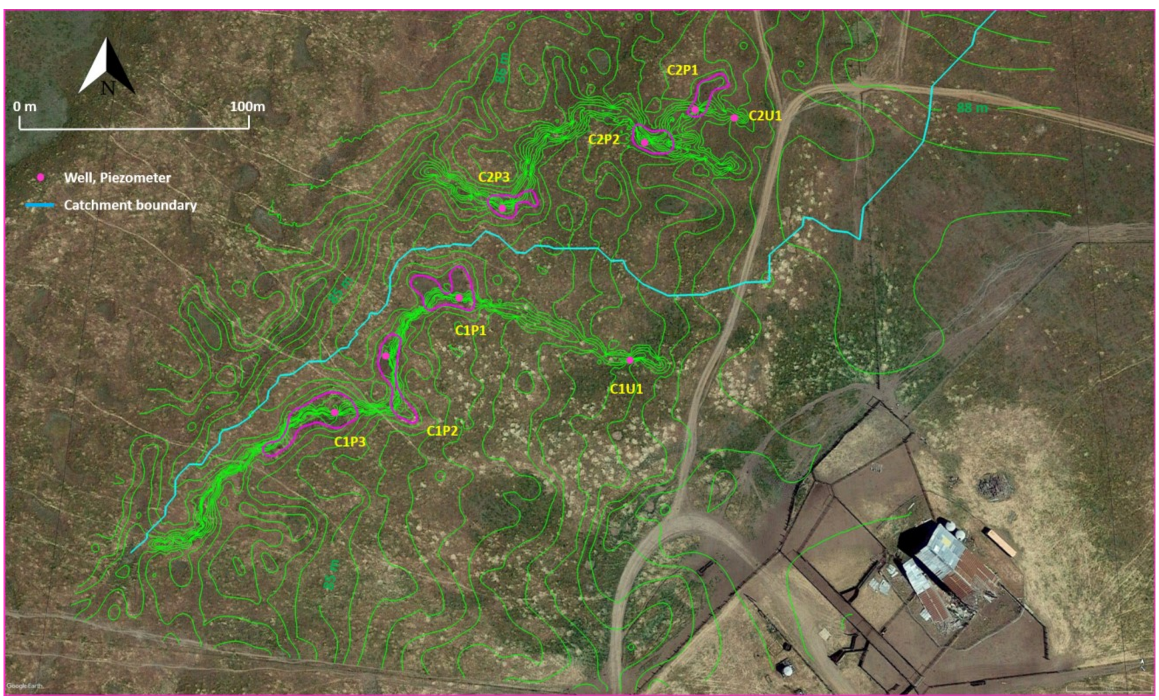

Figure 4 Contour map of study site overlaid onto Google Earth. It includes elevation, well and piezometer locations, and vernal pool and catchment boundaries. This was created in Surfer (version 13, Golden Software, 2015) based on 4,254 collected survey points and then overlaid onto Google Earth.

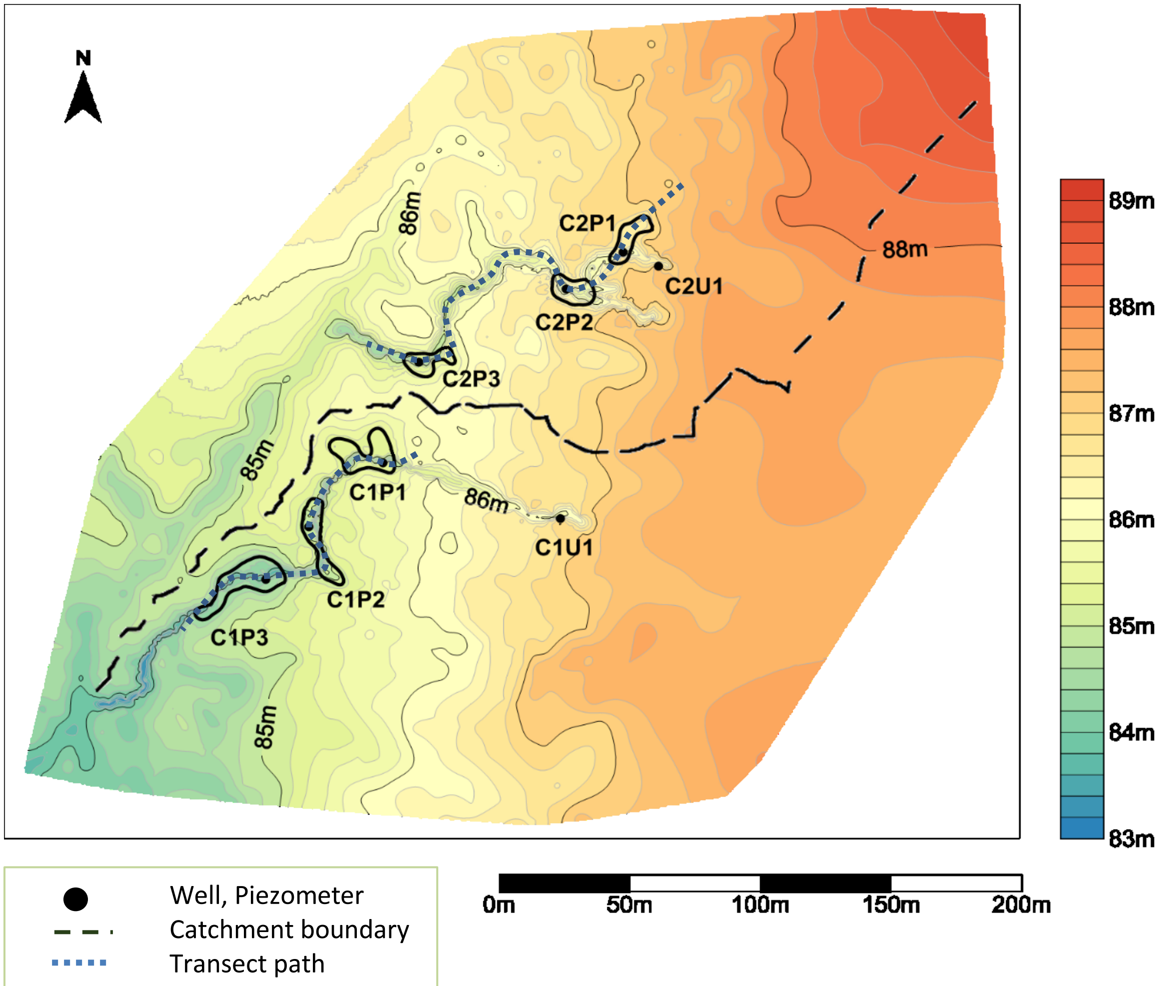

Figure 5 Contour map of study site– zoomed in. It includes elevation, well and piezometer locations, catchment and vernal pool boundaries, and transect paths. This was created in Surfer (version 13, Golden Software, 2015) based on 4,254 collected survey points.

Table 1 Summary of annual precipitation, reference evapotranspiration, and temperature of my study area.[1]

WY	Total Precipitation (cm)	Total Reference Evapotranspiration (cm)	Maximum Air Temperature (°C)	Minimum Air Temperature (°C)
2007	18.98	13.25	41.7	–7.8
2008	24.31	15.25	40.6	–4.4
2009	26.77	14.77	39.4	–3.9
2010	40.93	13.2	41.7	–6.7
2011	49.18	12.78	38.9	–5
2012	22.92	14.22	40	–8.9
2013	20.96	13.87	40	–6.1
2014	13.96	14.82	40.6	–8.9
2015	16.47	13.98	41.1	–5
2016	42.15	13.85	40	–4.4

[1]California Irrigation Management Information System (CIMIS) Station #148. Merced, California. Elevation 61 meters. (37.314139, –120.3867). Data of the last 10 years. Source: California Irrigation Management Information System (CIMIS) (http://cimis.water.ca.gov)

2.2 Topographic Survey

A topographic survey was conducted using a Trimble R8 Global Navigation Satellite System (GNSS) receiver (Trimble, Sunnyvale, California, USA) applying the real–time kinematic (RTK) technique to gather surface topographic and GPS data with an elevation accuracy of +/– 2 cm and spatial resolution accuracy of +/– 1 cm (Figures 6, 7). 4,254 survey points were collected during the summer of 2015 and imported into Surfer (version 13, Golden Software, 2015) to create a contour map of my study site to be used (1) to study its surface water flow patterns, (2) to outline and define two catchments and all vernal pool perimeters, and (3) to select three vernal pools of cascading elevation that would make up the series in each respective catchment.

Figure 6 Trimble R8 GNSS base station (Trimble, Sunnyvale, California, USA).

Figure 7 Trimble R8 GNSS receiver (Trimble, Sunnyvale, California, USA).

2.3 Ground Penetrating Radar

Like McCarten, et al. (2018a), a MALÅ Geoscience X3M ground penetrating radar (GPR) system (MALÅ Geoscience, Malå, Lapland, Sweden) connected to an 800 MHz shielded antenna was mounted on a cart and used to survey the depth of changes in soil horizon texture in my study site (Figure 8). GPR transects were conducted through each catchment traversing through each of my six vernal pools. The GPR system was programmed to collect a data sample every 0.05 m; the depth of radar penetration was set at 1.52 m, a calibration based on hand–augured soil pits used to determine the soil horizon textures and depth to impermeable layer. The GPR emits an energy wave from the antenna and collects a reflection wave from the soil based on density variation within the soil profile. Energy waves are accurate to +/– 2 cm and appear as blue and red– reflecting changes in soil density, which are the positive and negative parts of the energy wave.

To process and produce radargrams, GPR data files were loaded into RadExplorer (version 1.4, MALÅ Geoscience, 2005) and a uniform set of processing routines were performed to amplify the signal and optimize the quality of the profiles. Processing routines included (1) Direct Current Removal– to remove constant shifts (negative and positive) from the signal, (2) Time Adjustment– to establish the soil surface as depth zero, (3) Background Removal– to remove radar–caused signal that is a constant not associated with the real data in the reflected wave, (4) Amplitude Correction– to help display detail in the sub–bottom materials and increase signal strength at depth, and (5) Bandpass Filtering– to increase the signal:noise ratio. To represent changes in soil horizon texture observable in the radargram, a routine was used to automatically select traces across the transect by selecting the peak wave of a higher intensity energy wave, which were indicated by more intense blue and red wave coloration.

Figure 8 MALÅ Geoscience X3M ground–penetrating radar (GPR) system (MALÅ Geoscience, Malå, Lapland, Sweden) connected to an 800 MHz shielded antenna was mounted on a cart and used to survey the depth of changes in soil horizon texture.

2.4 Field Equipment Deployment

Two sets of three–vernal pool series were chosen based on geomorphology, as well as 4,254 elevation and GPS survey points (Figure 5). Each catchment contained one series of three vernal pools, which consisted of an upper, middle, and lower vernal pool, and all pools were of cascading elevation. A monitoring well and piezometer were installed at the lowest elevation of each vernal pool. An additional monitoring well and piezometer were installed upland in each catchment. Monitoring wells and piezometers were created by digging two–inch wide holes down to the shallow subsurface confining layer with a bucket auger (Table 2). Shallow subsurface confining layer was determined by the Redding series 2Bt soil layer description– yellowish red clay, extremely hard and firm. A two–inch, 0.010–inch slotted screen PVC pipe was placed and topped with a twist pressure top for monitoring wells. A two–inch PVC with eight holes drilled around the perimeter at 1 cm above the base was placed and capped for piezometers (Figures 9, 10, 11, 12). Model 3001 Junior M5 Leveloggers (Solinst, Georgetown, Ontario, Canada) were deployed in all monitoring wells and piezometers. A Model 1911–B.5 remote soil water sampler (SoilMoisture, Santa Barbara, California, USA), i.e. ceramic cup with a tube attached to it (see Water Sampling for description of cup), was installed in each monitoring well and filled with sludge (Figure 13). A Model Barologger Edge (Solinst, Georgetown, Ontario, Canada) was deployed nearby on a tree in a slotted two–inch PVC pipe with caps on either end (Figure 14). The Leveloggers and Barologger were programmed to sample every hour. They were left unattended until the end of the season for collection. Data collection was for WY 2016. Precautions (particularly in capping the wells and piezometers and being sure they did not protrude more than 10 cm above land surface) were taken to make sure deployed field equipment and installations were cow–proof.

Table 2 Coordinates, depth to confining layer, vernal pool depth, and surface area of vernal pools and catchments. Vernal pool depth was the difference between a topographic high and low point of a vernal pool and surface area was based on vernal pool boundary– all based on the contour map created in Surfer (version 13, Golden Software, 2015).

	Coordinates	Depth to Confining Layer (m)		Vernal Pool Depth (m)	Area (m^2)
		Well	Piezometer		
Catchment 1					10,775
C1U1 (Upland)	N 37 22.569, W 120 24.875	1.4	1.3	—	—
C1P1 (Upper)	N 37 22.580, W 120 24.922	0.505	0.51	0.37	251
C1P2 (Middle)	N 37 22.556, W 120 24.953	0.39	0.28	0.37	188
C1P3 (Lower)	N 37 22.535, W 120 24.986	0.295	0.45	1	308
Catchment 2					15,059
C2U1 (Upland)	N 37 22.622, W 120 24.848	5.1	4.05	—	—
P1 (Upper)	N 37 22.623, W 120 24.859	0.32	0.35	0.83	131
P2 (Middle)	N 37 22.616, W 120 24.870	0.29	0.32	1.03	143
P3 (Lower)	N 37 22.601, W 120 24.911	0.245	0.27	0.99	120

Figure 9 Inside a monitoring well. Model 3001 Junior M5 Levelogger (Solinst, Georgetown, Ontario, Canada) and Model 1911–B.5 remote soil water sampler (SoilMoisture, Santa Barbara, California, USA) deployed inside a two–inch slotted PVC pipe.

Figure 10 Monitoring well.

Figure 11 Piezometer preparation. Eight holes were drilled around the base of a two–inch PVC pipe.

Figure 12 Piezometer.

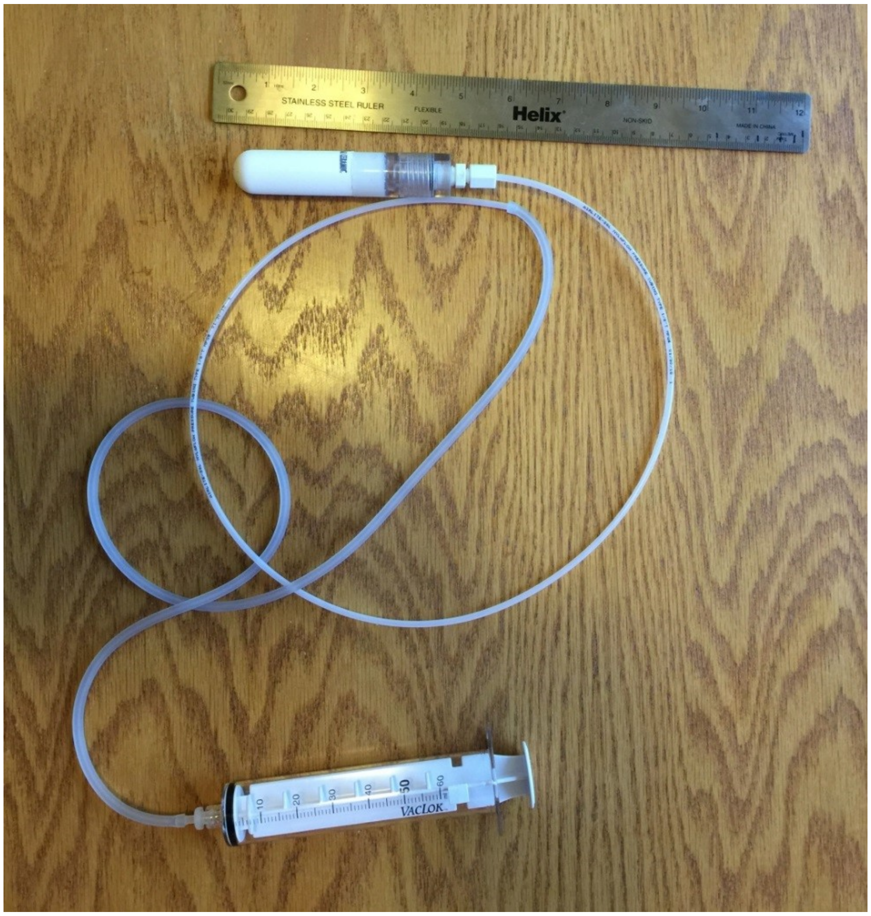

Figure 13 Model 1911–B.5 remote soil water sampler (SoilMoisture, Santa Barbara, California, USA).

Figure 14 Model Barologger Edge (Solinst, Georgetown, Ontario, Canada) placed inside a slotted PVC pipe and tied to a tree.

2.5 Water Sampling

Water samples (surface and perched groundwater) were collected almost weekly and post–precipitation with Model 1911–B.5 remote soil water samplers (SoilMoisture, Santa Barbara, California, USA), i.e. three–inch ceramic cup with 1/8–inch O.D. nylon tubing (Figure 13). These remote soil water samplers were good for water collection; the consisted of a fine pore ceramic material (6 µm) which would not permit seeds, branchiopods, or cysts from entering my water samples. Unused Nalgene bottles were rinsed several times with distilled water and air–dried in the laboratory before use in water sample collection. Approximately 20–30 mL of water (if available) was collected from vernal pool surface and monitoring wells with remote soil water samplers, filtered in the field through 0.45 µm polycarbonate membranes, and frozen until lab analysis. Another set of water sample was collected using the same method; these water samples were collected in 30mL glass vials (Fisherbrand™ Clear French Square Bottles with Black Phenolic PolyCone Cap), instead of Nalgene bottles, with no air space and stored at room temperature until lab analysis.

2.6 Analytical Procedure

Surface water and perched groundwater samples were analyzed in the laboratory for major ions, specific conductivity, pH, dissolved organic carbon (DOC), stable isotopes, and alkalinity. Major cations (i.e. sodium, ammonium, potassium, magnesium, and calcium) and anions (chlorine, sulfate, bromide, and nitrate) were measured on a Dionex ICS–2000 Reagent–Free Integrated Ion Chromatography System. Specific conductivity and pH were measured with a Fisher Scientific accumet excel XL 60. DOC was measured using the combustion catalytic oxidation/non–dispersive Infrared (NDIR) detection method on a Shimadzu TOC–Vcsh Total Organic Carbon Analyzer. Stable isotopes (i.e. D and ^{18}O) were measured on a DLT–100 Liquid Water Isotope Analyzer.

2.7 Calculations

2.7.1 Daily Precipitation and Reference Evapotranspiration (ET_o)

Daily precipitation and reference evapotranspiration (ET_o) were collected from California Irrigation Management Information System (CIMIS) Station #148, located southeast (37.314139, –120.3867) of my study site. CIMIS–calculated ET_o is from CIMIS hourly values using the CIMIS Penman Equation– a version of the Pruitt/Doorenbos–modified, Penman equation using a wind function (developed at the University of California, Davis), a unique cloud factor value for the station location, and grass as a reference crop. Because CIMIS Station #148 is on irrigated land, we had to correct it with a canopy coefficient (Drexler et al., 2004). We multiplied CIMIS–calculated ET_o values with canopy coefficients provided in McCarten et al. (2018b) (Table 3).

Table 3 Canopy coefficients provided in McCarten et al. (2018b).

Month	Canopy Coefficient
October	0.25
November	0.4
December	0.54
January	1.05
February	0.96
March	0.92
April	0.89
May	0.86
June	0.59
July	0.41
August	0.35
September	0.21

2.7.1 Water Column

According to McCarten et al. (2018b), Redding soil has a porosity of 50%. To calculate water column, we assumed 50% soil porosity and used the following equation:

$$\boldsymbol{y = x - (d \cdot 0.50)} \qquad \textbf{Equation 2}$$

where

y is water column (cm)

x is daily average pool stage (cm)

d is depth to shallow surface confining layer (cm)

2.7.2 Water Storage

We used the following equation to over–estimate vernal pool water storage:

$$\boldsymbol{S = y \cdot A} \qquad \textbf{Equation 3}$$

where

S is water storage (cm^3)

y is water column (cm)

A is surface area (cm^2)

2.7.3 Hydraulic Gradient

We used the following equations to calculate hydraulic gradient:

$$\boldsymbol{i} = \frac{\Delta \boldsymbol{h}}{\boldsymbol{d}}$$ **Equation 4**

where

i is hydraulic gradient

Δh is difference in hydraulic head between two vernal pools (m)

d is distance between two vernal pools (m)

$$\boldsymbol{h} = \boldsymbol{z} + \boldsymbol{\varphi}$$ **Equation 5**

where

h is hydraulic head (m)

z is elevation head (m)

φ is pressure head (m)

$$\boldsymbol{z} = \boldsymbol{a} - \boldsymbol{b}$$ **Equation 6**

where

z is elevation head (m)

a is elevation (m)

b is piezometer depth (m)

These equations refer to a saturated system. Since my system is perched aquifer, they are inappropriate as the system dries out, i.e. when the system is no longer hydrologically connected.

Chapter 3 Results

The data represented in my study is from November 11, 2015 to May 20, 2016. It took a series of precipitation events between November 11, 2015 and December 21, 2015 (totaling 5.02 cm of water) for all three pools to reach soil saturation. Between November 11, 2015 and December 21, 2015, there was no surface water inundation. Once the soil was fully saturated, the water table rose and fell in direct response to precipitation events.

3.1 Physical Characteristics

3.1.1 Topography

Based on the 4,254 GPS and elevation survey points, my study site showed two distinct catchments– a lower catchment, or Catchment 1 (C1), and an upper catchment, or Catchment 2 (C2) (Figure 5). C1 is at a lower elevation compared to C2. Each catchment contains a series of three vernal pools; each series is made up of an upper (P1), middle (P2), and lower (P3) vernal pool– all of cascading elevation (Figure 15). Each vernal pool varied in area (Table 4). Vernal pool perimeters were determined based on perimeters formed by dried remnants of vernal pool plants during the summer of the fourth drought year (2015).

Table 4 Number of days of inundation, depth to confining layer, and surface area of vernal pools and catchments. Surface area was based on vernal pool boundaries on the contour map created in Surfer (version 13, Golden Software, 2015).

	Days of Inundation	Well Depth to Confining Layer (m)	Area (m^2)
Catchment 1			10,775
C1P1 (Upper)	18	0.505	251
C1P2 (Middle)	15	0.39	188
C1P3 (Lower)	8	0.295	308
Catchment 2			15,059
C2P1 (Upper)	66	0.32	131
C2P2 (Middle)	99	0.29	143
C2P3 (Lower)	96	0.245	120

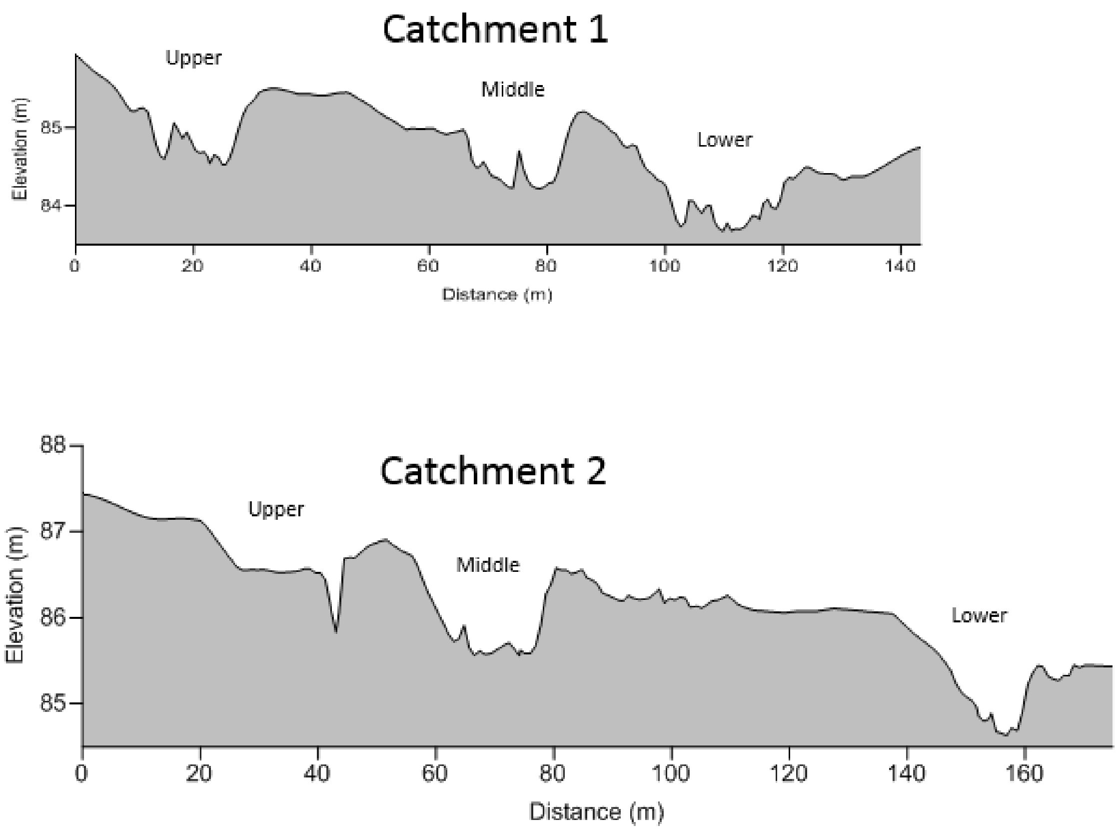

Figure 15 Transects of Catchments 1 and 2– and its upper, middle, and lower vernal pools. This was based on and created from the contour map created in Surfer (version 13, Golden Software, 2015).

3.1.2 GPR Radargrams

Radargrams of all six vernal pool transects showed that the shallow subsurface confining layer did not parallel the soil surface, except for C2P1 (Figures 16–21). Because these radargrams are single vernal pool transects, piezometers/ monitoring wells may appear to penetrate the shallow subsurface confining layer, but they did not; they were located off the transect. The shallow subsurface confining layer of C1 pools averaged 15–30 cm deep, while C2 pools averaged 20–30 cm deep. The shallow subsurface confining layer in C2P2 pinched up at the downgradient end of the pool. All radargrams also showed that the topography of the duripan layer matched closer to the shallow subsurface confining layer than to the soil surface.

Vernal pools in Catchment 1 pools were closer together in distance compared to those in Catchment 2 (Figures 22, 23). Shallow subsurface confining layer was thicker in Catchment 1 than it was in Catchment 2, but shallow subsurface confining layer in Catchment 2 had a more consistent thickness throughout the transect.

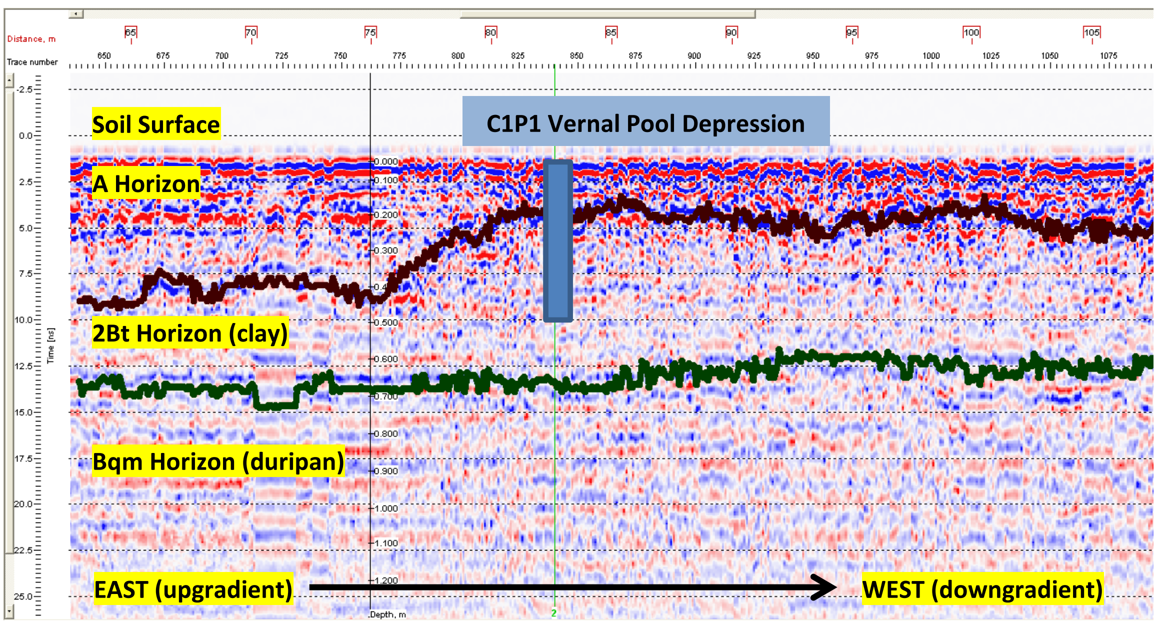

Figure 16 Interpreted GPR radargram of East to West transect of C1P1 showing position and depth of piezometer/monitoring well and soil horizons (scale in cm, +/– 5cm). The thick, brown line represents the start of the clay layer (2Bt horizon). The thick, green line represents the start of the duripan layer (Bqm horizon).

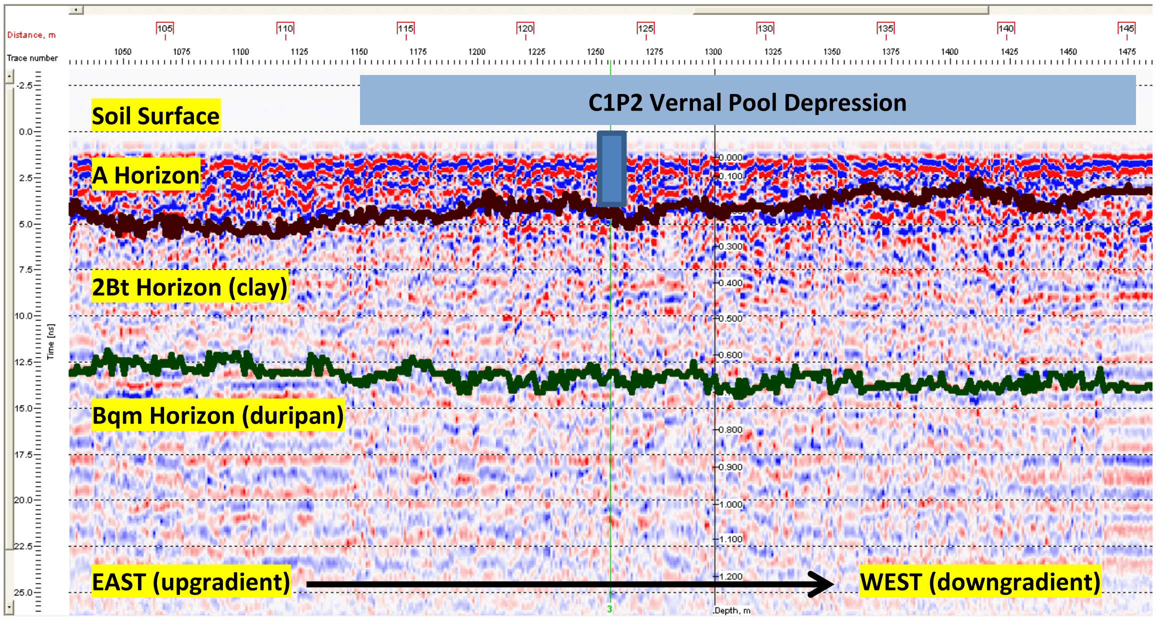

Figure 17 Interpreted GPR radargram of East to West transect of C1P2 showing position and depth of piezometer/monitoring well and soil horizons (scale in cm, +/– 5cm). The thick, brown line represents the start of the clay layer (2Bt horizon). The thick, green line represents the start of the duripan layer (Bqm horizon).

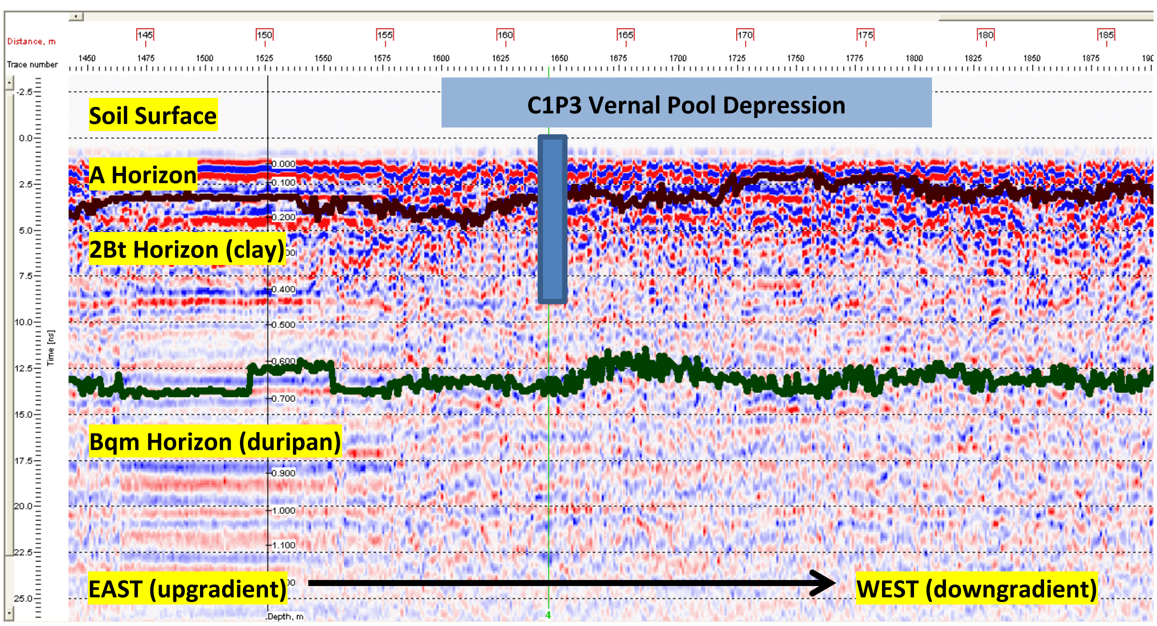

Figure 18 Interpreted GPR radargram of East to West transect of C1P3 showing position and depth of piezometer/monitoring well and soil horizons (scale in cm, +/– 5cm). The thick, brown line represents the start of the clay layer (2Bt horizon). The thick, green line represents the start of the duripan layer (Bqm horizon).

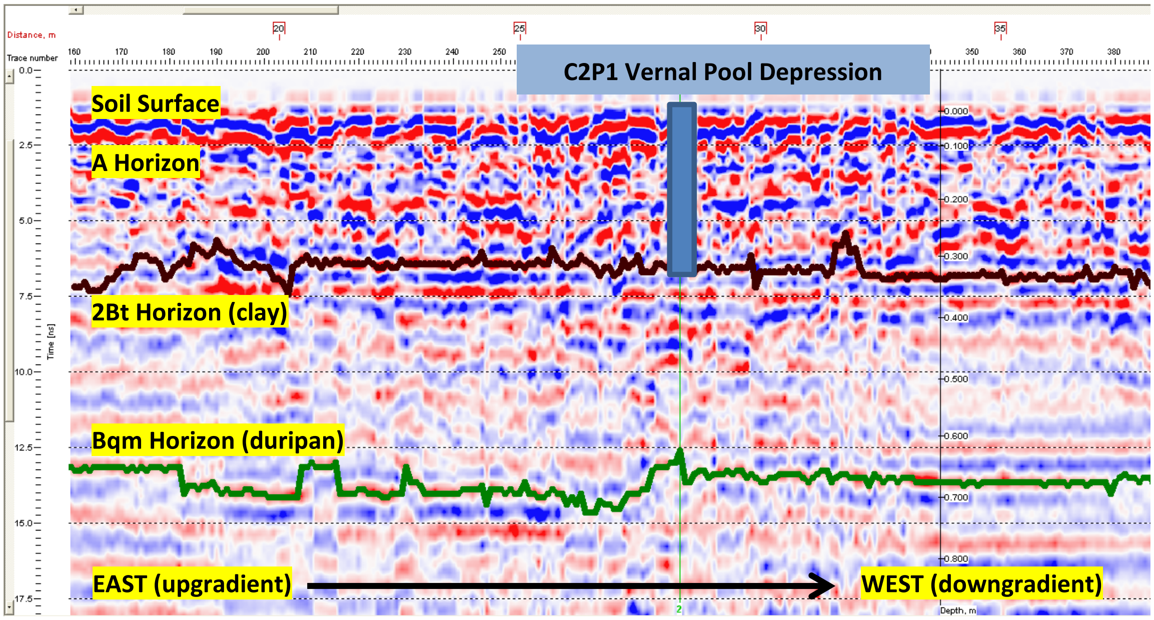

Figure 19 Interpreted GPR radargram of East to West transect of C2P1 showing position and depth of piezometer/monitoring well and soil horizons (scale in cm, +/– 5cm). The thick, brown line represents the start of the clay layer (2Bt horizon). The thick, green line represents the start of the duripan layer (Bqm horizon).

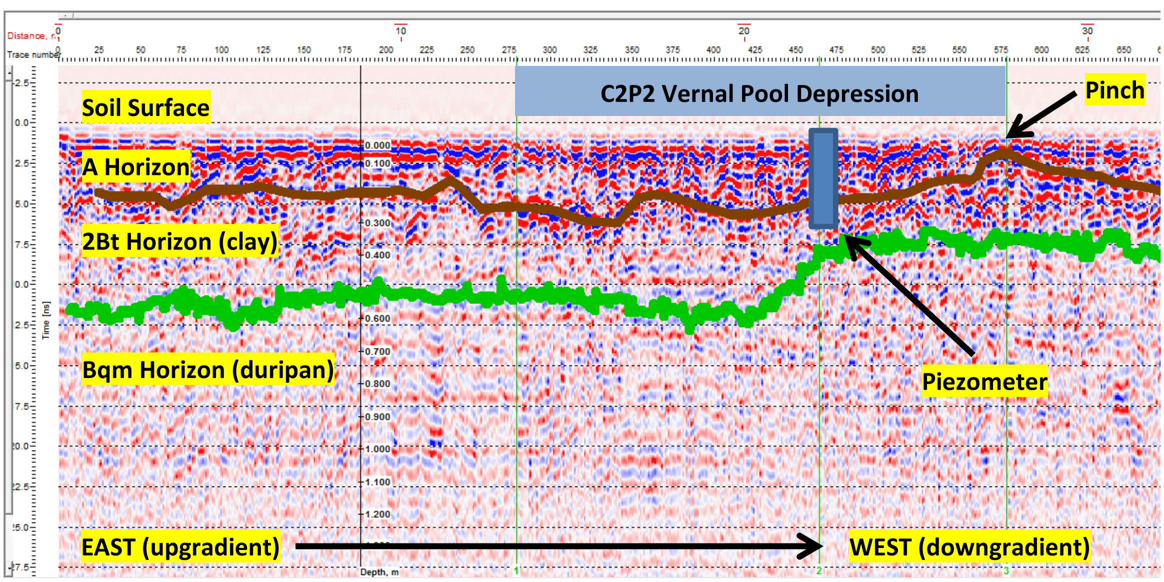

Figure 20 Interpreted GPR radargram of East to West transect of C2P2 showing position and depth of piezometer/monitoring well and soil horizons (scale in cm, +/– 5cm). The thick, brown line represents the start of the clay layer (2Bt horizon). The thick, green line represents the start of the duripan layer (Bqm horizon).

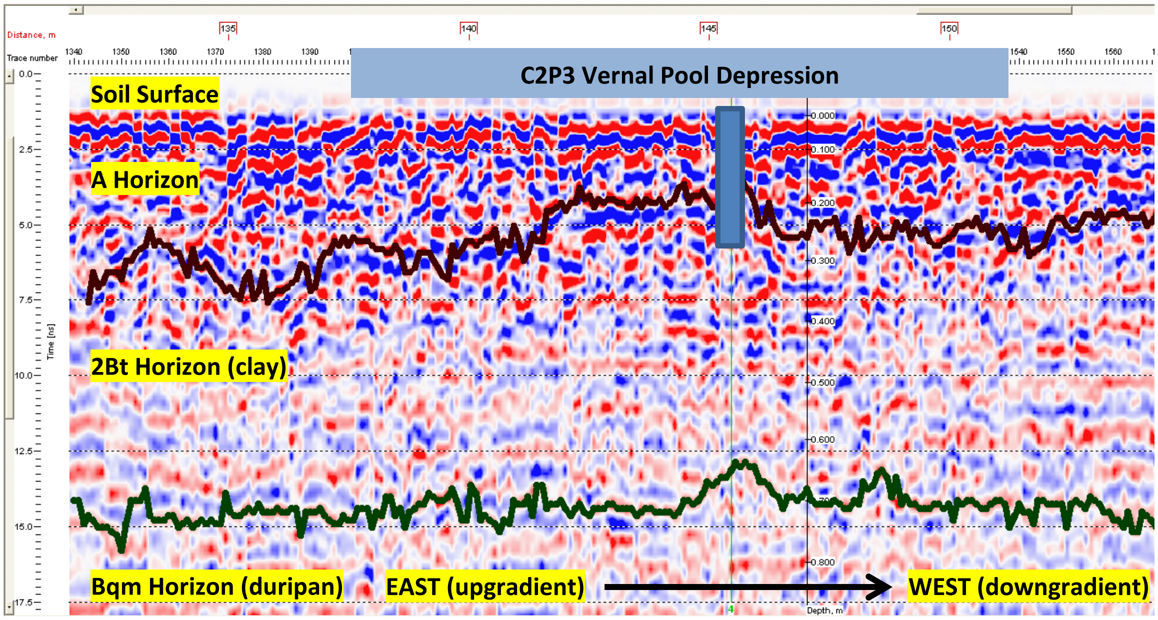

Figure 21 Interpreted GPR radargram of East to West transect of C2P3 showing position and depth of piezometer/monitoring well and soil horizons (scale in cm, +/– 5cm). The thick, brown line represents the start of the clay layer (2Bt horizon). The thick, green line represents the start of the duripan layer (Bqm horizon).

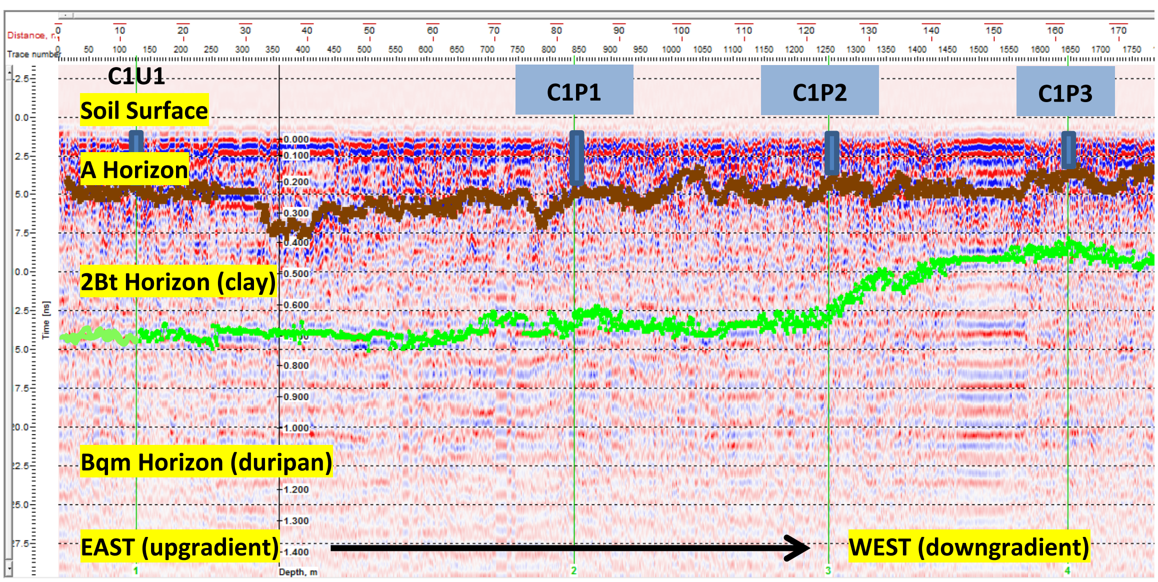

Figure 22 Catchment 1 GPR transect. Green vertical lines are locations of a monitoring well/ piezometer in each vernal pool. The thick, brown line represents the start of the clay layer (2Bt horizon). The thick, green line represents the start of the duripan layer (Bqm horizon).

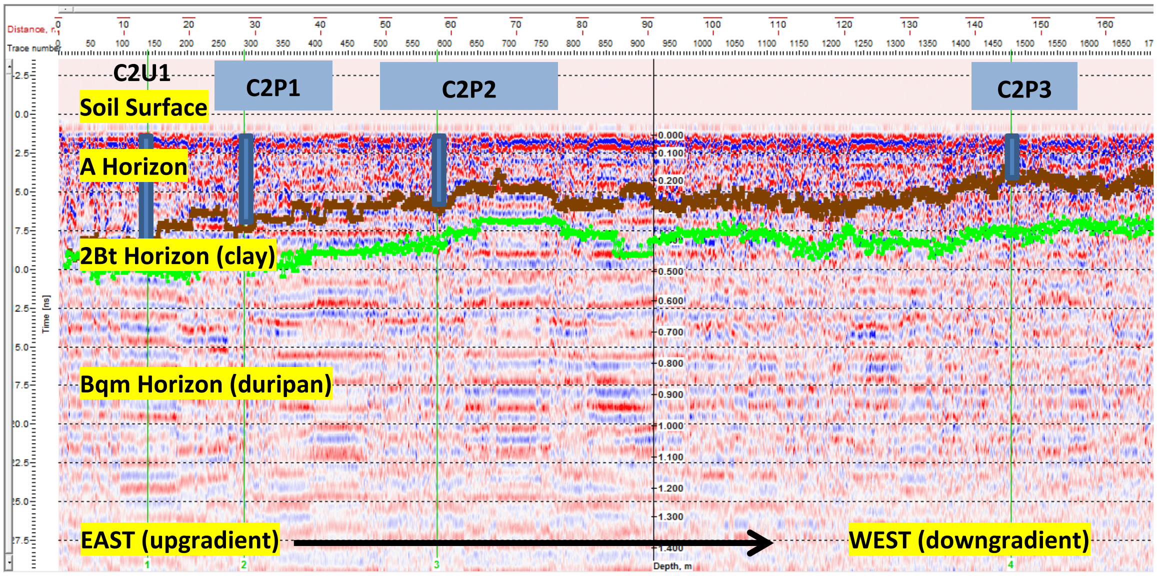

Figure 23 Catchment 2 GPR transect. Green vertical lines are locations of a monitoring well/ piezometer in each vernal pool. The thick, brown line represents the start of the clay layer (2Bt horizon). The thick, green line represents the start of the duripan layer (Bqm horizon).

3.1.3 Perched Groundwater Table and Surface Water Level

3.1.3.1 Catchment 1

The upland soil water table showed response to precipitation events with over 1.25 cm of water starting mid–January, except for the last major precipitation of the wet season that occurred in early April (Figure 24). It wetted and dried up for shorter periods compared to the vernal pools.

All pools showed surface water ponding starting January 6 (Figure 25). C1P1, C1P2, and C1P3 showed surface water ponding for 18, 15, and 8 days, respectively (Table 4**)**. C1P1 water table was higher than C1P2 (especially at the start of the season), except during December 22–24, December 28–January 5, January 17, January 23, February 5–21, and March 4–end of collection season, which was late April. Overall, C2P3 water table was lower than the others, except for December 28–January 5, where it had the highest water table, and March 4–16, where it had the second highest water table after C1P2.

Pool levels responded to a series of precipitation in January and March. The last storm of the season (April 8–9) prompted response in C1P1 and C1P2 water tables, but not C1P3. Sharp and rapid drops in C1P3 water table indicated its sensitive response to cessation of precipitation, except at the beginning of the season (December 28–January 5).

3.1.3.2 Catchment 2

The upland soil water table showed response to precipitation events with over 1 cm of water starting late December (Figure 24). The upland water table was more responsive in C2 than C1 and had longer wetting periods than C1, but, unlike the vernal pools, was overall less sensitive to precipitation events.

Vernal pools showed surface water ponding starting December 22 (Figure 25). C2P1, C2P2, and C2P3 showed surface water accumulation for 67, 99, and 96 days, respectively (Table 4). C2P2 exhibited the highest water table throughout the season, reaching at much as 29.23 cm above soil surface. C2P3 reached soil saturation before C2P1 and C2P2, as its water table responded to precipitation events that occurred earlier on (November 15 and 24). C2P2 water table maintained the highest for majority of the season, except for December 22 and December 25–January 4. C2P2 had the lowest water table, except for December 27–January 4. From February onward, C2P3 water table was higher than that of C2P2.

C2P1 showed the quickest and most extreme decline in water table immediately after precipitation events ceased. All pool levels quickly responded positively to precipitation events.

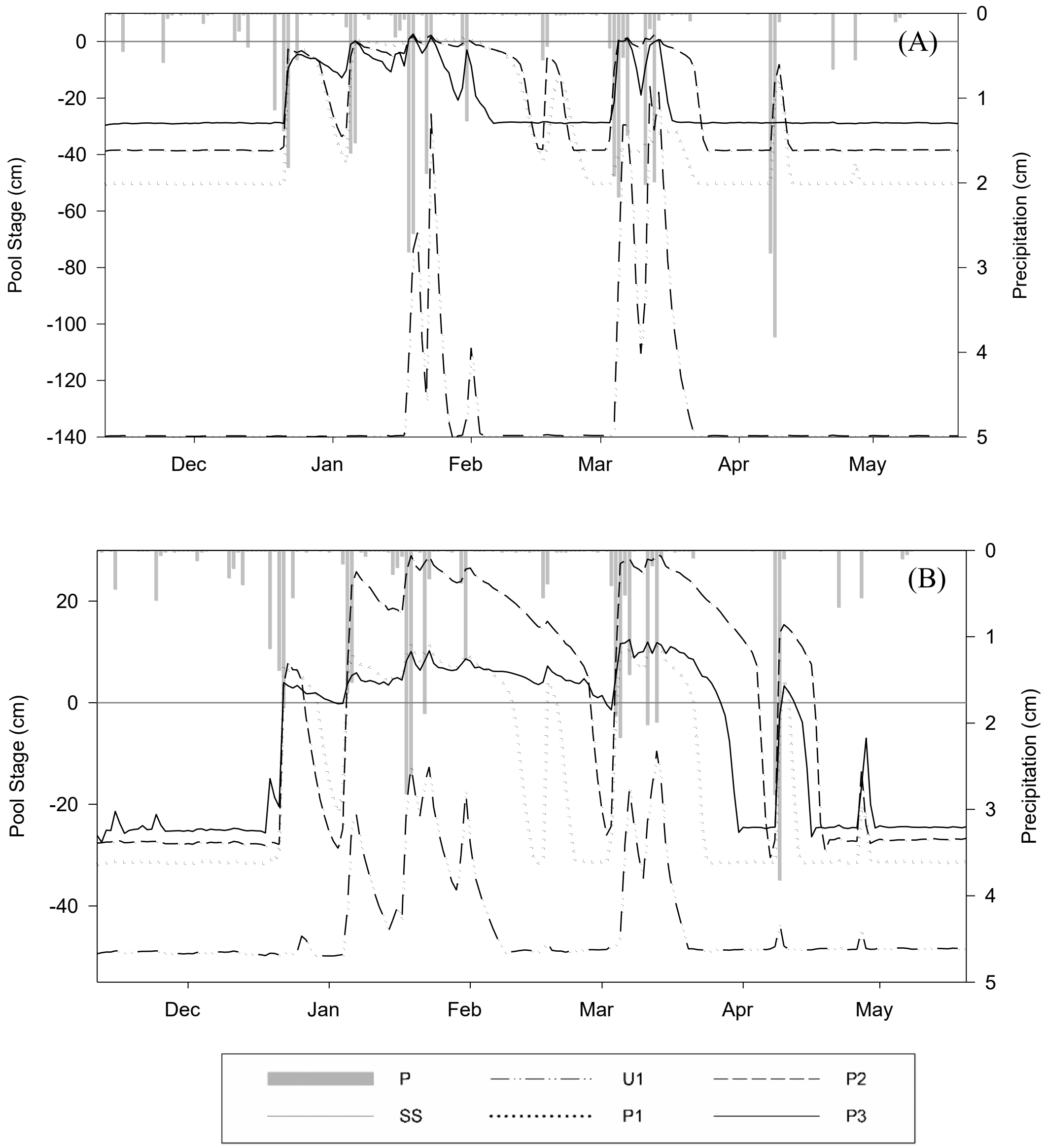

Figure 24 Average daily precipitation (P) and average daily water table height of upland (U), upper pool (P1), middle pool (P2), and lower pool (P3) in (A) Catchment 1 and (B) Catchment 2. Average daily precipitation was obtained from CIMIS Station #148. Pool stages were measured with pressure transducers that were placed in the field in summer 2015. Pressure transducers were corrected for barometric pressure changes. At the bottom of the vernal pool, pool stage is 0 cm, also referred to as the soil surface (SS).

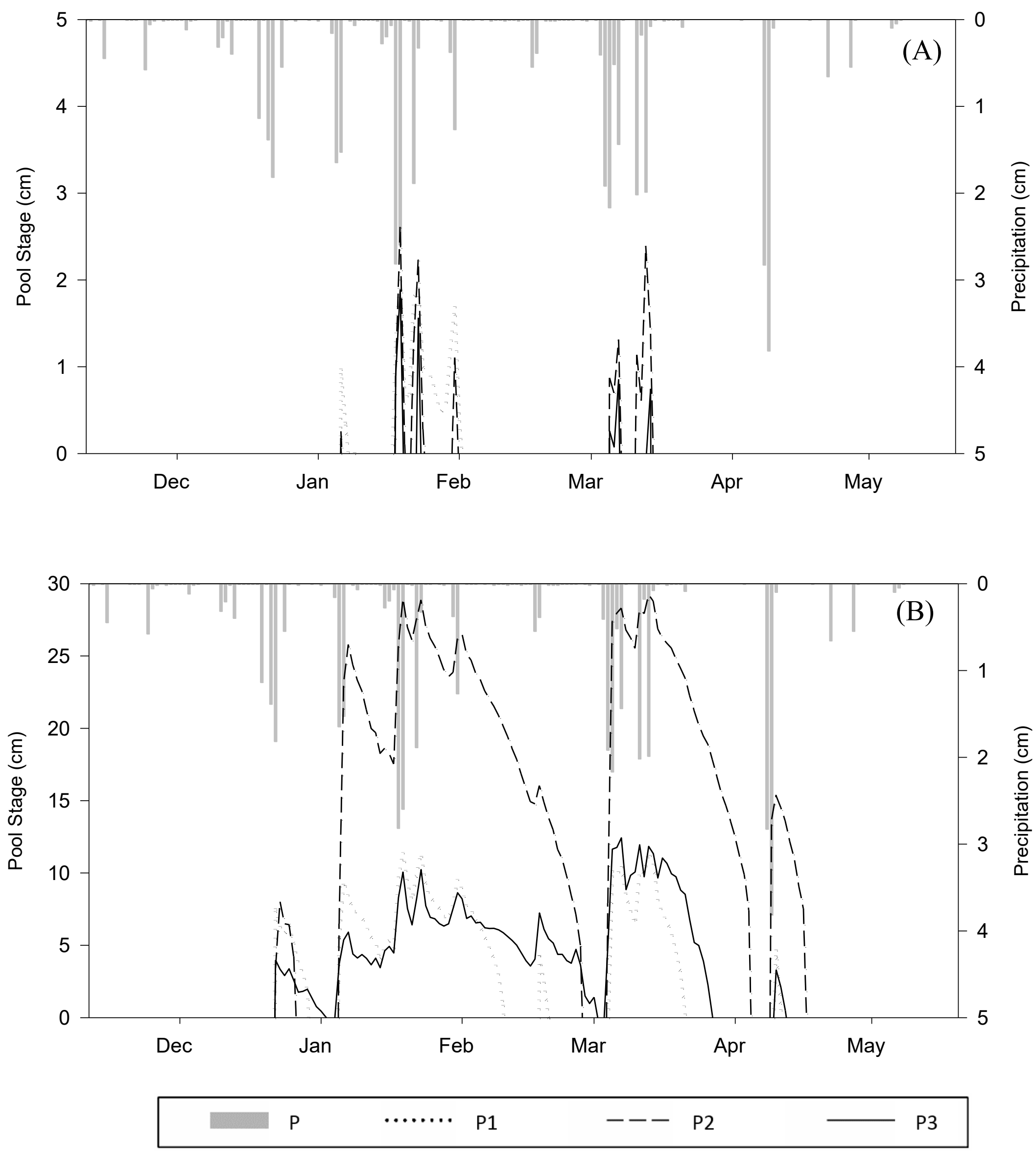

Figure 25 Average daily precipitation (P) and inundation period of upper pool (P1), middle pool (P2), and lower pool (P3) in (A) Catchment 1 and (B) Catchment 2. Average daily precipitation was obtained from CIMIS Station #148. Pool stages were measured with pressure transducers that were placed in the field in summer 2015. Pressure transducers were corrected for barometric pressure changes. At the bottom of the vernal pool, pool stage is 0 cm, also referred to as the soil surface (SS).

3.1.4 Pressure Head and Hydraulic Gradient

The pressure head, shown as an elevation in Figure 26, increased in response to a series of precipitation events starting in December then showed a relatively rapid drop in elevation often within a week following cessation of the precipitation for the vernal pools higher up in the catchment (C1P1, C1P2 and C2P1, C2P2). The relatively shallow C1P3 vernal pool experienced a strong diurnal signal and little change in hydraulic head while C2P3 experienced a relatively constant hydraulic head increase due to recharge from the uplands (Figure 26). In figure 26, the bottom of the vernal pool represents the soil surface elevation. Therefore, vernal pools in the upper elevations of the catchment dry down, due to downgradient drainage and evaporation of surface water, to the soil surface while C2P3 only dried down to the soil surface at the end of March after the majority of the precipitation events finished (Figure 26B).

Hydraulic gradient values for P2–P3 were greater than those from P1–P2 for both three–pool series (Figure 27). There were non–zero C1P1–C1P2 hydraulic gradient values (0.1–0.3) throughout the wet season, whereas C1P2–C1P3 hydraulic gradient values (0.5–0.8) only occurred during the period with the highest precipitation, predominately in late December and late March. C2P1–C2P2 hydraulic gradient values were more variant than those from C2P2–C2P3 and correlated with precipitation events (Figure 27). C2P2–C2P3 hydraulic gradient remained quite constant throughout the wet season. This may be due to C2P2 remaining inundated for a longer period and maintaining a constant water elevation. The upper vernal pools (C1P1 and C2P1) had higher downgradient flow relative to the amount of evaporative flux from the vernal pools, while the middle and lower vernal pools had lower downgradient flow, which is also reflected in the stable isotope signatures described below. Once the perched groundwater was fully discharged from the upper elevation vernal pools, the lower elevation vernal pools (C2P3) began to dry down later in the season. In Figure 27, a flat “hydraulic gradient” indicates that the system has begun to dry out and the vernal pools are not hydraulically connected.

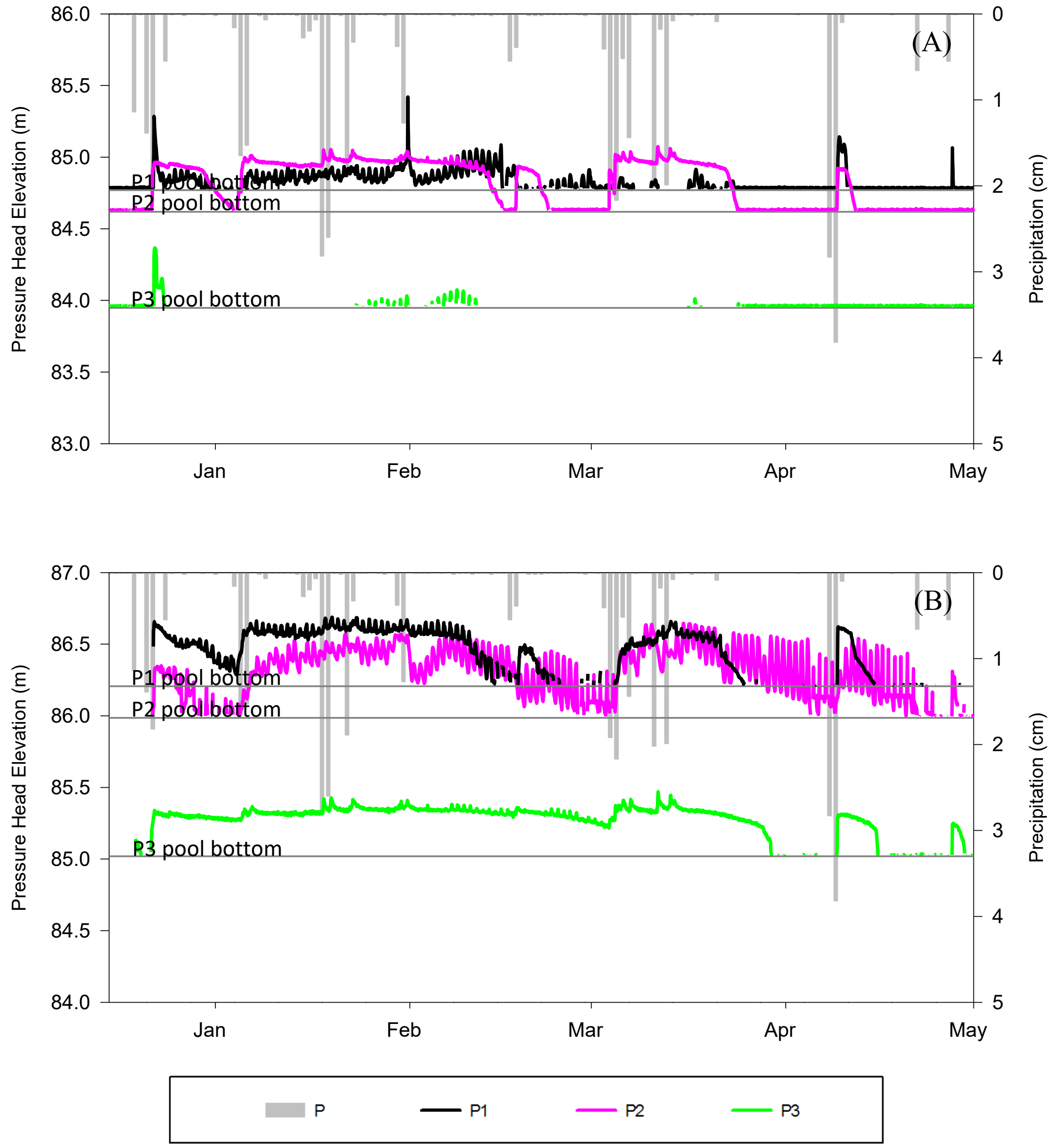

Figure 26 Elevation of water column (piezometer head) of upper (P1), middle (P2), and lower pool (P3) of (A) Catchment 1 (B) and Catchment 2. The pool bottom is the soil surface.

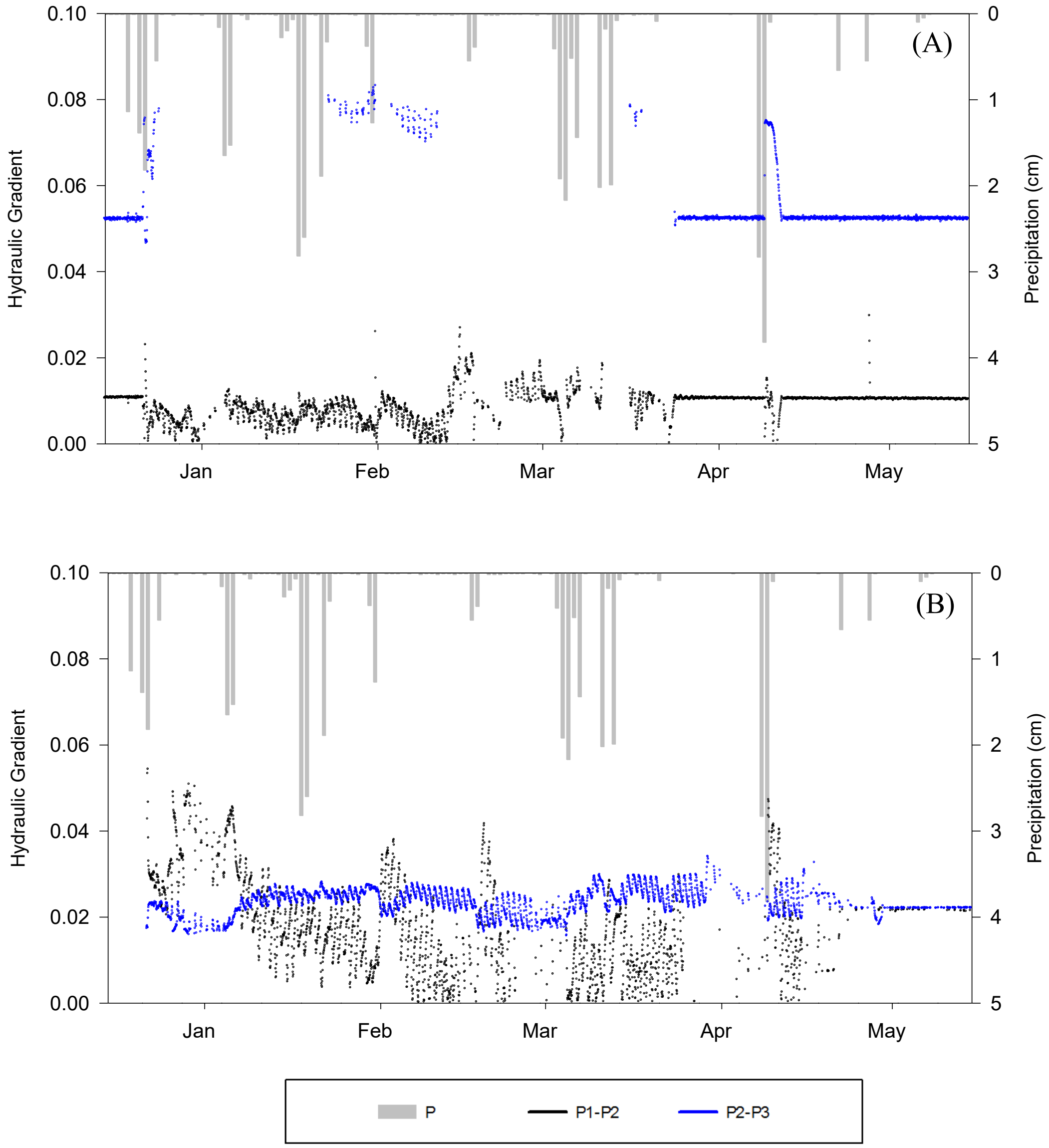

Figure 27 Hydraulic gradient of Pools 1 and 2 (P1–P2) and Pools 2 and 3 (P2–P3) of (A) Catchment 1 (B) and Catchment 2. Depth to shallow subsurface confining layer and a 50% soil porosity assumption were used in calculating hydraulic gradient. When the lines labelled as hydraulic gradient are flat, the system is drying out and wells are no longer hydrologically connected.

3.2 Chemical Characteristics

3.2.1 Specific Conductivity, DOC, Isotopes, pH

Specific conductivities of my vernal pools were high compared to local river water (32.7 µS/cm) and local groundwater (81.6 µS/cm); they ranged from 108.0 to 420.1 µS/cm (Figures 28, 29). Seasonal averages for C1 perched groundwater, C1 surface water, and C2 surface water were 199.7 µS/cm, 199.7 µS/cm, and 234 µS/cm, respectively. Specific conductivity responded inversely to precipitation; values decreased with precipitation and increased with prolonged dry periods. Specific conductivity of C2P2 surface water was only observed between a narrow range of 150 to 200 µS/cm for most of the wet season, and then increased towards and at the end of the wet season. Water samples had small pH range– 6.96 to 7.50 (Table 5).

Like specific conductivity, DOC concentrations were also inversely related to precipitation (Figure 30). Unlike the all other water samples, C2P2 surface water samples showed low and invariant values until mid–March. Specific conductivity and DOC were directly related (Figure 31). The vernal pools served as a sink for fine particles. Many water samples had a brown tint even after passing through a 0.45 µm polycarbonate membrane for lab analysis, but the majority of the samples became clear after the fine particles settled down, suggesting particulate organic matter was present rather than dissolved organic matter. One organic carbon–contributing variable in this system was green vegetation in and around the vernal pools throughout the wet season. My study site is an active grazing space for cows. Cows could have added organic carbon from previous years by turning up soil and through manure deposition, since they were constantly walking through the shallow vernal pools throughout the season.

Stable water isotopes, δD and $\delta^{18}O$, got heavier over time, especially with prolonged dry periods throughout the wet season, and lighter with precipitation– a typical pattern of evaporation and dilution by precipitation events (Figure 32). C1P1 perched groundwater and Catchment 2 surface water showed similar evaporation signals (Figure 32). Within Catchment 2, C2P3 had a stronger evaporation signal than C2P2 at the beginning of the wet season. After major precipitation events in March, C2P2 had a stronger evaporation signal than C2P3.

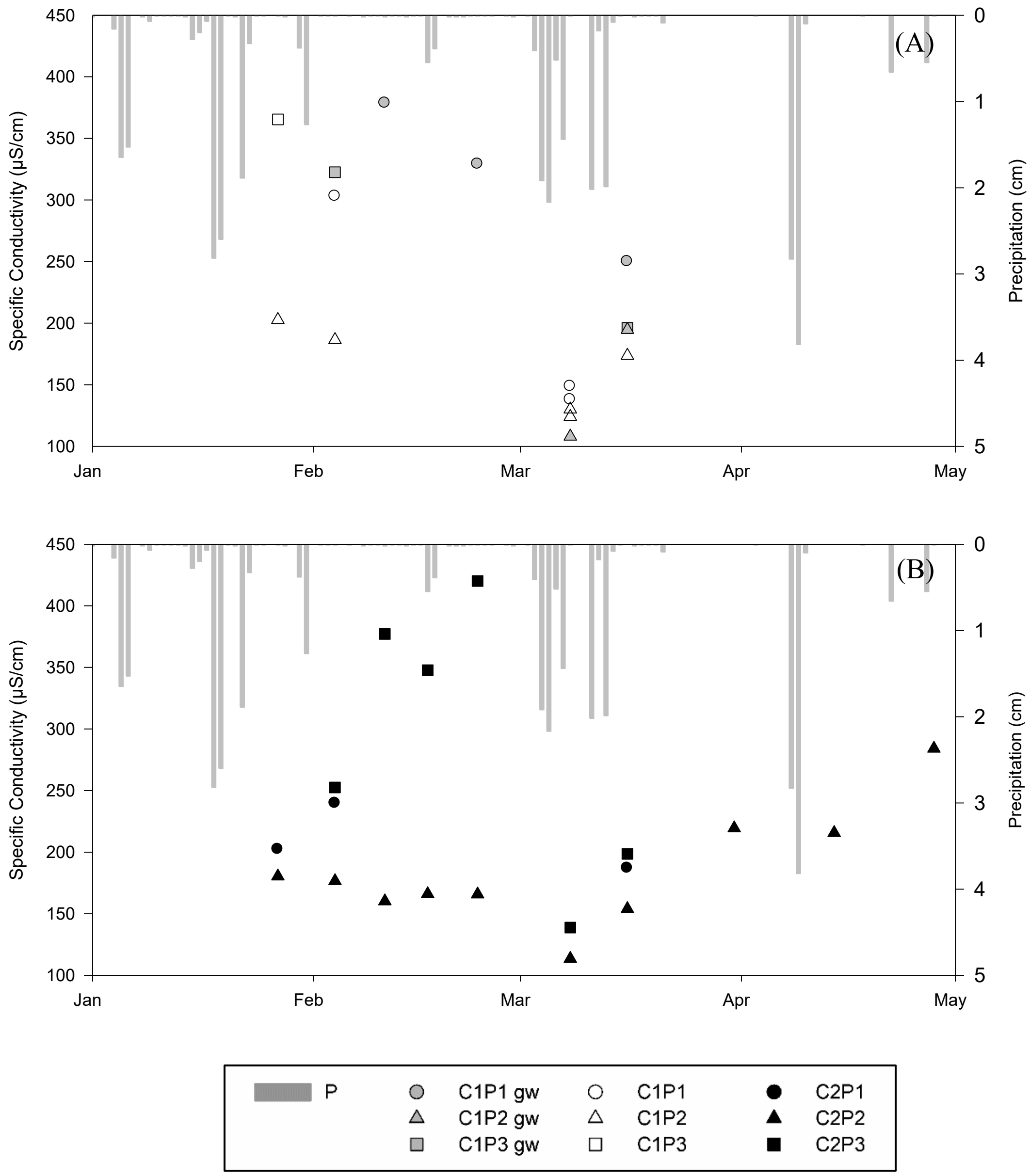

Figure 28 Average daily precipitation (P) and specific conductivity of surface water and perched groundwater (gw) samples of upper (P1), middle (P2), and lower (P3) pools in (A) Catchment 1 (C1) and (B) Catchment 2 (C2). Average daily precipitation was obtained from CIMIS Station #148.

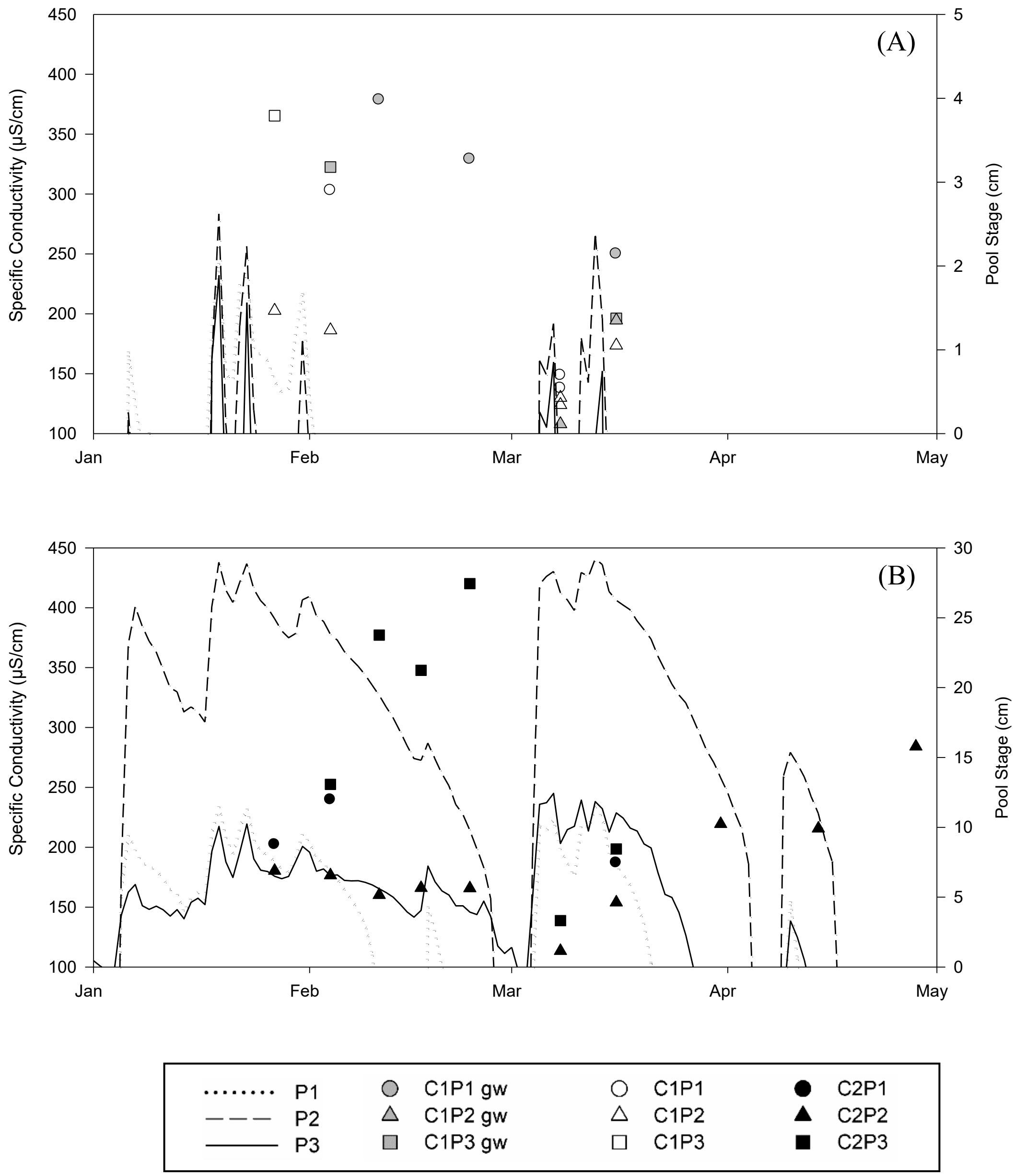

Figure 29 Specific conductivity of surface water and perched groundwater (gw) samples, pool stage, and inundation period of upper (P1), middle (P2), and lower (P3) pools in (A) Catchment 1 (C1) and (B) Catchment 2 (C2). Pool stages were measured with pressure transducers that were placed in the field in summer 2015. Pressure transducers were corrected for barometric pressure changes.

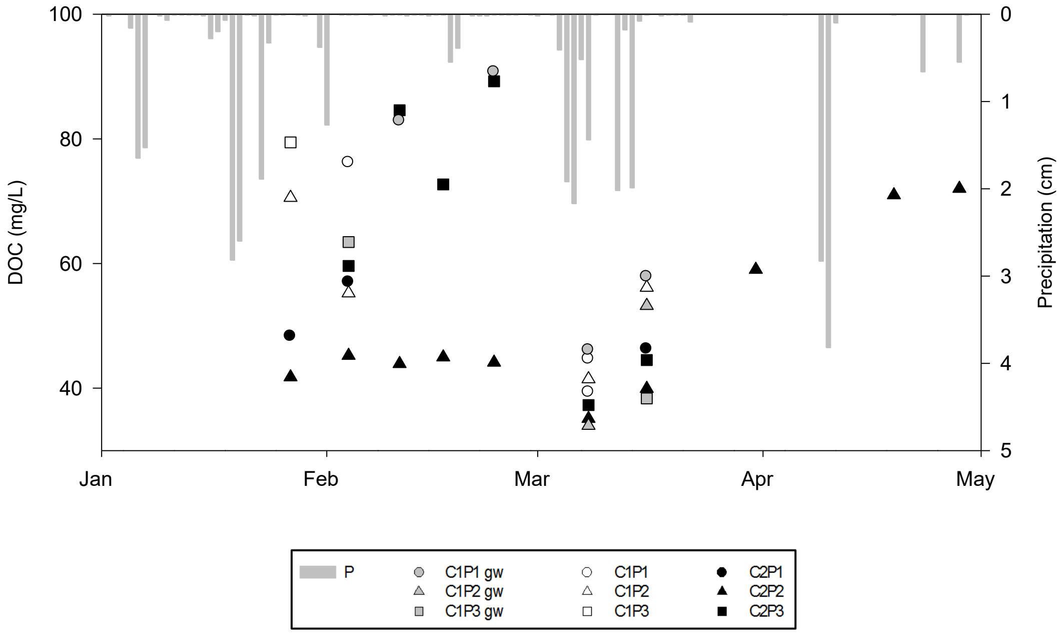

Figure 30 Dissolved organic carbon (DOC) average daily precipitation (P) of surface water and perched groundwater (gw) samples of upper (P1), middle (P2), and lower (P3) pools in Catchment 1 (C1) and Catchment 2 (C2). Average daily precipitation was obtained from CIMIS Station #148.

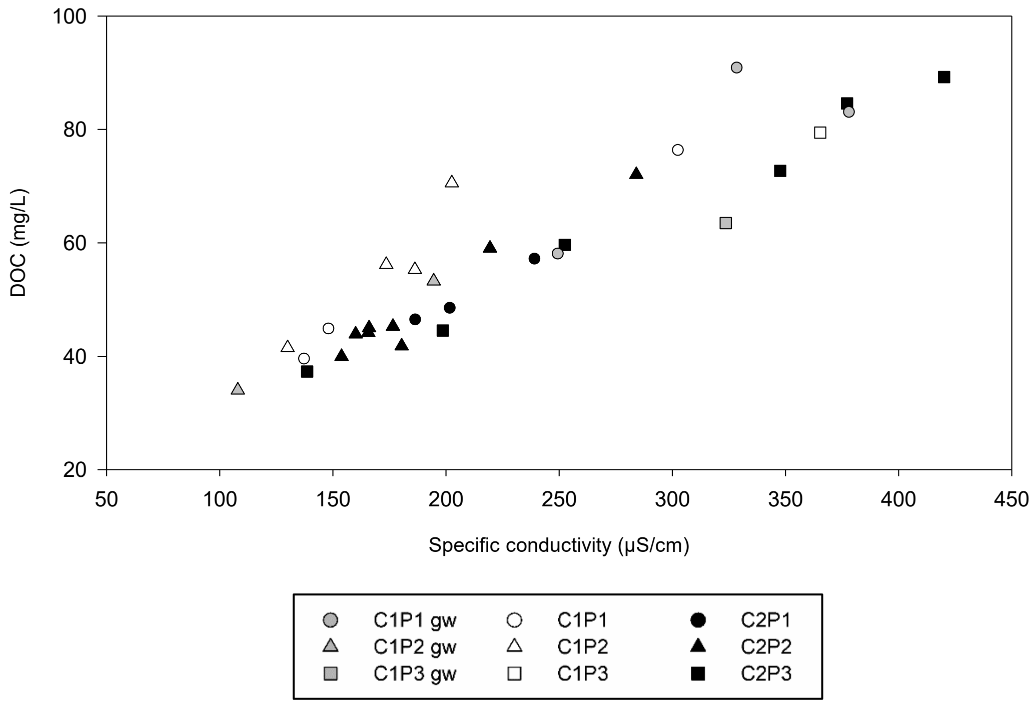

Figure 31 Specific conductivity and dissolved organic carbon (DOC) concentrations of surface water and perched groundwater (gw) samples of upper (P1), middle (P2), and lower (P3) pools in Catchment 1 (C1) and Catchment 2 (C2).

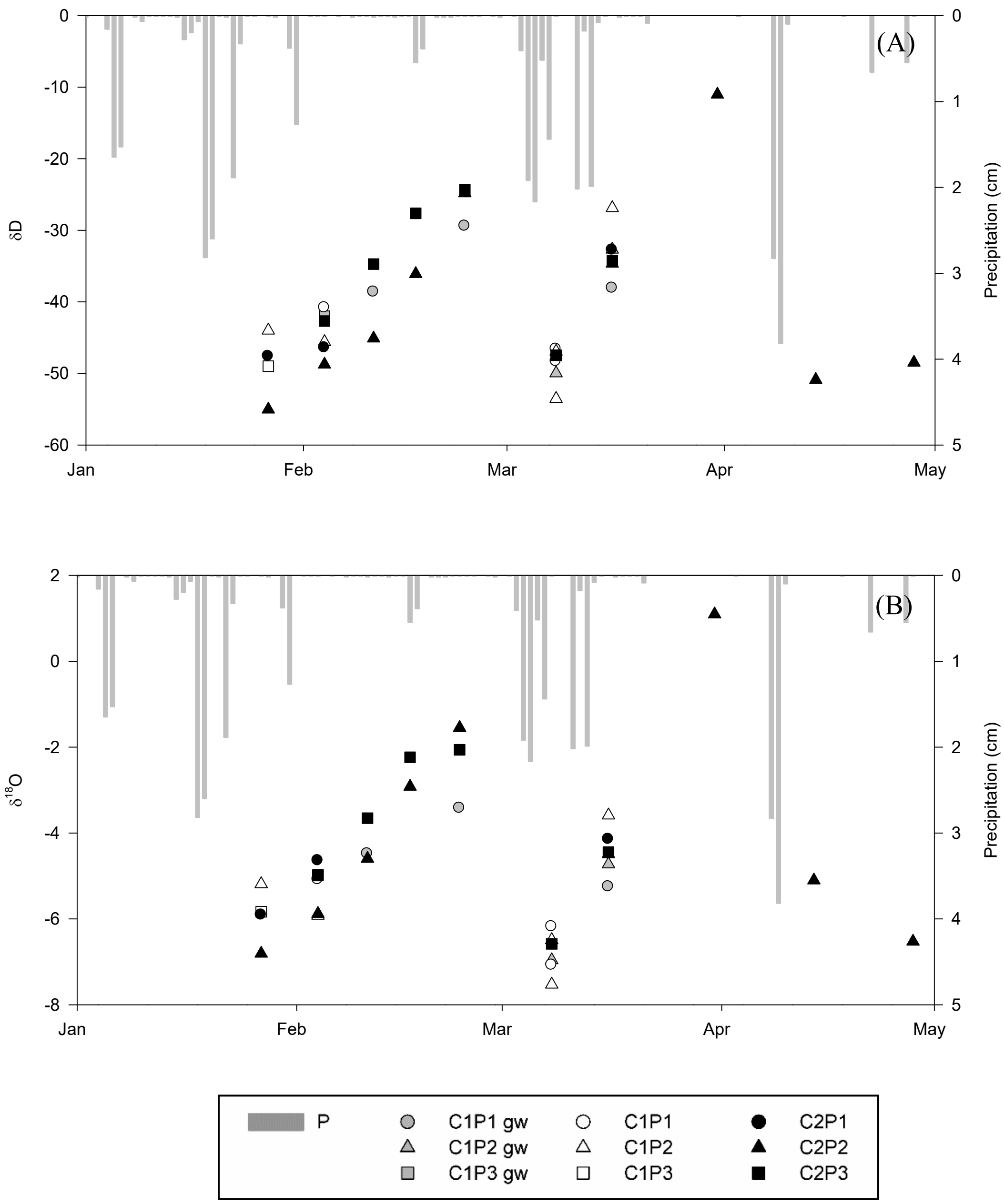

Figure 32 Average daily precipitation (P) and (A) δD and (B) $\delta^{18}O$ of surface water and perched groundwater (gw) samples of upper (P1), middle (P2), and lower (P3) pools in Catchment 1 (C1) and Catchment 2 (C2). Average daily precipitation was obtained from CIMIS Station #148.

Table 5 pH measurements.[1]

	n	pH	SD
Catchment 1			
C1P1 (Upper)	3	7.21	0.13
C1P2 (Middle)	5	7.19	0.21
C1P3 (Lower)	1	7.36	N/A
C1P1 gw (Upper)	3	6.96	0.09
C1P2 gw (Middle)	2	7.50	0.71
C1P3 gw (Lower)	1	7.04	N/A
Catchment 2			
C2P1 (Upper)	3	7.31	0.09
C2P2 (Middle)	9	7.28	0.22
C2P3 (Lower)	6	7.33	0.23

[1]Taken from isotope analysis samples; temperature around 21.9 to 22.4 degrees Celsius.

3.2.1 Ions

3.2.1.1 Ca^{2+}

Perched groundwater and surface water concentrations of Ca^{2+} in all C1 pools decreased with precipitation events and increased after precipitation events (Figure 33). Changes in C1 vernal pool concentration were variant throughout the season. Surface water concentrations in C2P1 and C2P2 were invariant. C2P3 changed dramatically–responding quickly to both the presence and absence of precipitation events.

3.2.1.2 K^{+}

Perched groundwater concentrations of K^{+} were lower than all surface water samples for both catchments (Figure 34). Concentrations from all pools were close in range with each other throughout the season. C1P1 and C1P2 surface water were invariant. An initial C1P3 sample had a very high concentration at the start of the season, but no pattern was concluded because only one sample could be obtained. All surface water concentrations in C2 were low and invariant. C2P2 concentrations increased at the end of the season (late April).

3.2.1.3 Mg^{2+}

Perched groundwater concentrations of Mg^{2+} were higher than those of surface water in both catchments (Figure 35). All surface water concentrations were similar in value, except for one C1P1 sample, which was taken on February 17, 2016. C1P1 and C1P2 concentrations showed minimal change thought out the season, except for when C1P2 concentration increased after the early March precipitation events. Surface water concentrations in C2P1 and C2P3 decreased and then increased during and after early March precipitation events. C2P2 was invariant throughout the season and then increased towards the end.

3.2.1.4 Na^{+}

C1 perched groundwater concentrations of Na^{+} were higher than those from its surface water (Figure 36). All pools showed a decrease in perched groundwater concentration over time, except for C1P2. C1P1 surface water concentrations increased and then decreased with early March precipitation events, whereas C1P2 stayed stagnant throughout the season. There was only one C1P3 sample, so no behavioral pattern was concluded. Surface water concentrations in C2P1 and C2P2 were invariant, except for C2P2 concentrations increasing in May. C2P3 was stagnant in the early part of the season and then decreased with March precipitation events.

3.2.1.5 NH_4^{+}

C1 perched groundwater concentrations of NH_4^{+} were higher than those from its surface water (Figure 37). All pools showed an increase in perched groundwater concentration over time, except for C1P1. C1P1 surface water concentrations increased and then decreased with early March precipitation events, whereas C1P2 stayed invariant throughout the season. C1P3 concentration values were below the detection limit. C2 surface water concentrations in all pools did not show much change, except for C2P2 concentrations increasing in May.

3.2.1.6 Br^{-}

Perched groundwater and surface water concentrations of Br^{-} from both catchments showed very low values, with all values in the range of 0.000–0.008 mmol/L, except for one surface water sample from C1P3 that had a Br^{-} concentration at 0.008 mmol/L (Figure 38). C2P2 surface water concentrations tapered off at the end of the wet season (late April).

3.2.1.7 Cl^-, SO_4^{2-}

Perched groundwater concentrations of Cl^-, and SO_4^{2-} were generally higher than all surface water samples for both catchments (Figures 39, 40). In both perched groundwater and surface water, C1P3 had the highest concentration values, followed by C1P1 and C1P2. All surface water concentrations were in a similar range of values. All pools in C2 had similar concentration values throughout the wet season, with C2P3 increasing towards the end of the wet season.

3.2.1.8 NO_3^-

Perched groundwater and surface water concentrations of NO_3^- in all C1 pools were decreasing as the season progressed (Figure 41). There was only one surface water sample from C1P2 and C1P3, so a pattern could not be determined. C2P1 surface water concentrations increased the most. C2P2 started with a high concentration at the start of the season and then stagnated throughout the season before tapering off at the end of the wet season. Overall, all vernal pools showed a decrease in concentration as the wet season progressed.

3.2.1.9 Charge Balance

Our water samples displayed a difference in charge balance that ranged from 0.82 to 3.42 (m eq/L) (Appendix, Table 9). Catchment 1 charge balance differences averaged 1.69 m eq/L for perched groundwater and 1.75 m eq/L for surface water. Catchment 2 charge differences averaged 1.57 m eq/L for surface water. There was an abundance of cations, shortage of anions, or a combination of the two. Water samples showed that Ca^{2+} was the cation with the highest concentration and there was a significant amount of DOC, a negatively charged molecule. DOC and Ca^{2+} concentrations had a direct relationship, since DOC was not included in the charge balance, accounting for DOC and its effects on Ca^{2+} concentrations may address the charge imbalances in my vernal pool system (Sapek, 2013) (Figure 42).

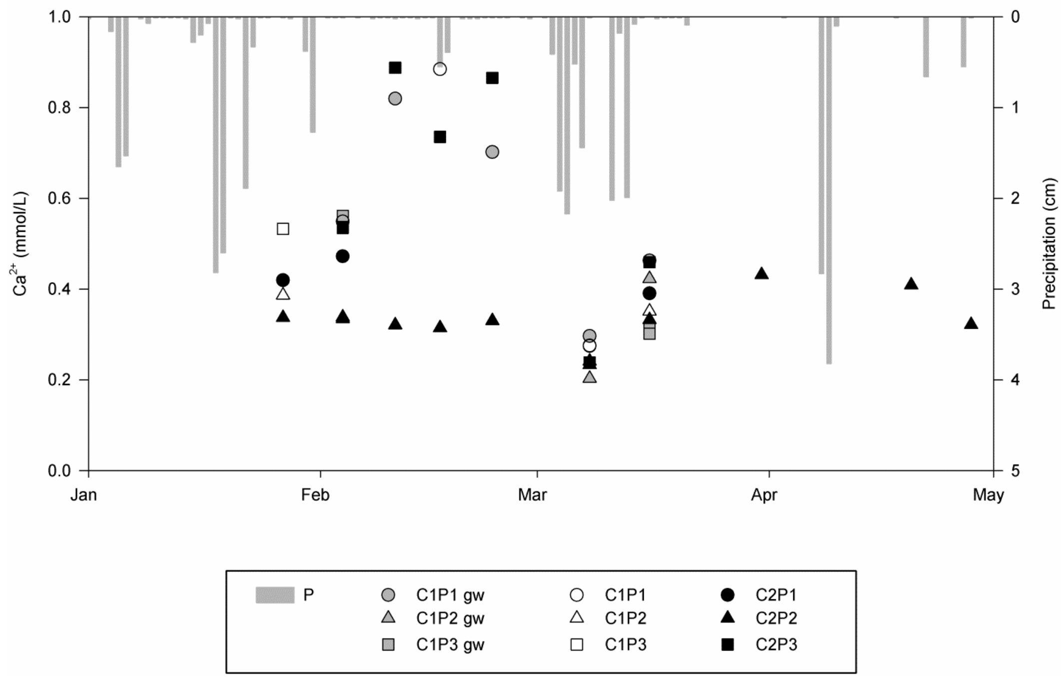

Figure 33 Average daily precipitation (P) and Ca^{2+} concentration of surface water and perched groundwater (gw) samples of upper (P1), middle (P2), and lower (P3) pools in Catchment 1 (C1) and Catchment 2 (C2). Average daily precipitation was obtained from CIMIS Station #148.

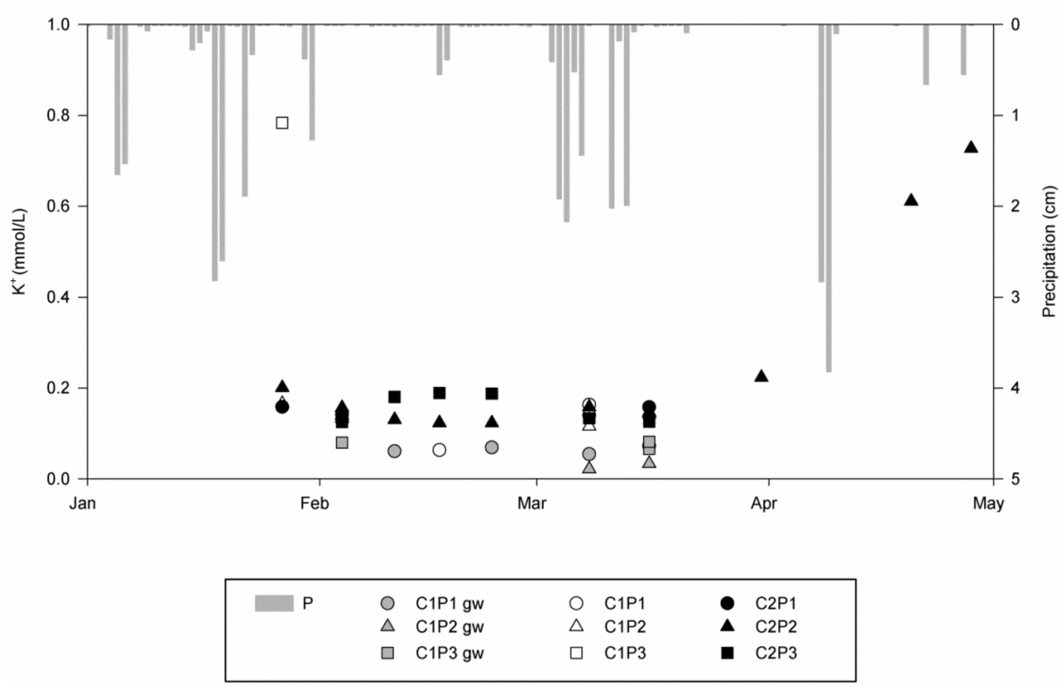

Figure 34 Average daily precipitation (P) and K^{+} concentration of surface water and perched groundwater (gw) samples of upper (P1), middle (P2), and lower (P3) pools in Catchment 1 (C1) and Catchment 2 (C2). Average daily precipitation was obtained from CIMIS Station #148.

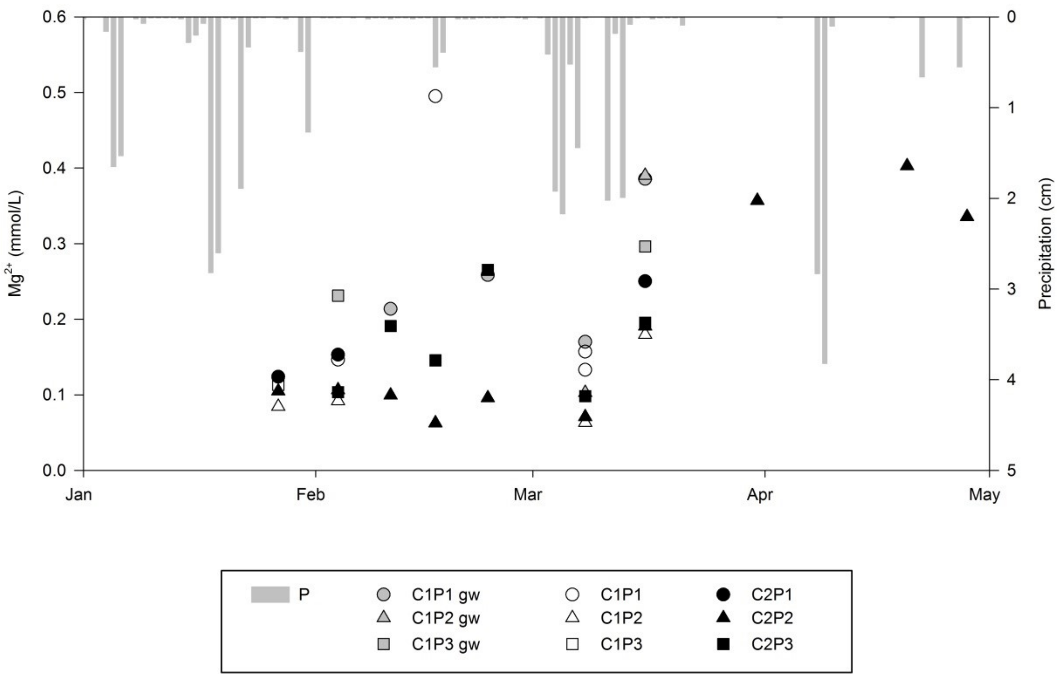

Figure 35 Average daily precipitation (P) and Mg^{2+} concentration of surface water and perched groundwater (gw) samples of upper (P1), middle (P2), and lower (P3) pools in Catchment 1 (C1) and Catchment 2 (C2). Average daily precipitation was obtained from CIMIS Station #148.

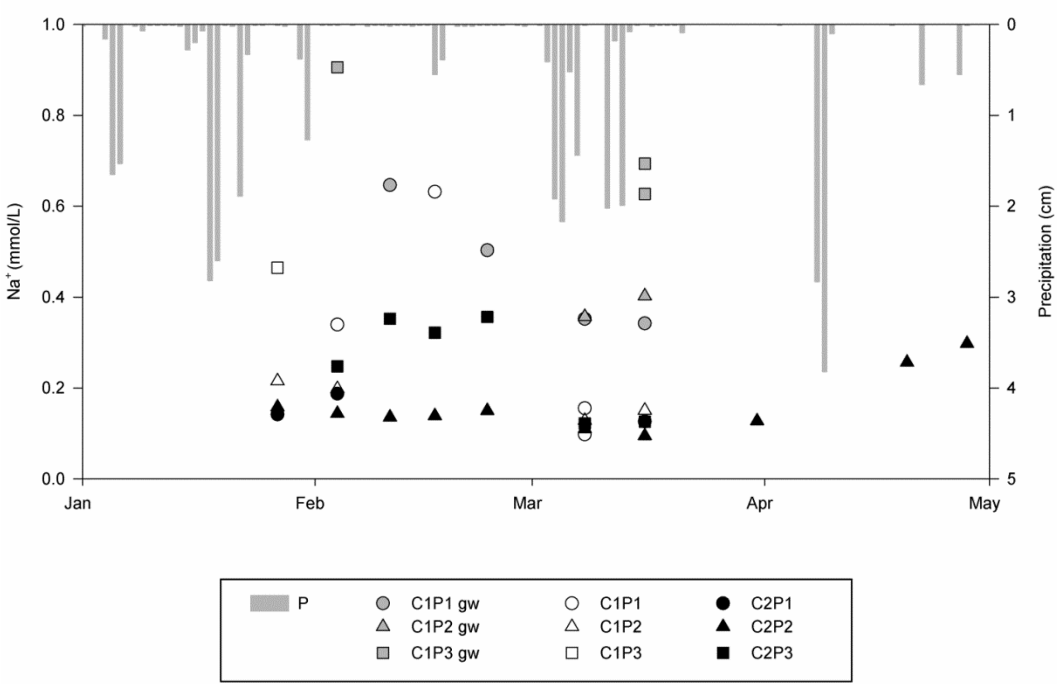

Figure 36 Average daily precipitation (P) and Na^{+} concentration of surface water and perched groundwater (gw) samples of upper (P1), middle (P2), and lower (P3) pools in Catchment 1 (C1) and Catchment 2 (C2). Average daily precipitation was obtained from CIMIS Station #148.

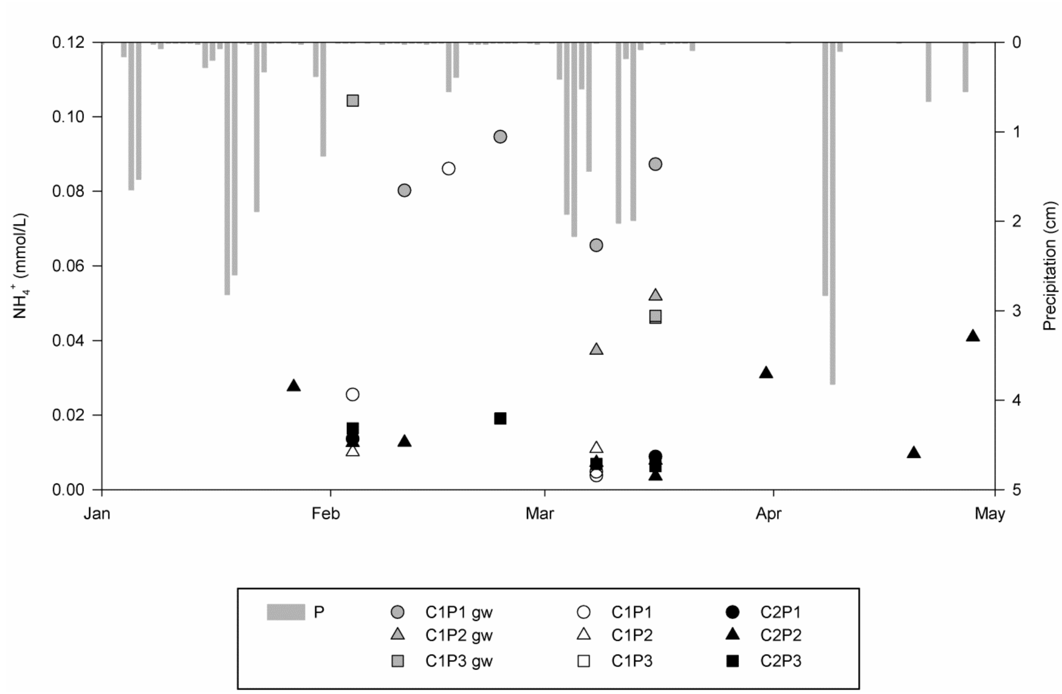

Figure 37 Average daily precipitation (P) and NH_4^+ concentration of surface water and perched groundwater (gw) samples of upper (P1), middle (P2), and lower (P3) pools in Catchment 1 (C1) and Catchment 2 (C2). Average daily precipitation was obtained from CIMIS Station #148.

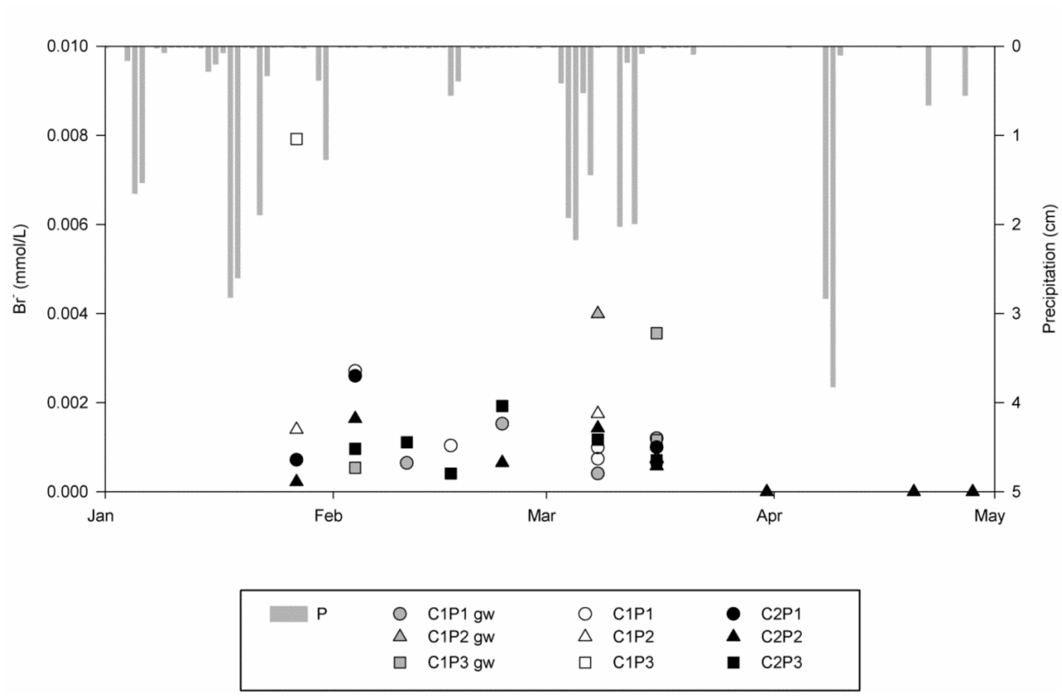

Figure 38 Average daily precipitation (P) and Br^- concentration of surface water and perched groundwater (gw) samples of upper (P1), middle (P2), and lower (P3) pools in Catchment 1 (C1) and Catchment 2 (C2). Average daily precipitation was obtained from CIMIS Station #148.

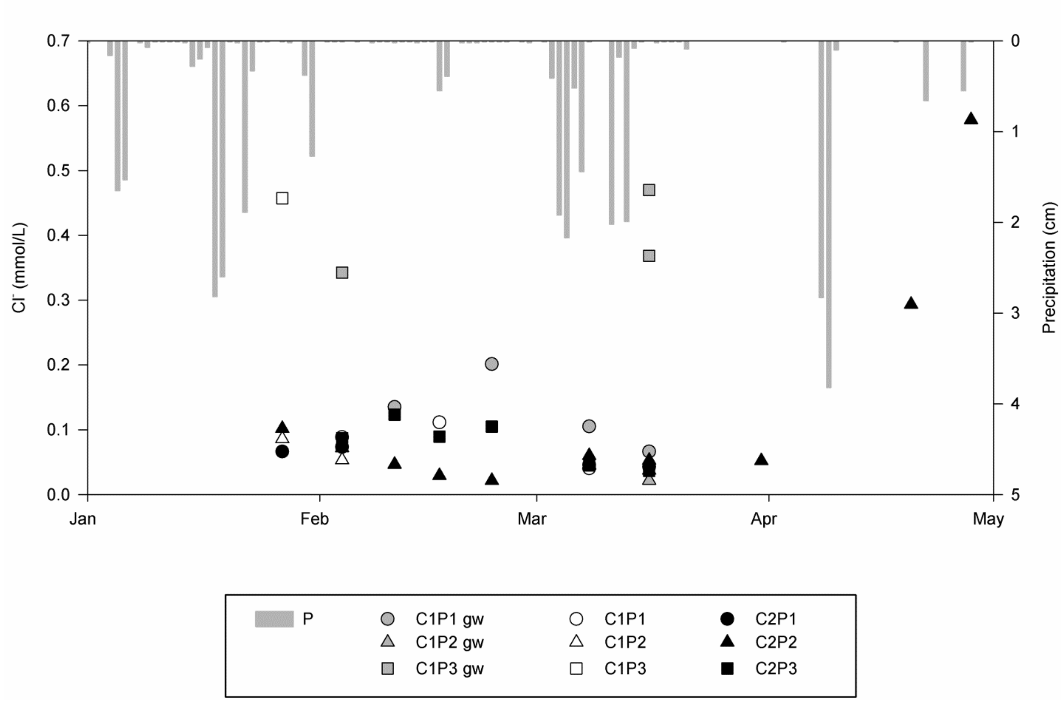

Figure 39 Average daily precipitation (P) and Cl^- concentration of surface water and perched groundwater (gw) samples of upper (P1), middle (P2), and lower (P3) pools in Catchment 1 (C1) and Catchment 2 (C2). Average daily precipitation was obtained from CIMIS Station #148.

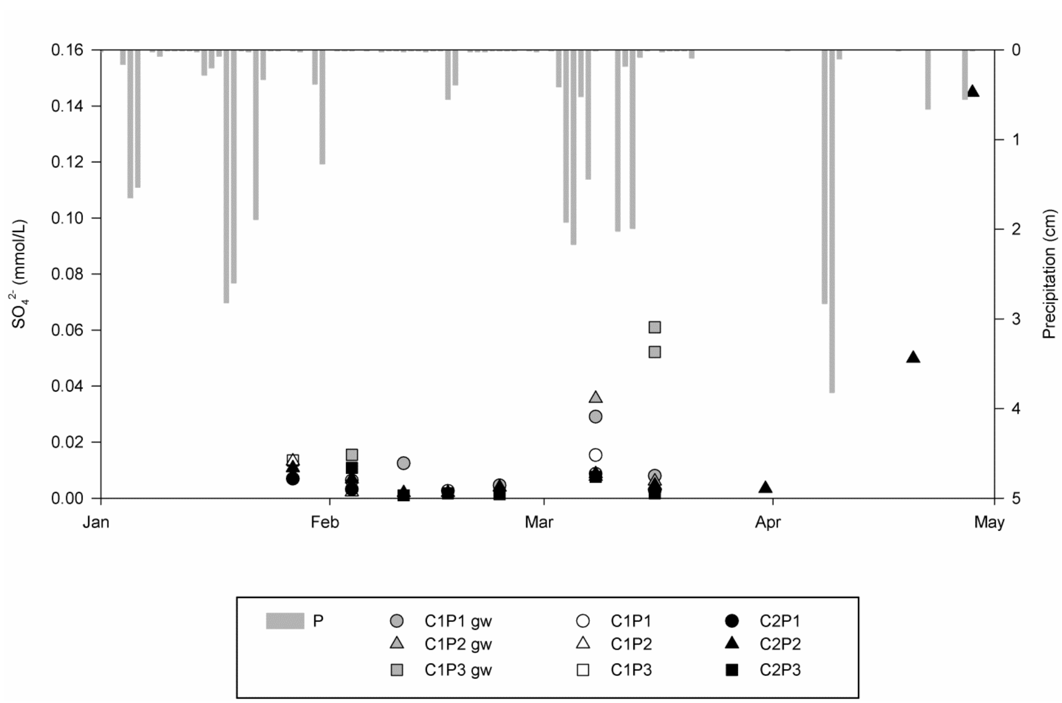

Figure 40 Average daily precipitation (P) and SO_4^{2-} concentration surface water and perched groundwater (gw) samples of upper (P1), middle (P2), and lower (P3) pools in Catchment 1 (C1) and Catchment 2 (C2). Average daily precipitation was obtained from CIMIS Station #148.

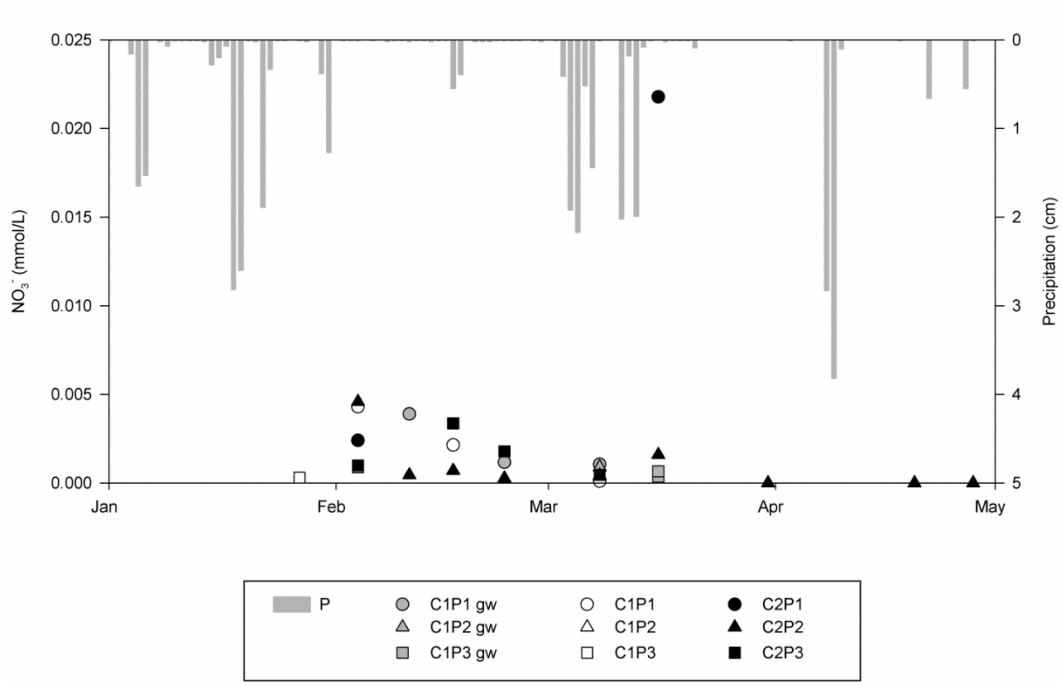

Figure 41 Average daily precipitation (P) and NO_3^- concentration of surface water and perched groundwater (gw) samples of upper (P1), middle (P2), and lower (P3) pools in Catchment 1 (C1) and Catchment 2 (C2). Average daily precipitation was obtained from CIMIS Station #148.

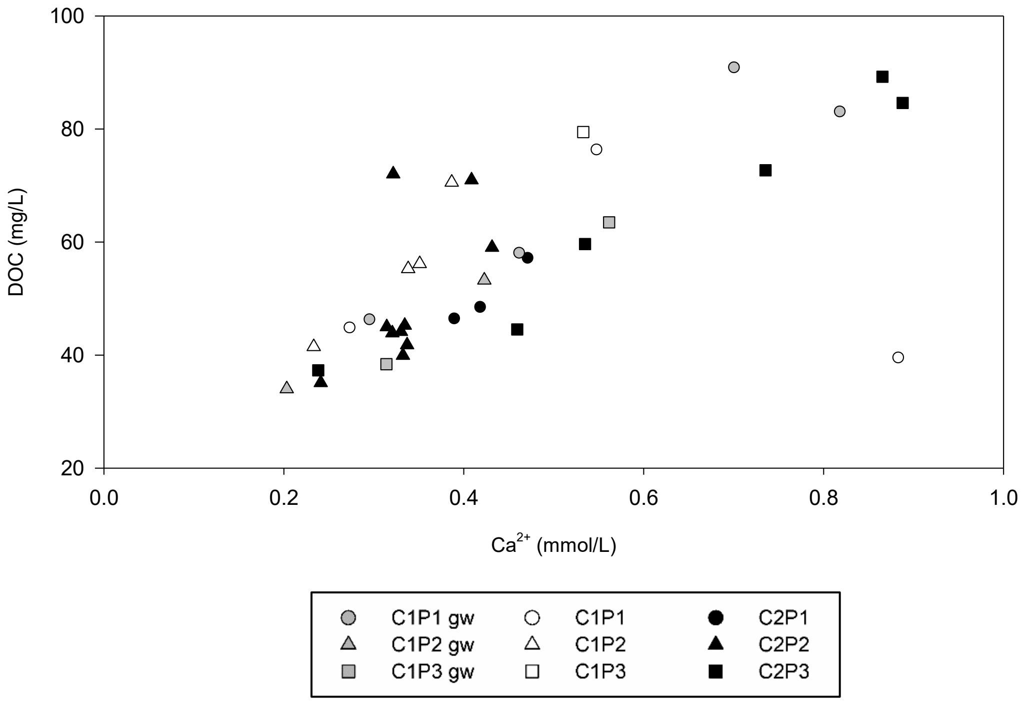

Figure 42 DOC and Ca^{2+} concentration of surface water and perched groundwater (gw) samples of upper (P1), middle (P2), and lower (P3) pools in Catchment 1 (C1) and Catchment 2 (C2).

Chapter 4 Discussion

Vernal pools have often been considered “isolated” wetlands (Winter & LaBaugh, 2003; Zedler, 2003). Hanes and Stomberg (1998) suggested that upland water input, including from upslope vernal pools, was small compared to direct precipitation. Their water balance model did not take into consideration any subsurface water. Similarly, Pyke (2004) created a vernal pool hydrology model (called PHYDO) that assumed the vernal pools were isolated and only received direct precipitation as water input, and evapotranspiration was the main output, although the downslope rim of the vernal pool could release water when the vernal pool water reached an elevation higher than the downslope rim. The perception that these wetlands function, more or less, like a bathtub receiving water directly from precipitation and losing water from evapotranspiration has been challenged in recent years (Winter & LaBaugh, 2003; Zedler, 2003; Mushet et al., 2015; Calhoun et al., 2017). The concept of wetlands being isolated from streams and rivers is now an important area of study, and field data are slowly being shown to contradict the “isolated” wetland myth. Rains et al. (2006) demonstrated connectivity of the uplands and flow through vernal pools using stable isotopes. McCarten et al. (2018b) showed that the geophysical structure of a vernal pool landscape contributed to the overall water balance of vernal pools. It is these concepts that were being tested in this study and to contribute to a better understanding of vernal pool hydrology.

The results of my study show there are several dimensions to the hydrological connectivity of vernal pool systems– the shallow subsurface confining layer, perched groundwater and surface water flow, and inundation. Like Rains et al. (2006), perched groundwater and surface water flow are significant water sources in my vernal pools system, in addition to precipitation. Inundation is an indicator of subsurface characteristic and the shallow subsurface confining layer is a source of constriction. These dimensions are important in the determining the degree of hydrological connectivity amongst vernal pools, and between vernal pools and their surrounding landscape. Previous studies (Ameli & Creed, 2017; Leibowitz & Brooks, 2008; Rains et al., 2006) have explained contributing variables that influence water path ways in vernal pool systems. The shallow subsurface confining layer is a contributing variable that has not been previously explored; it does not necessarily parallel the soil surface, it plays a role in where a vernal pool forms in the landscape, and it determines when and how long a vernal pool inundates. With vernal pool destruction and degradation, mitigation often comes in the form of the creation of new pools or restoration of degraded ones (Black & Zedler, 1998; Ferren et al., 1998). In a natural vernal pool landscape, there are a variety of inundations times, and reconstructed vernal pools should mimic that. Understanding the hydrology of this unique abiotic environment is vital for the success of vernal pools and vernal pool species, as they face habitat loss and experiences new selective pressures associated with climate change (Calhoun et al., 2014).

4.1 Hydrological Connectivity

Vernal pool hydrological connectivity is important because it affects the hydrological, biogeochemical, and biological functions of vernal pools. McDonough et al. (2015) suggested that hydrological connectivity ecologically links wetlands and nearby water bodies. Ameli and Creed (2017) suggested that groundwater transit time affects the structure and function of aquatic ecosystems, because water can adsorb nutrients and metals as it travels through soil. My study expands on the factors that influence hydrological connectivity in vernal pools by focusing on the role of the shallow subsurface confining layer, perched groundwater and surface water flow, and inundation.

4.1.1 Shallow Subsurface Confining Layer

This vernal pool system showed that the depth to the shallow subsurface confining layer plays a significant role in the inundation period of vernal pools. Rains et al. (2006) explained how the shallow subsurface confining layer in their vernal pool system created perched aquifers that were not connected to the regional aquifer– indicating that surface water and perched groundwater flow through their vernal pools. Ameli and Creed (2017) explained how geology and landscape were significant in how vernal pools hydrologically connect on the surface and subsurface. Both studies exemplify the importance of geology and landscape in how water flows through vernal pools systems, but the relationship between geology and landscape and vernal pool inundation have not been characterized until now. In addition, including the shallow subsurface confining layer as a parameter to Ameli and Creed's (2017) subsurface–surface model could enhance their assessment of the timing and length of hydrological connectivity of vernal pools.

C2P2 exemplifies the important role of the shallow subsurface confining layer in a vernal pool system. GPR images showed that the shallow subsurface confining layer topography does not match the surface soil topography, and depths to the shallow subsurface confining layer vary across my study site (Figures 16–23). C2P2 had the longest inundation period of 99 days, followed by C2P3 with 96 days, and C2P1 with 66 days (Table 5). My data supported no correlation between vernal pools' length of inundation period to its surface area. C2P2 does not have a significantly larger surface area than the other pools but inundated for the most days. In addition to precipitation, this could be caused by the inflow of surface water, perched groundwater, or a combination of the two. One observed physical feature unique to C2P2 is its shallow subsurface confining layer rising nearly to the soil surface on the downslope side, or "pinch," which can cause water to stay in the pool longer, causing a "dam effect" (Figure 20). In addition, assuming the soil has a 50% porosity, the water column and volumes of my two vernal pool series showed similar behavior and measurements, yet we observed a huge difference in the inundation period amongst the two series (Figures 43, 44; Table 5).

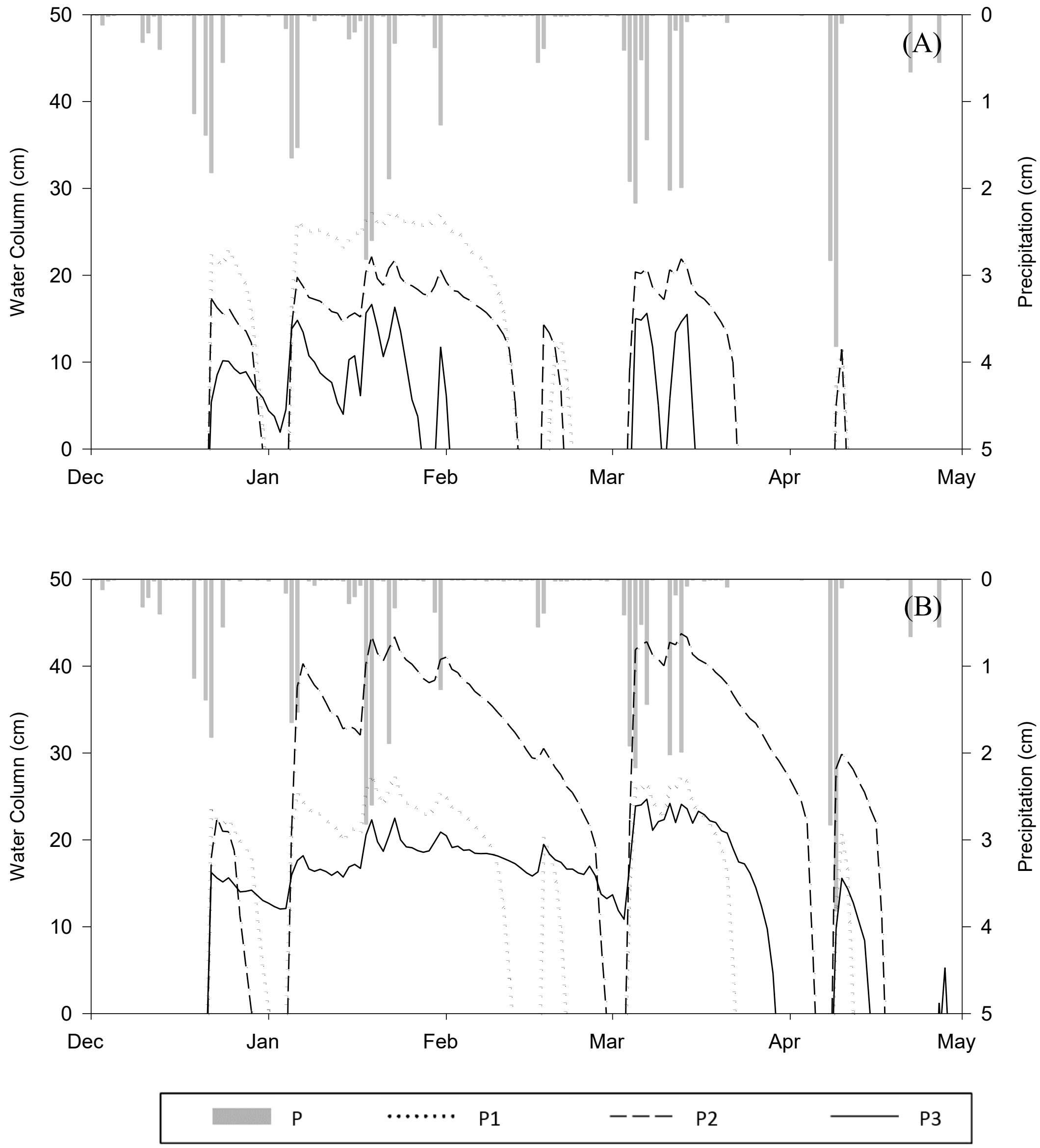

Figure 43 Daily water column of upper (P1), middle (P2), and lower (P3) pools in (A) Catchment 1 (C1) and (B) Catchment 2 (C2). Water column at 0 cm is the top of the shallow subsurface confining layer. Soil is assumed to have 50% porosity. Average daily precipitation was obtained from CIMIS Station #148.

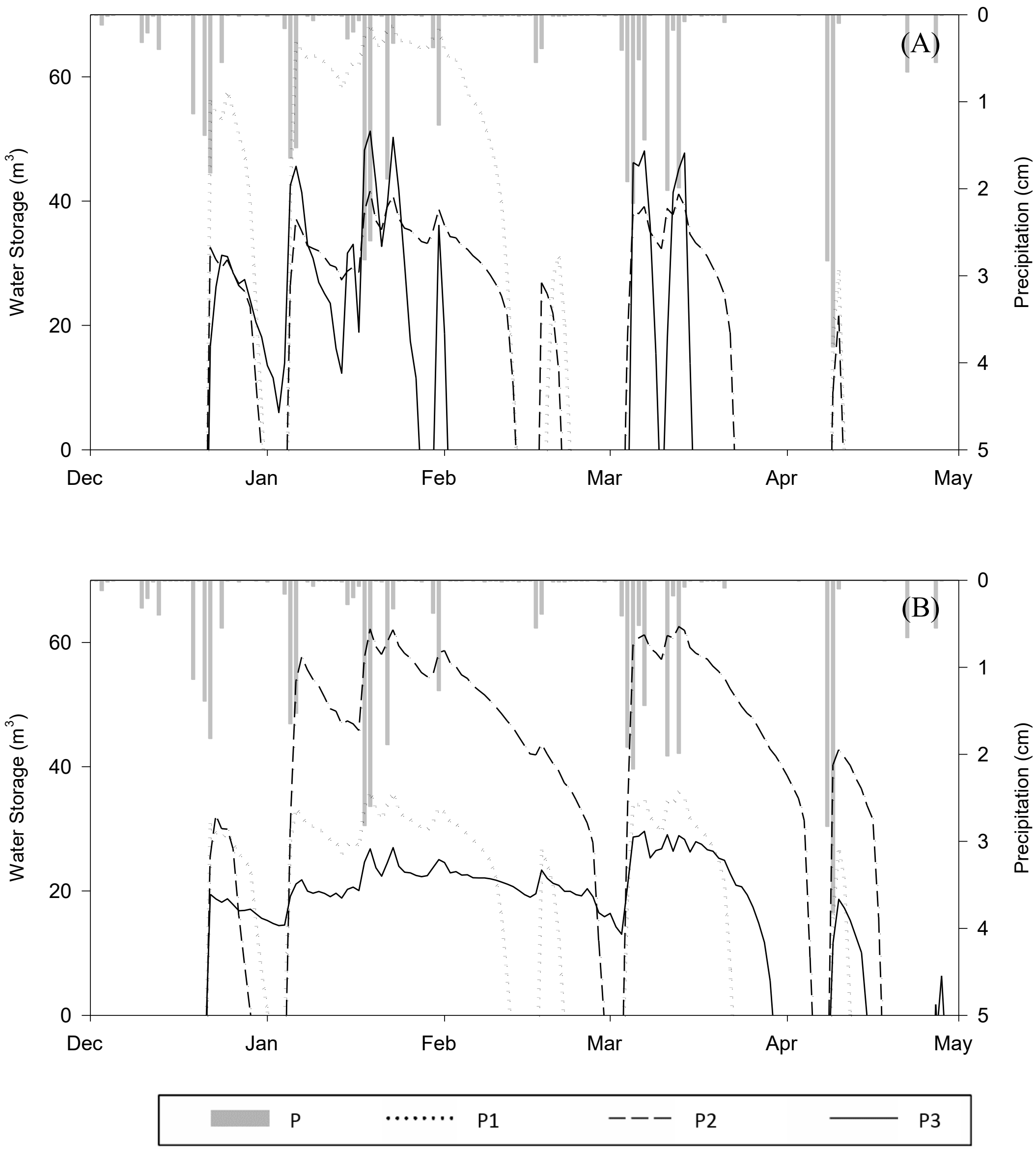

Figure 44 Estimation of water storage of upper (P1), middle (P2), and lower (P3) pools in (A) Catchment 1 (C1) and (B) Catchment 2 (C2). Soil is assumed to have 50% porosity. Average daily precipitation was obtained from CIMIS Station #148.

4.1.2 Perched Groundwater and Surface Water Flow

The temporal patterns in specific conductivity in my vernal pool system suggested a longitudinal and lateral movement of water– indicating likely vernal pool hydrological connectivity. As noted by Rains, et al. (2006), if the primary water loss in vernal pools was solely due to evapotranspiration, then specific conductivity of vernal pool surface water would increase over time due to evapoconcentration. Specific conductivity for all my vernal pools fluctuated over time (Figure 28). Similar to the vernal pools in Rains, et al. (2006) and Chow, et al. (2016), high specific conductivity occurred when there was a prolonged period without precipitation (e.g. C2P3 in early February), low specific conductivity after precipitation (e.g. C2P3 in mid–February), and high specific conductivity towards the end of the wet season (e.g. C2P2 starting in April) (Figure 28). C2P2, on the other hand, from January to April, had narrow–range, low values of specific conductivity (113.4–284.1 μS/cm)– signifying a continuous flushing of water and/or a larger body of surface pool water, which limited local effects of evapoconcentration.

Conservative ion ratios [Cl^-]:[Na^+] and [SO_4^{2-}]:[Cl^-] showed a large range in values throughout the wet season, 0.18–1.94 and 0.01–0.33, respectively. We focused on anions, as anions are more likely to be conservative since they tend to not adsorb into the soil (Goldscheider et al., 2008). Soil functions as a chemical reactor altering the chemistry of water as it passes through soil, e.g. picking up ions (e.g. Parsons et al., 2003). Constant ion ratios are indicative of single–sourced water (Nwankwoala & Udom, 2011); ion ratios from a single–water source would remain constant during evaporation and dilution processes. Anions ratios from C2P2 and C2P3 ranged from 0.05–1.94 μS/cm, which suggested multiple water input sources other than precipitation (Figures 45, 46). C2P2 and C2P3 also showed similar ion ratio behaviors with a lag in time, which suggested that C2P3 was receiving water input from C2P2 and/or C2P2 and C2P3 shared overlapping water inputs (Figures 45, 46). One possible explanation is that as this catchment wetted up, water was contributed from different parts of the landscape and may be indicative of soil–water processes, since the area surrounding my study site was of different soil series (Raynor, Hopeton, and Corning). These non–constant ion ratios further support hydrological connectivity of vernal pools, connectivity to the landscape, or both, through longitudinal and lateral water movements.

Isotopes from vernal pool surface water and perched groundwater samples got heavier as the wet season progressed but got lighter with precipitation events because lighter isotopes were introduced (Figure 32). This suggested that perched groundwater experienced evaporative and dilution processes, which also further supports hydrological connectivity of vernal pools and its connectivity to the landscape.

The vernal pool system showed that its water balance is not solely reliant on direct precipitation and evapotranspiration. Figures 47–49 showed the estimated water storage based on the vernal pool's water column and surface area and assuming 50% soil porosity; and compared it to the difference between daily precipitation and ET_o multiplied by canopy coefficients (McCarten et al., 2018b); this supported that perched groundwater was a significant contributor to vernal pool inundation, which was suggested by Rain et al. (2006) using stable isotopes demonstrating connectivity with the uplands. For example, C1P1 showed no water storage during March precipitation events, suggesting new precipitation all went into the perched groundwater. In April, a large precipitation event only gave C1P1 a small water level, again suggesting that the recharged precipitation all contributed to the perched groundwater (Figure 47). These incidents further support hydrological connectivity of vernal pools, specifically supporting perched groundwater flow because inundation occurred when ET_o exceeded precipitation and no inundation occurred when precipitation exceeded ET_o.

Vernal pool longitudinal flow of water is restricted due to its depth to the shallow subsurface confining layer– meaning water travels as far as it can longitudinally before it hits the shallow subsurface confining layer and then water is forced to travel laterally in response to the hydraulic gradient. The differences in hydraulic gradient in all four vernal pool pairs (C1P1–C1P2, C1P2–C1P3, C2P1–C2P2, and C2P2–C2P3) were positive, implying that the higher elevation pool was discharging into the lower elevation pool (Figure 27). The four vernal pool pairs had varying hydraulic gradients– this again demonstrates variable hydrological connectivity between my vernal pools. This heterogeneity between pools may be important for the ecological functioning of this system.

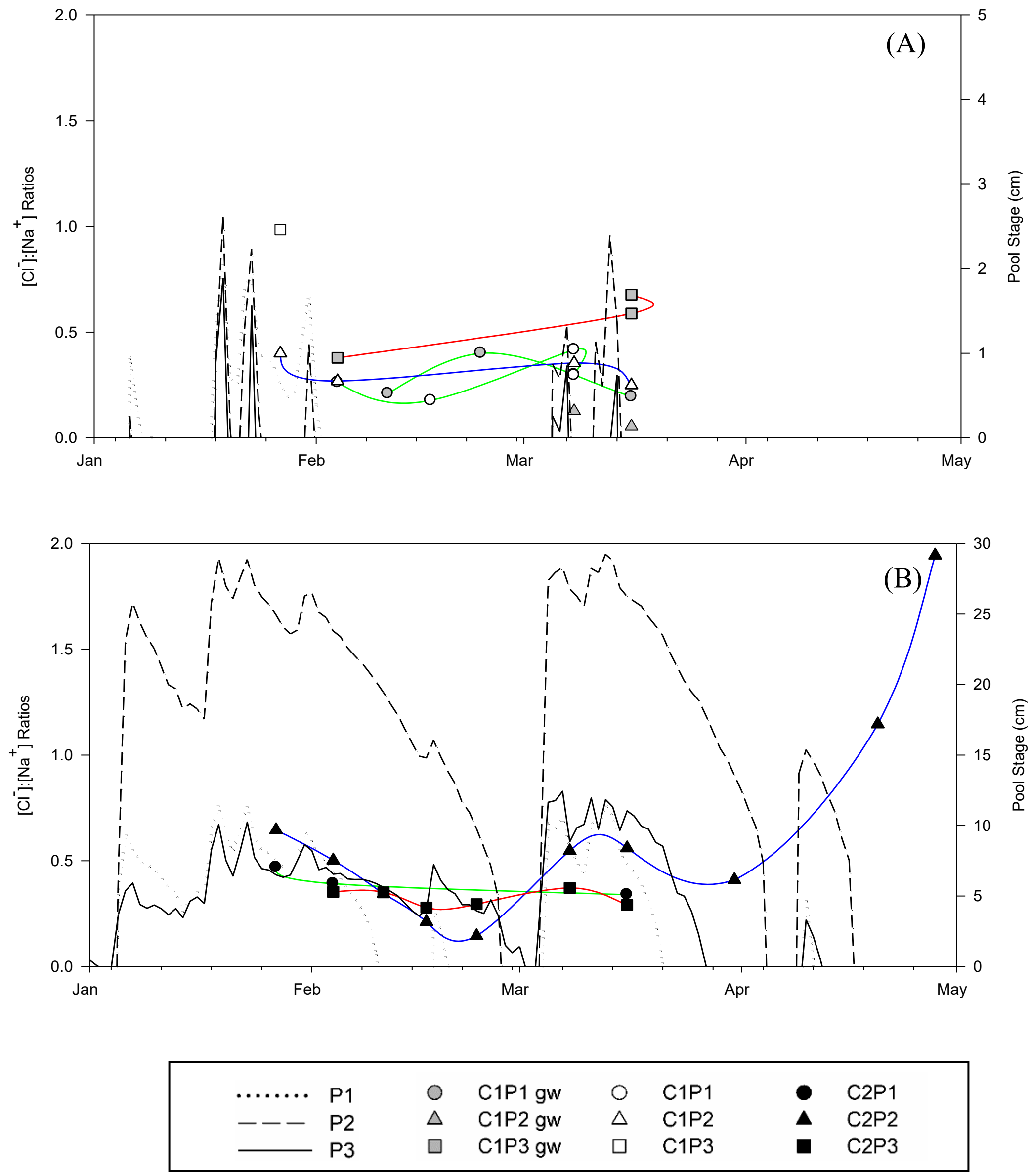

Figure 45 Pool stage and Cl^- and Na^+ concentration ratios of surface water and perched groundwater (gw) samples of upper (P1), middle (P2), and lower (P3) pools in (A) Catchment 1 (C1) and (B) Catchment 2 (C2). Colored lines connecting the vernal pools are added to serve as visual aids– showing changes in ion ratio. Pool stages were measured with pressure transducers that were placed in the field in summer 2015. Pressure transducers were corrected for barometric pressure changes.

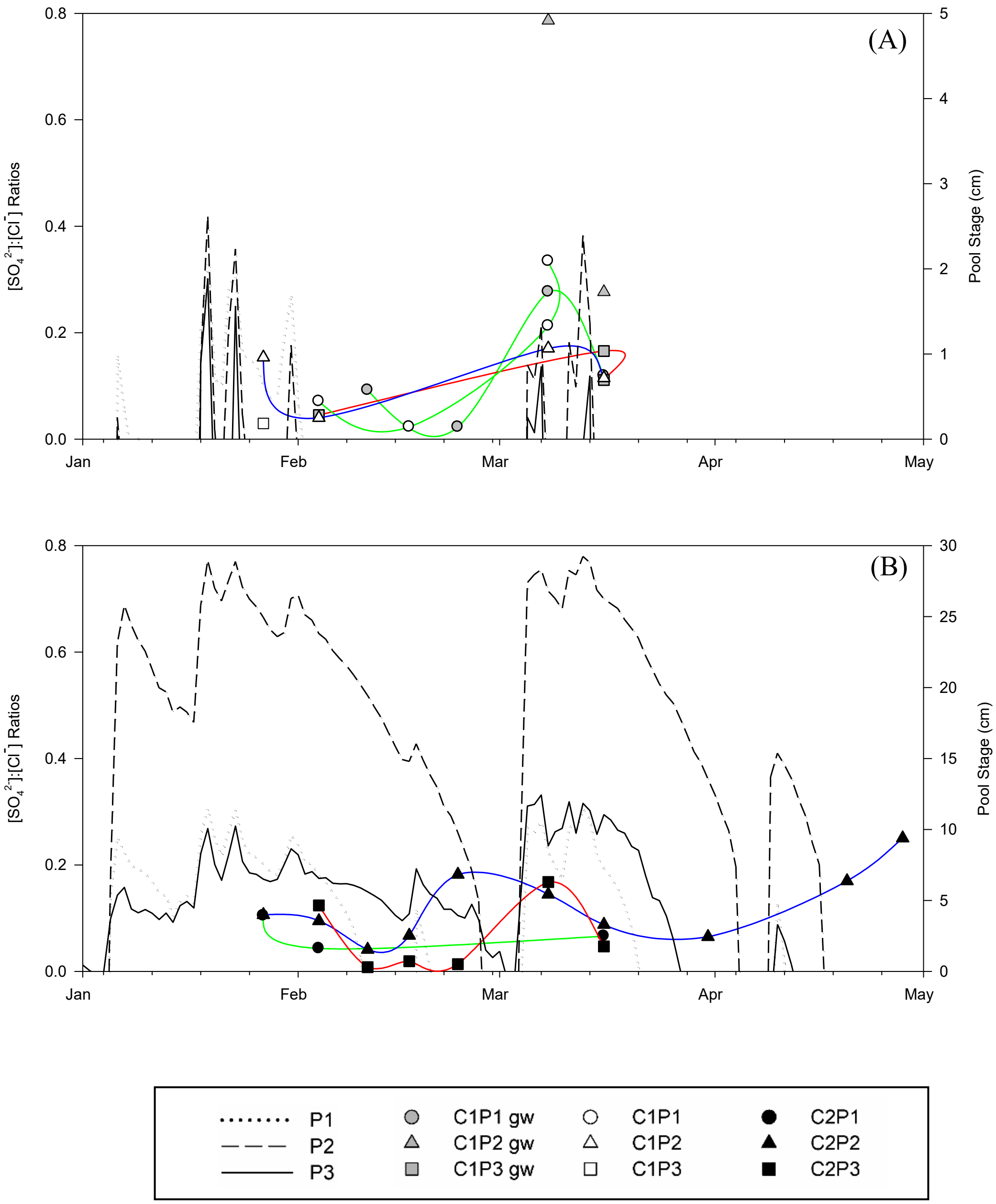

Figure 46 Pool stage and SO_4^{2-} and Cl^- concentration ratios of surface water and perched groundwater (gw) samples of upper (P1), middle (P2), and lower (P3) pools in (A) Catchment 1 (C1) and (B) Catchment 2 (C2). Colored lines connecting the vernal pools are added to serve as visual aids– showing changes in ion ratio. Pool stages were measured with pressure transducers that were placed in the field in summer 2015. Pressure transducers were corrected for barometric pressure changes.

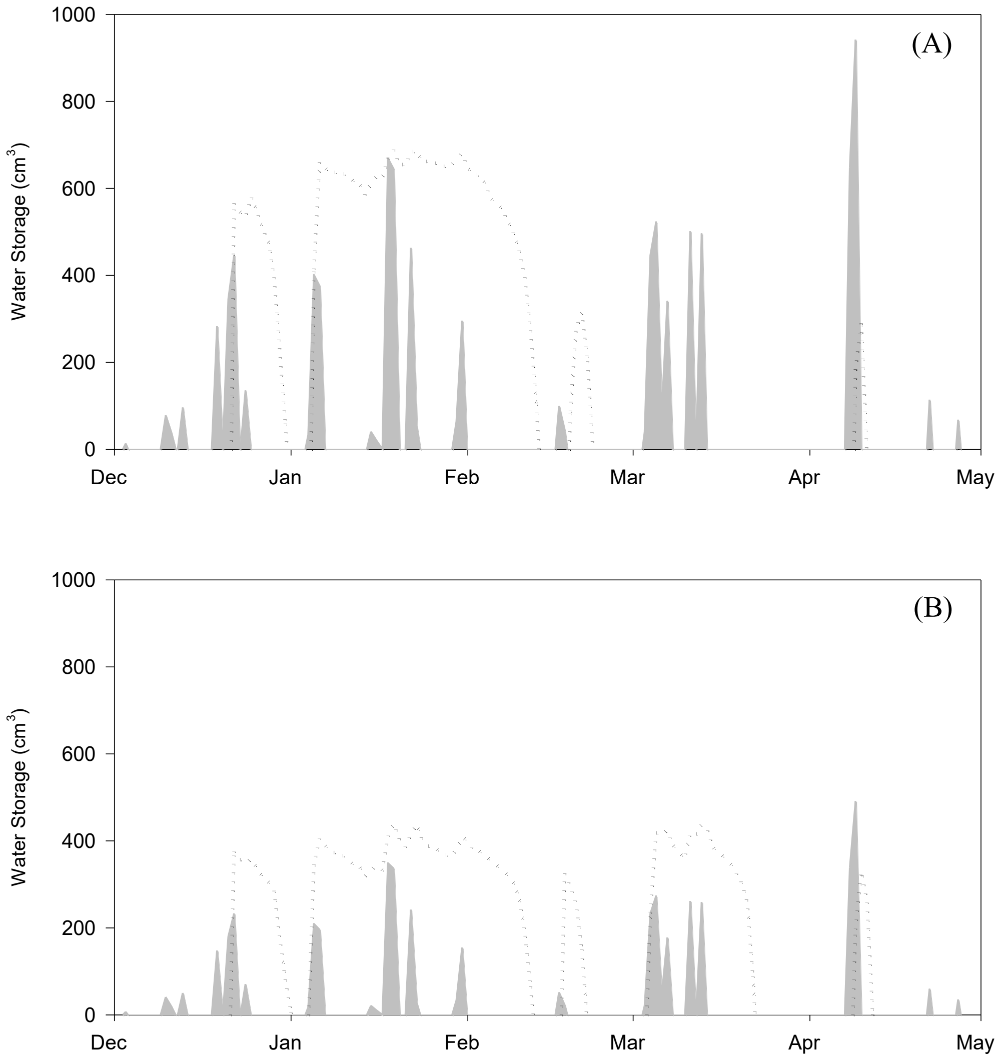

Figure 47 Estimation of water storage based on water column (dotted) and the difference between daily precipitation and ET_o multiplied by canopy coefficients (McCarten et al., 2018b) (see text for calculations) (shaded grey area) of upper pool in (A) Catchment 1 (C1) and (B) Catchment 2 (C2). Average daily precipitation and ET_o were obtained from CIMIS Station #148.

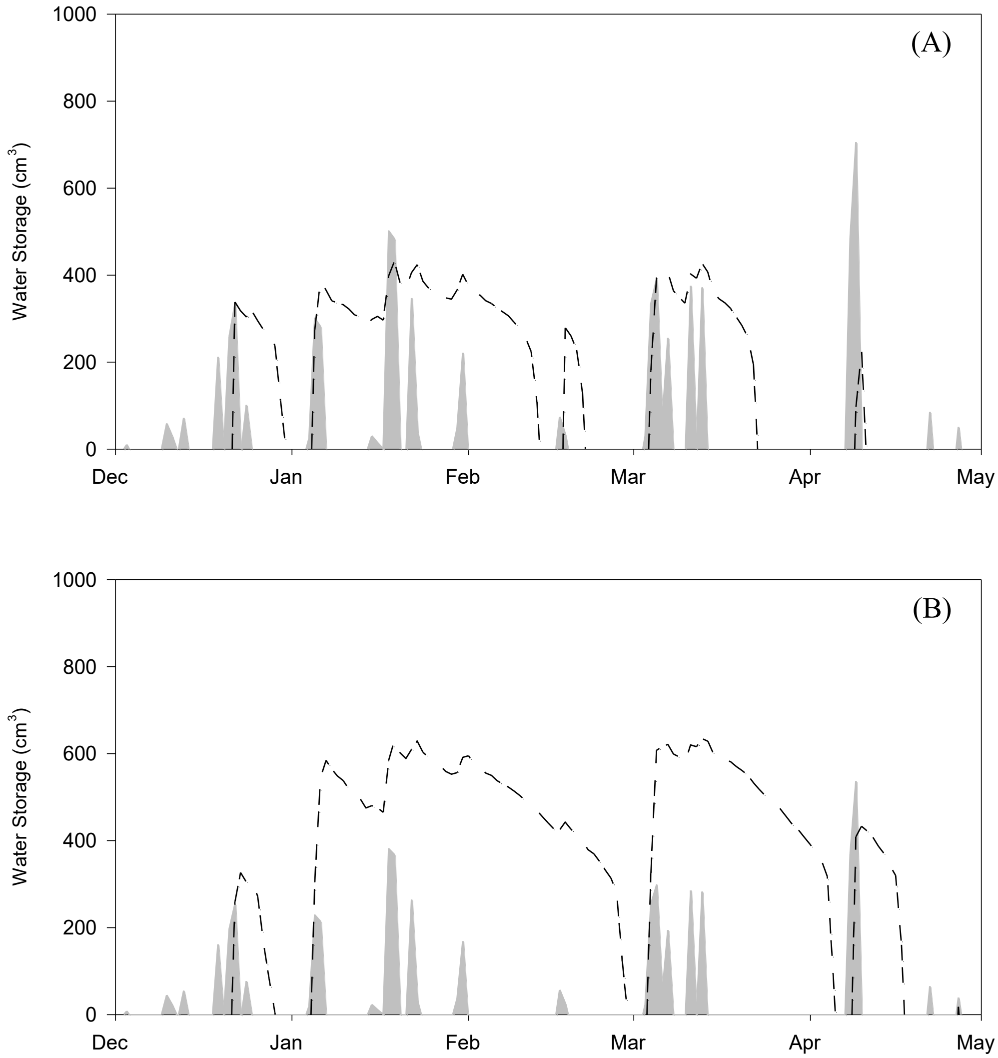

Figure 48 Estimation of water storage based on water column (dashed) and the difference between daily precipitation and ET_o multiplied by canopy coefficients (McCarten et al., 2018b) (see text for calculations) (shaded grey area) of middle pool in (A) Catchment 1 (C1) and (B) Catchment 2 (C2). Average daily precipitation and ET_o were obtained from CIMIS Station #148.

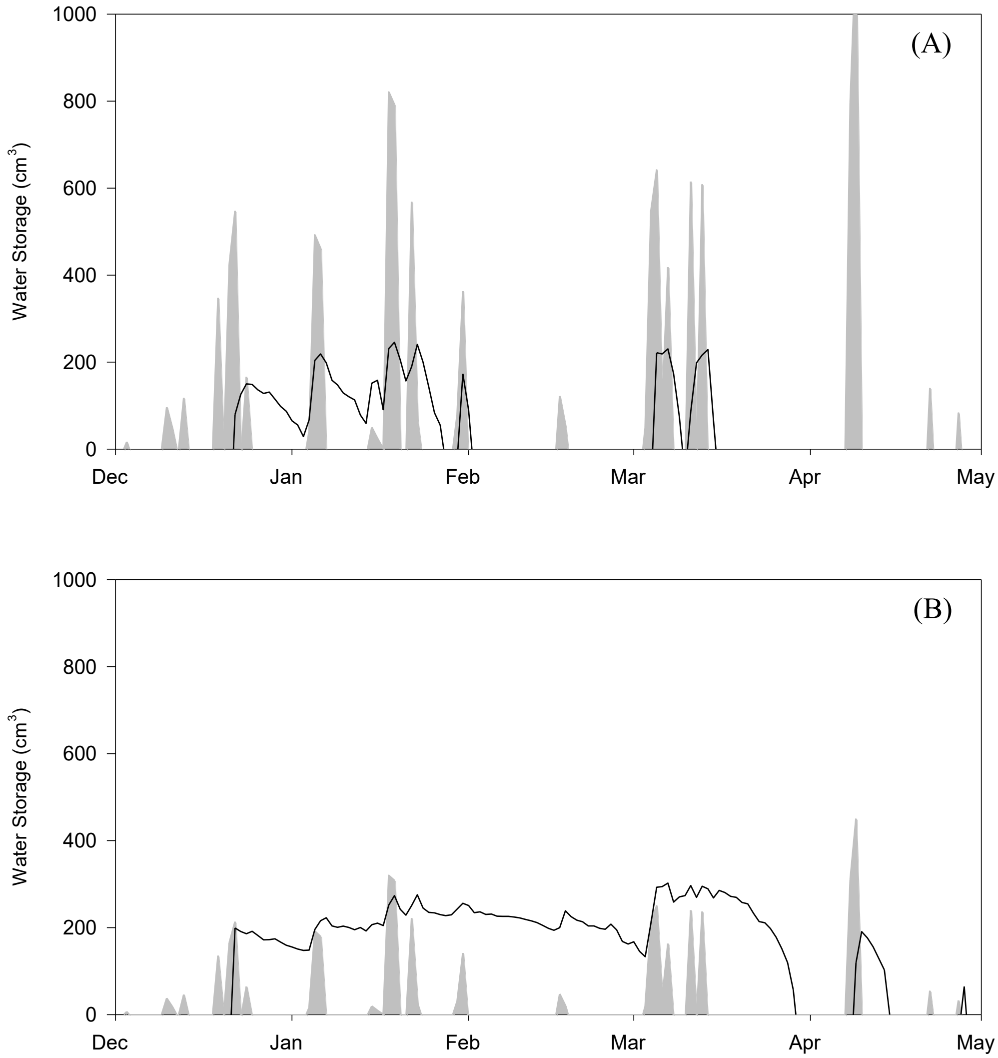

Figure 49 Estimation of water storage based on water column (solid) and the difference between daily precipitation and ET_o multiplied by canopy coefficients (McCarten et al., 2018b) (see text for calculations) (shaded grey area) of middle pool in (A) Catchment 1 (C1) and (B) Catchment 2 (C2). Average daily precipitation and ET_o were obtained from CIMIS Station #148.

4.1.3 Inundation

Inundation is important in vernal pool systems, because it gives a sense of the water input origin, which can further support hydrological connectivity amongst wetlands. Cabezas et al. (2011) characterized hydrological connectivity between surrounding water bodies with change in pool stage over time. The rapid changes in pool stages from vernal pools post–precipitation would indicate such connectivity. Except for C2P2 and its possible "dam effect," all vernal pools showed a relatively rapid decrease in pool stage post–precipitation (Figure 25). The amount of water loss in a short time frame could be from perched groundwater flowing downgradient which would further support that vernal pools are hydrologically connected, and that perched groundwater flow, as well as evapotranspiration, contribute to the drying out the pools. As seen in Figure 50, water column exceeded the precipitation and evapotranspiration difference even after assuming a 50% soil porosity, which points to significant surface and perched groundwater hydrological connectivity– higher elevation vernal pools recharging the groundwater and groundwater discharging into the lower vernal pools.

Gimbel et al. (2016) looked at the impacts of droughts on hydrological systems. They found that soil takes time to recover from hydrophobicity and infiltration patterns change after a prolonged dry period, e.g. clayey and loamy soils developed preferential flows. My study took place in WY 2016, the first normal year after four years of drought; therefore, the system was very dry to begin with. Sections of the same catchment can inundate and hydrologically connect at different times during the season, and this can vary water year to water year. Hydrological connectivity may not even occur in some water years, e.g. if total water input is less than total water output. Soil needs to be saturated for water to travel and for systems to hydrologically connect. Precipitation intensity, frequency, and duration play a crucial role in creating such an environment; and because WY 2016 was the first normal year after the drought, the hydrological connectivity patterns that were observed may have occurred for the very first time.

Vernal pool and plant dynamics are complex; with annual, varied inundation periods, different plant species could appear each water year. If inundation period is too long, marsh species take over and threaten vernal pool species; if inundation period is too short, vernal pool species are also stressed (Barry, 1998). More recently, Gosejohan et al. (2017) measured specific plant associations in northern California vernal pools being correlated with hydrological regimes. Though plant surveys were not conducted in this study, further research could be conducted to examine the relationship between inundation and plant species richness.

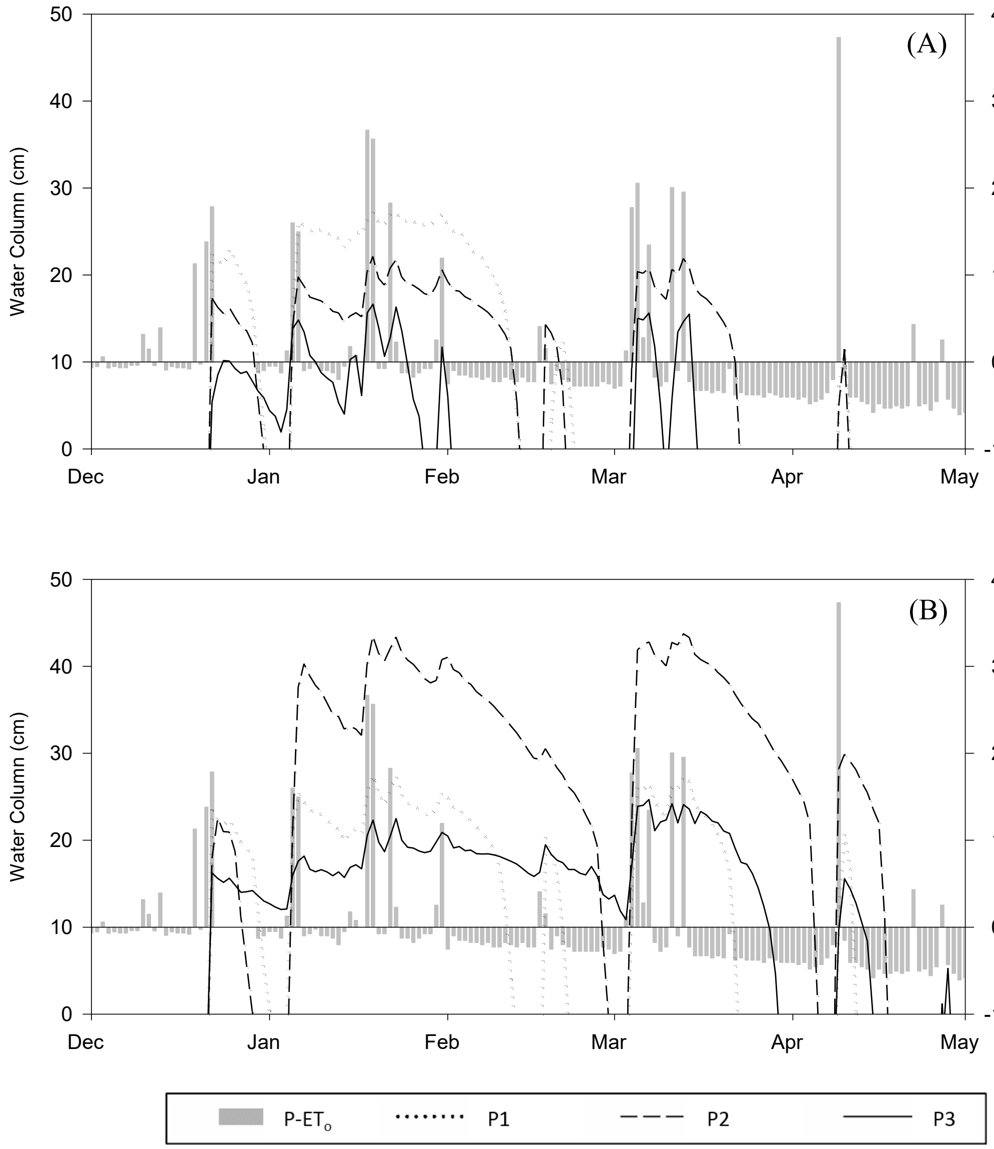

Figure 50 Daily water column and difference in precipitation (P) and reference evapotranspiration (ET_o) multiplied by canopy coefficients provided in McCarten et al. (2018b) of upper (P1), middle (P2), and lower (P3) pools in (A) Catchment 1 (C1) and (B) Catchment 2 (C2). Water column at 0 cm is the top of the shallow subsurface confining layer. Soil is assumed to have 50% porosity. Average daily precipitation and ET_o were obtained from CIMIS Station #148.

4.2 Hydrological Connectivity and Impacts on Water Quality and Ecological Effects

The shallow, subsurface confining layer topography is a contributing factor to vernal pool hydrology that has not been previously explored. Because its topography does not parallel the soil surface across the landscape, the shallow subsurface confining layer plays a significant role in determining where vernal pools form and sit on the landscape (e.g. GPR radargrams in Figures 16–23); there is no homogeneity to the shallow subsurface confining layer. Not only does the soil surface need to be a topographic low for a vernal pool to form, but the shallow subsurface confining layer needs to be at a depth where soil can successfully saturate in a timely manner, so the vernal pool can inundate.

The shallow subsurface confining layer can also suggest drainage patterns. For example, Catchment 1 vernal pools do not have a deep subsurface confining layer and the confining layer tightly parallel the soil surface, which could contribute to its short inundation period (Table 3). Another example of this is the shallow subsurface confining layer rising nearly to the soil surface on the downslope side in C2P2, which could have caused water to stay in the vernal pool longer, causing a "dam effect" (Figure 20). Like C2P2, C2P3 has a varied shallow subsurface confining layer topography (Figure 21)– this topography could have led to C2P3 having the second largest inundation period in Catchment 2 after C2P2. These examples support how the shallow subsurface confining layer plays an important role in hydrological connectivity because the subsurface confining layer topography can affect local water movement, and the depths to shallow subsurface confining layer can affect the timing of soil saturation; altogether affecting inundation periods of vernal pools. Ultimately water is coming from many directions, inferring vernal pools are connecting at different times, and not just to each other, but to the landscape as well.

Vernal pools are biologically diverse hotspots, containing species with unique physiological adaptations and life cycles adapted to a habitat defined by distinct wet and dry seasons (Gosejohan et al., 2017; Hanes & Stromberg 1998; Keeley & Zedler 1998; Solomeshch et al., 2007). The presence and lifespan of branchiopods and vernal pool plants are related to vernal pool depth, size, volume, and inundation period (Gosejohan et al., 2017; Helm, 1998). For example, Conservancy Fairy Shrimp have a longer period of maturity and reproduction (36.5 days average to mature, 46.2 days average to reproduce, and lifespan average of 113.9 days) and are associated with certain endemic vernal pool grasses, which are typically found in larger, deeper vernal pools with longer inundation periods; whereas Vernal Pool Fairy Shrimp have shorter maturation and reproduction periods (18 days average to mature, 39.7 days average to reproduce, and lifespan average of 90.6 days) making their presence common in many more vernal pools (Helm, 1998; Kneitel, 2014; Simovich, 1998). In managing vernal pool landscapes to sustain these branchiopods and vernal pool plants, the integrity of the landscapes' hydrology must be maintained.

In addition to biological functions, hydrological connectivity affects the biogeochemical functions of vernal pool systems (Ameli & Creed, 2017). McLaughlin and Cohen (2017) noted that biogeochemical processes affect water quality and local groundwater recharge. There was a cation imbalance in my vernal pool water samples, suggesting a high concentration of Ca^{2+}, a major cation in fresh waters (Brooks et al., 2012). There was also a high concentration of DOC in my water samples, which is a negatively charged molecule. Where there is an increase in DOC, the system draws more cations, typically Ca^{2+}, from soil and/or rock so that the water can be charge balanced, which could explain the direct relationship between Ca^{2+} and DOC observed in this study (Brooks et al., 2012) (Figure 42). Rains et al. (2008) observed high DOC concentrations in their clay–rich vernal pools as well and suggested it was from the soil eroding in the high sodium concentrated water. Hosen et al. (2018) observed high DOC concentrations and implied DOC is consistently contributed by groundwater flow paths and/or occasionally contributed by temporary surface connectivity. DOC may play an important role in sustaining local vernal pool inhabitants. Further investigation needs to be done in identifying DOC sources in this vernal pool system and its role in ion balance and ecological activities.

When restoring vernal pools, studies, like those done by Collinge et al. (2013) and Javornik and Collinge (2016), copied the reference vernal pool surface topography and claimed these restored vernal pools had similar hydrology to their reference vernal pools. These studies excluded the role of the shallow subsurface confining layer in their vernal pool hydrology. My study showed the importance of the shallow subsurface confining layer and its role in vernal pool hydrology, i.e. affecting the direction and rate of water movement, the time it takes for soil to saturate, and the inundation period. As noted by Collinge et al. (2013), it is very challenging to have a successful vernal pool restoration due to the complex relationships between hydrological features and organism and plant dynamics. If the inundation period is increased, marsh species take over and threaten vernal pool species; if the inundation period is decreased, this also stresses vernal pool species (Barry, 1998; Bauder, 1987). Subtle differences may exist in the plant species transitions in a hydrologically fluctuating environment due to the depth of the water–restricting soil horizons. These observations all point to the need to have a detailed understanding of vernal pool hydrology and the specific landscape in which restoration is proposed. A literature review by Calhoun et al. (2014) found many restored or constructed vernal pool failed to provide hydrological conditions for some target species. They concluded it was due to a lack of understanding of the topography, geology, and other factors that affect the hydrology and ecology. The application of methods used in my study, including GPS, GPR, and subsurface hydrology measurements could all be used to improved restoration engineering design. The U.S. Army Corps of Engineers recently released new Regional Compensatory Mitigation and Monitoring Guidelines (2015) that identified the need to use landscape level site assessments for wetland mitigation restoration and creation, as well as using information on soils and geology and a water budget to calculate potential hydrology. Further, for monitoring they require using water level dataloggers, such as the Solinst leveloggers used in my study, for monitoring all constructed vernal pools.

The importance and understanding of hydrology, specifically the shallow subsurface confining layer, and connectivity to the landscape is brought forth here. I hope my study will encourage future studies to better understand how the shallow subsurface confining layer relates to vernal pool hydrological connectivity, since we only studied a small subset of vernal pools; and contribute in a regulatory context to enhance existing mitigation requirements, to evaluate impacts to vernal pools, and in a non–regulatory context to support vernal pools restoration efforts.

Chapter 5 Conclusion

This study showed that vernal pools are hydrologically connected to each other and to the landscape. There are several factors to the hydrological connectivity of this vernal pool system– the shallow subsurface confining layer, perched groundwater and surface water flow, inundation, and the location of pools relative to each other in the landscape. The last factor, location, is important for the establishment of a hydraulic gradient between vernal pools, because it determines whether the vernal pools drain into one another. While the area of the uplands drained more water to the vernal pools at lower elevations, the upper elevation vernal pools were geophysically positioned within a drainage system, observed in the soil surface topography as well as in the location of the subsurface confining layer, to recharge to vernal pools at lower elevation. The shallow subsurface confining is a contributing variable that has not been addressed in previous studies; it does not necessarily parallel the soil surface, it plays a role in where a vernal pool forms in the landscape, and it determines when and how long a vernal pool inundates. In addition to precipitation– the main water source– perched groundwater and surface water flow are significant water sources in the water budget of this vernal pool system. Inundation is indicative of subsurface characteristics. In the relatively small sample of vernal pools studied (two three–pool series), there was significant hydrological differences between all vernal pools. Understanding the varying hydrology of this unique abiotic environment is vital for the success of vernal pools and vernal pool species, as they face habitat loss and experiences new selective pressures associated with climate change.

References

Ameli, A. A. and I. F. Creed. 2017. Quantifying hydrologic connectivity of wetlands to surface water systems. Hydrology and Earth System Sciences 21: 1791–1808.

Barry, S. J. 1998. Managing the Sacramento Valley vernal pool landscape to sustain native flora. p. 236–240. *In* C. W. Witham, E. T. Bauder, D. Belk, W. R. Ferren Jr., and R. Ornduff, (eds.) Ecology, Conservation, and Management of Vernal Pool Ecosystems. California Native Plant Society, Sacramento, CA, USA.

Bauder, E. T. 1987. Threats to San Diego vernal pools and a case study in altered pool hydrology. p. 209–213. *In* T.S. Elias (ed.) Conservation and Management of Rare and Endangered Plants. California Native Plant Society, Sacramento, CA, USA.

Bauder, E. T. 2005. The effects of an unpredictable precipitation regime on vernal pool hydrology. Freshwater Biology. 50: 2129–2135. doi:10.1111/j.1365–2427.2005.01471.

Black, C. and P. H. Zedler. 1998. An overview of 15 years of vernal pool restoration and construction activities in San Diego County, California. Ecology, conservation, and management of vernal pool ecosystems. p. 195–205. *In* C. W. Witham, E. T. Bauder, D. Belk, W. R. Ferren Jr., and R. Ornduff, (eds.) Ecology, Conservation, and Management of Vernal Pool Ecosystems. California Native Plant Society, Sacramento, CA, USA.

Brooks, K. N., P. F. Ffolliott, and J. A. Magner. 2012. Hydrology and the Management of Watersheds. Ames, Iowa: Wiley–Blackwell.

Brooks, T. T. 2004. Weather–related effects on woodland vernal pool hydrology and hydroperiod. Wetlands 24:104–114.

Brooks, T. T. 2005. A review of basin morphology and pool hydrology of isolated ponded wetlands: implications for seasonal forest pools on the northeastern United States. Wetlands Ecology and Management 13: 335–348.

Cabezas, A., M. Gonzalez–Sanchís, B. Gallardo, and F. Comín. 2011. Using continuous surface water level and temperature data to characterize hydrological connectivity in riparian wetlands. Environmental Monitoring and Assessment 183: 485. doi: 10.1007/s10661–011–1934–9.

Calhoun, A. J. K., J. Arrigoni, R. P. Brooks, M. L. Hunter, and S. C. Richter. 2014. Creating successful vernal pools: a literature review and advice for practitioners. Wetlands 34: 1027–1038.

Calhoun, A. J. K., D. M. Mushet, L. C. Alexander, E. S. DeKeyser, L. Fowler, C. R. Lane, M. W. Lang, M. C. Rains, S. C. Richter, and S. C. Walls. 2017. The significant surface–water connectivity of “geographically isolated wetlands.” Wetlands 37: 801–806.

California Department of Water Resources. 2016. Hydroclimate report water year 2016. California Department of Water Resources. Sacramento, CA, USA.

Chow, A. T., A. L. Pitt, R. F. Baldwin, D. Suhre, and J. Wang. 2016. Water quality dynamics of ephemeral wetlands in the Piedmont ecoregion, South Carolina, USA. Ecological Engineering 94: 555–563. doi:10.1016/j.ecoleng.2016.06.075.

CIMIS. 2010, California Irrigation Management Information System. Department of Water Resources. http://wwwcimis.water.ca.gov/cimis/welcome.jsp

Collinge, S. K., C. Ray, and J. T. Marty. 2013. A long–term comparison of hydrology and plant community composition in constructed versus naturally occurring vernal pools. Restoration Ecology 21: 704–712. doi: 10.1111/rec.12009.

Dahl, T. E. 1990. Wetlands losses in the United States 1780's to 1980s. U.S. Department of the Interior, Fish and Wildlife Service. Washington, D.C., USA.

Doerr, S. H. and A. D. Thomas. 2000. The role of soil moisture in controlling water repellency: new evidence from forest soils in Portugal. Journal of Hydrology 231–232: 134–47. doi:10.1016/S0022–1694(00)00190–6.

Dore, M. H. 2005. Climate change and changes in global precipitation patterns: what do we know? Environment International 31:1167–1181. doi:10.1016/j.envint.2005.03.004.

Drexler, J. Z., R. L. Snyder, D. Spano, and U. K. T. Paw. 2004. A review of models and micrometeorological methods used to estimate wetland evapotranspiration. Hydrological Processes 18: 2071–2101.

Epting, S. M., J. D. Hosen, L. C. Alexander, M. W. Lang, A. W. Armstrong, and M. A. Palmer. 2018. Landscape metrics as predictors of hydrologic connectivity between Coastal Plain forested wetlands and streams. Hydrological Processes, 32: 516–532.

Ferren, W. R., D. M. Hubbard, S. Wiseman, A. K. Parikh, and N. Gale. 1998. Review of ten years of vernal pool restoration and creation in Santa Barbara, California. Ecology, conservation, and management of vernal pool ecosystems. p. 206–216. *In* C. W. Witham, E. T. Bauder, D. Belk, W. R. Ferren Jr., and R. Ornduff, (eds.) Ecology, Conservation, and Management of Vernal Pool Ecosystems. California Native Plant Society, Sacramento, CA, USA.

Gimbel, K. F., H. Puhlmann, and M. Weiler. 2016. Does drought alter hydrological functions in forest soils? Hydrology and Earth System Sciences 20: 1301–1317.

Goldscheider, N., J. Meiman, M. Pronk, and C. Smart. 2008. Tracer tests in karst hydrogeology and speleology. International Journal of Speleology, 37: 27–40. doi:10.5038/1827–806X.37.1.3

Gosejohan, M. C., P. J. Weisberg, and K. E. Merriam. 2017. Hydrologic influences on plant community structure in vernal pools of northeastern California. Wetlands 37: 257–268. doi:10.1007/s13157–016–0863–3.

Griffin, D. and K. J. Anchukaitis. 2014. How unusual is the 2012–2014 California drought? Geophysical Research Letters 41: 9017–9023. doi:10.1002/2014GL062433.

Hanes, T. and L. Stromberg. 1998. Hydrology of vernal pools on non–volcanic soils in the Sacramento Valley. p. 38–49. *In* C. W. Witham, E. T. Bauder, D. Belk, W. R. Ferren Jr., and R. Ornduff, (eds.) Ecology, Conservation, and Management of Vernal Pool Ecosystems. California Native Plant Society, Sacramento, CA, USA.

Helm, B. P. 1998. Biogeography of eight large brachiopods endemic to California. p.124–139. *In* C. W. Witham, E. T. Bauder, D. Belk, W. R. Ferren Jr., and R. Ornduff, (eds.) Ecology, Conservation, and Management of Vernal Pool Ecosystems. California Native Plant Society, Sacramento, CA, USA.

Hobson, W. A. and R. A. Dahlgren. 1998. Soil forming processes in vernal pools of northern California, Chico area. p. 24–37. *In* C. W. Witham, E. T. Bauder, D. Belk, W. R. Ferren, Jr., and R. Ornduf (eds.) Ecology, Conservation, and Management of Vernal Pool Ecosystems. California Native Plant Society, Sacramento, CA, USA.

Holland, R. F. 1998. Great Valley vernal pool distribution, photo revised 1996. p. 71–75. *In* C.W. Witham, E. T. Bauder, D. Belk, W. R. Ferren, Jr., and R. Ornduf (eds.) Ecology, Conservation, and Management of Vernal Pool Ecosystems. California Native Plant Society, Sacramento, CA, USA.

Holland R. F. and S. K. Jain. 1977. Vernal Pools. p. 515–533. *In* M.G. Barbour, J. Major (eds.) Terrestrial vegetation of California. Wiley Interscience, New York, New York, USA.

Hosen, J. D., A.W. Armstrong, and M. A. Palmer. 2018. Dissolved organic matter variations in coastal plain wetland watersheds: The integrated role of hydrological connectivity, land use, and seasonality. Hydrological Processes 32: 1664–1681.

Javornik, C. J. and S. K. Collinge. 2016. Influences of annual weather variability on vernal pool plant abundance and community composition. Aquatic Botany 134: 61–67.

Jokerst, J. D. 1990. Floristic analysis of volcanic mudflow vernal pools. p. 1–29. *In* Ikeda D. H. and Schlising R. A. (eds.) Vernal Pool Plants– Their Habitat and Biology. Studies from the Herbarium No. 8. California State University, Chico.

Keeley, J. E. and P. H. Zedler. 1998. Characterization and global distribution of vernal pools. p. 1–14. *In* C. W. Witham, E. T. Bauder, D. Belk, W. R. Ferren, Jr., and R. Ornduf (eds.) Ecology, Conservation, and Management of Vernal Pool Ecosystems. California Native Plant Society, Sacramento, CA, USA.

Kneitel, J. M. 2014. Inundation timing, more than duration, affects the community structure of Californian vernal pool mesocosms. Hydrobiologia 732: 71–83. doi:10.1007/s10750–014–1845–1.

Leibowitz, S. G. and K. C. Vining. 2003. Temporal connectivity in a prairie pothole complex. Wetlands 23:13–25.

Leibowitz, S. G. and R. T. Brooks. 2008. Hydrology and landscape connectivity of vernal pools. p. 31–53. *In* A. J. K. Calhoun and P. G. deMaynadier (eds.), Science and Conservation of Vernal Pools in Northeastern North America, Boca Raton, FL, USA.

McCarten, N. F. and R. Dahlgren. 2018a. Manuscript in review. Efficacy of ground–penetrating radar for mapping subsurface stratigraphy in vernal pool wetlands. Soil Science Society of America Journal.

McCarten, N. F., T. H. Harter, G. Fogg, and R. Dahlgren. 2018b. Manuscript in review. Water balance of a vernal pool wetland catchment. Hydrological Processes.

McCarten, N. F., T.H. Harter, A. O'Geen, G. Fogg, and R. Dahlgren. 2018c. Manuscript in preparation. Geophysical structure and meteorological effects on the hydrological functioning of vernal pool wetlands. Wetlands.

McDonough, O. T., M. W. Lang, J. D. Hosen, and M. A. Palmer. 2015. Surface hydrologic connectivity between Delmarva Bay wetlands and nearby streams along a gradient of agricultural alteration. Wetlands, 35: 41–53.

McLaughlin, D. L. and M. J. Cohen. 2013. Realizing ecosystem services: wetland hydrologic function along a gradient of ecosystem condition. Ecological Applications 23: 1619–1631.

Mushet, D. M., A. J. K. Calhoun, L. C. Alexander, M. J. Cohen, E. S. DeKeyser, L. Fowler, C. R. Lane, M. W. Lang, M. C. Rains, and S. C. Walls. 2015. Geographically isolated wetlands: rethinking a misnomer. Wetlands 35: 423–431.

Nikiforoff, C. C. 1941. Hardpan and microrelief in certain soil complexes of California. U.S. Department of Agriculture. Washington, D.C., USA.

Nwankwoala H. O. and G. J. Udom. 2011. Investigation of hydrogeochemical characteristics of groundwater in Port Harcourt City, Nigeria: Implications for use and vulnerability. Journal of Applied Science and Environmental Management 15: 479–488.

Parsons, A. 2003. Draft Burned Area Emergency Rehabilitation (BAER) soil burn severity definitions and mapping guidelines. USDA–Forest Service, Remote Sensing Application Center. Salt Lake City, UT, USA.

Pyke, C. 2004. Simulating vernal pool hydrologic regimes for two locations in California, USA. Ecological Modeling 173: 109–127.

Rains, M. C., G. E. Fogg, T. Harter, R. A. Dahlgren, and R. J. Williamson. 2006. The role of perched aquifers in hydrological connectivity and biogeochemical processes in vernal pool landscapes, Central Valley, California. Hydrological Processes 20: 1157–1175.

Rains, M. C., R. A. Dahlgren, G. E. Fogg, T. Harter, and R. J. Williamson. 2008. Geological control of physical and chemical hydrology in California vernal pools. Wetlands 28: 347–362. doi:10.1672/07–132.1.

Schlatter, K.J., A.M. Faist, and S.K. Collinge. 2016. Using performance standards to guide vernal pool restoration and adaptive management. Restoration Ecology 24:145–152.

Smith, D. W. and W. L. Verrill. 1998. Vernal Pool–Soil–Landform Relationships in the Central Valley, California. p. 15–22. *In* C. W. Witham, E. T. Bauder, D. Belk, W. R. Ferren, Jr., and R. Ornduf (eds.) Ecology, Conservation, and Management of Vernal Pool Ecosystems. California Native Plant Society, Sacramento, CA, USA.

Solomeshch, A., M. G. Barbour, and R. F. Holland. 2007. Vernal pools. p. 398–428. *In* M.G. Barbour et al. (eds.) Terrestrial vegetation of California, third edition. University of California Press, Berkeley, CA, USA.

Sapek, B. 2013. Relationship between dissolved organic carbon and calcium and magnesium in soil water phase and their uptake by meadow vegetation. Journal of Water and Land Development 19: 69–76. doi: 10.2478/jwld–2013–0018.

Trenberth, K. E. 2010. Changes in precipitation with climate change. Climate Research 47: 123–138. doi:10.3354/cr00953.

U.S. Army Corps of Engineers. Regional Compensatory Mitigation and Monitoring Guidelines. South Pacific Division. 2004. http://www.spd.usace.army.mil/Portals/13/docs/regulatory/mitigation/MitMon.pdf.

Walther, G., E. Post, P. Convey, A. Menzel, C. Parmesan, T. J. C. Beebee, J. Fromentin, O. Hoegh–Guldberg, and F. Bairlein. 2015. Ecological responses to recent climate change. Nature 416: 389–395. doi:10.1038/416389a.

Weitkamp, W. A., R. C. Graham, M. A. Anderson and C. Amrhein. 1996. Pedogenesis of a vernal pool Entisol–Alfisol–Vertisol catena in southern California. Soil Science Society of America Journal 60: 316–323.

Williams, A. P., R. Seager, J. T. Abatzoglou, B. I. Cook, J. E. Smerdon, and E. R. Cook. 2015. Contribution of anthropogenic warming to California drought during 2012–2014. Geophysical Research Letters 42: 6819–6828. doi:10.1002/2015GL064924.

Winter, T. C. and J. W. LaBaugh. 2003. Hydrologic considerations in defining isolated wetlands. Wetlands 23: 532.

Zedler, P. H. 2013. Vernal pools and the concept of “isolated wetlands”. Wetlands 23: 597.

Appendix

Table 6 CIMIS station #148 precipitation and ET_o data.

Date	ETo (mm)	Precipitation (mm)
11/10/2015	1.2	0.9
11/11/2015	1.48	0.1
11/12/2015	1.48	0.2
11/13/2015	1.78	0
11/14/2015	1.86	0.1
11/15/2015	0.69	4.5
11/16/2015	2.74	0
11/17/2015	1.48	0
11/18/2015	1.62	0
11/19/2015	1.71	0
11/20/2015	1.47	0.1
11/21/2015	1.72	0.1
11/22/2015	1.77	0.1
11/23/2015	1.68	0
11/24/2015	1.16	5.8
11/25/2015	1.04	0.6
11/26/2015	1.37	0.2
11/27/2015	1.2	0
11/28/2015	1.39	0.2
11/29/2015	1.37	0.1
11/30/2015	1.12	0.1
12/1/2015	1.36	0.1
12/2/2015	1.09	0.1
12/3/2015	1.23	1.2
12/4/2015	1.73	0.2
12/5/2015	0.98	0.1
12/6/2015	1.29	0
12/7/2015	1.25	0
12/8/2015	0.88	0
12/9/2015	0.66	0
12/10/2015	0.15	3.2
12/11/2015	1.08	2.1
12/12/2015	1.27	0.2
12/13/2015	0.32	4
12/14/2015	1.68	0.1
12/15/2015	1.1	0.1
12/16/2015	1.23	0.1

12/17/2015	1.22	0.1
12/18/2015	1.41	0.1
12/19/2015	0.23	11.4
12/20/2015	0.58	0.1
12/21/2015	0.26	13.9
12/22/2015	0.79	18.2
12/23/2015	1.35	0
12/24/2015	0.2	5.5
12/25/2015	1.04	0.1
12/26/2015	1.11	0
12/27/2015	0.76	0.2
12/28/2015	0.39	0
12/29/2015	1.08	0
12/30/2015	1.19	0.1
12/31/2015	1.14	0
1/1/2016	0.84	0.2
1/2/2016	0.56	0
1/3/2016	1.15	0
1/4/2016	0.27	1.6
1/5/2016	0.49	16.5
1/6/2016	0.33	15.3
1/7/2016	1.11	0
1/8/2016	0.9	0.2
1/9/2016	0.95	0.7
1/10/2016	0.99	0.1
1/11/2016	1.06	0.1
1/12/2016	1.32	0.1
1/13/2016	1.94	0.1
1/14/2016	0.79	0.2
1/15/2016	1.13	2.8
1/16/2016	1.16	2
1/17/2016	0.65	0.7
1/18/2016	1.48	28.2
1/19/2016	0.3	26
1/20/2016	0.65	0.1
1/21/2016	1.14	0.2
1/22/2016	0.43	18.9
1/23/2016	1.06	3.3
1/24/2016	1.29	0.1
1/25/2016	1.21	0.1
1/26/2016	1.74	0
1/27/2016	1.16	0.1

1/28/2016	1.07	0.2
1/29/2016	0.77	0
1/30/2016	1.18	3.8
1/31/2016	0.87	12.7
2/1/2016	2.62	0
2/2/2016	0.96	0.1
2/3/2016	1.55	0.1
2/4/2016	1.56	0.1
2/5/2016	1.83	0
2/6/2016	1.85	0.1
2/7/2016	1.97	0
2/8/2016	2.1	0.2
2/9/2016	2.19	0.1
2/10/2016	2.23	0.1
2/11/2016	2.01	0.2
2/12/2016	2.15	0.1
2/13/2016	2.32	0.1
2/14/2016	1.95	0.2
2/15/2016	2.32	0.1
2/16/2016	2.4	0.1
2/17/2016	1.61	5.5
2/18/2016	2.3	3.9
2/19/2016	2.43	0
2/20/2016	1.26	0.2
2/21/2016	2.17	0.2
2/22/2016	2.63	0.2
2/23/2016	2.74	0.1
2/24/2016	2.82	0.1
2/25/2016	2.8	0.1
2/26/2016	2.74	0.1
2/27/2016	2.78	0
2/28/2016	2.21	0.1
2/29/2016	2.84	0.2
3/1/2016	3.08	0
3/2/2016	2.69	0.1
3/3/2016	2.73	4.1
3/4/2016	1.57	19.2
3/5/2016	0.95	21.7
3/6/2016	2.2	5.2
3/7/2016	0.89	14.4
3/8/2016	1.88	0.1
3/9/2016	2.71	0

3/10/2016	2.34	0
3/11/2016	0.25	20.2
3/12/2016	2.73	1.8
3/13/2016	0.15	19.9
3/14/2016	3.1	0.8
3/15/2016	3.36	0.1
3/16/2016	3.33	0
3/17/2016	3.57	0.2
3/18/2016	3.54	0.1
3/19/2016	3.29	0.1
3/20/2016	3.58	0.1
3/21/2016	1.67	0.9
3/22/2016	3.83	0
3/23/2016	3.48	0
3/24/2016	3.73	0
3/25/2016	3.92	0
3/26/2016	3.9	0
3/27/2016	4.06	0
3/28/2016	3.66	0
3/29/2016	3.78	0
3/30/2016	3.98	0
3/31/2016	4.05	0
4/1/2016	4.08	0
4/2/2016	4.21	0
4/3/2016	4.08	0.1
4/4/2016	4.89	0
4/5/2016	4.54	0
4/6/2016	4.35	0
4/7/2016	3.58	0
4/8/2016	2.76	28.3
4/9/2016	0.77	38.2
4/10/2016	2.61	1
4/11/2016	4.09	0
4/12/2016	4.11	0
4/13/2016	4.52	0
4/14/2016	4.75	0
4/15/2016	5.92	0
4/16/2016	4.7	0
4/17/2016	5.28	0
4/18/2016	5.26	0.1
4/19/2016	5.01	0
4/20/2016	5.43	0

4/21/2016	5.2	0
4/22/2016	2.3	6.6
4/23/2016	4.98	0
4/24/2016	4.9	0
4/25/2016	5.56	0
4/26/2016	4.6	0
4/27/2016	3.13	5.5
4/28/2016	4.28	0.1
4/29/2016	5.22	0
4/30/2016	5.98	0
5/1/2016	5.95	0
5/2/2016	5.8	0
5/3/2016	4.15	0
5/4/2016	4.03	0
5/5/2016	2.76	0
5/6/2016	1.69	1
5/7/2016	2.35	0.5
5/8/2016	5.01	0.1
5/9/2016	5.46	0
5/10/2016	5.99	0
5/11/2016	6.27	0
5/12/2016	6.43	0
5/13/2016	6.54	0
5/14/2016	6.14	0
5/15/2016	6.3	0
5/16/2016	6.87	0
5/17/2016	6.58	0
5/18/2016	6.63	0
5/19/2016	6.36	0
5/20/2016	5.27	0
5/21/2016	5.12	0

Table 7 Stable isotopes, specific conductivity, and pH.

Source	Vernal Pool	Collection Date	∂D	∂O18	Specific Conductivity (µS/cm)	pH
s	c1p2	1/27/16	–43.997257	–5.191191	202.6	7.17
s	c1p3	1/27/16	–48.996393	–5.835952	365.4	7.36
s	c2p1	1/27/16	–47.638294	–5.914459	202.2	7.39
s	c2p2	1/27/16	–55.032639	–6.808991	180.4	7.46
s	c1p1	2/4/16	–40.846399	–5.087339	303.0	7.28
s	c1p2	2/4/16	–45.617808	–5.925358	186.3	7.11
gw	c1p3	2/4/16	–42.008955	–4.973053	322.6	7.04
s	c2p1	2/4/16	–46.439218	–4.649135	239.6	7.34
s	c2p2	2/4/16	–48.756039	–5.880114	176.6	7.31
s	c2p3	2/4/16	–42.678762	–4.989309	252.5	7.33
gw	c1p1	2/11/16	–38.653243	–4.487968	378.6	7.02
s	c2p2	2/11/16	–45.119864	–4.598013	160.1	7.65
s	c2p3	2/11/16	–34.728003	–3.655625	377.2	7.35
s	c2p2	2/17/16	–36.095922	–2.922452	166.0	7.31
s	c2p3	2/17/16	–27.634979	–2.238654	347.7	7.34
gw	c1p1	2/24/16	–29.437752	–3.425661	329.0	7.00
s	c2p2	2/24/16	–24.823227	–1.550733	165.7	7.46
s	c2p3	2/24/16	–24.61815	–2.258868	420.1	7.14
gw	c1p1	2/24/16	–50.920078	–6.74712	149.3	6.83
gw	c1p2	3/8/16	–49.979329	–6.961089	108.0	8.00
s	c2p3	3/8/16	–47.473918	–6.584096	138.7	7.07
gw	c1p1	3/16/16	–38.097888	–5.256979	249.9	6.85
s	c1p2	3/16/16	–26.901665	–3.592353	173.6	7.06
gw	c1p2	3/16/16	–32.688849	–4.729699	194.6	6.99
s	c2p1	3/16/16	–32.781322	–4.149923	186.9	7.21
s	c2p2	3/16/16	–34.652655	–4.493416	153.9	7.21
s	c2p3	3/16/16	–34.237036	–4.446635	198.6	7.74
s	c2p2	3/31/16	–11.024317	1.092132	219.5	7.10
s	c2p2	4/14/16	–50.895366	–5.105032	215.6	7.12
s	c2p2	4/28/16	–48.485093	–6.530549	284.1	6.91
s	c1p1	3/8/16	–46.633701	–6.188789	137.8	7.30
s	c1p2	3/8/16	–46.949088	–6.491132	130.0	7.05
s	c1p2	3/8/16	–53.561203	–7.528974	124.0	7.55
s	c1p1	3/8/16	–48.327303	–7.081895	148.6	7.06

Table 8 Ions and DOC.

Source	Vernal Pool	Date	Na^+ (mg/L)	NH_4^+ (mg/L)	K^+ (mg/L)	Mg^+ (mg/L)	Ca^{2+} (mg/L)	Cl^- (mg/L)	SO_4^{2-} (mg/L)	Br^- (mg/L)	NO_3^- (mg/L)	DOC (mg/L)
GW	C1P1	3/16/16	7.86	1.57	2.84	9.37	18.55	2.36	0.76	0.10		57.86
GW	C1P3	3/16/16	14.41	0.83	2.59	7.20	12.59	130.59	58.58	0.92	0.21	38.37
S	C2P2	3/16/16	2.17	0.06	5.73	4.63	13.33	561.74	133.56	13.84	29.60	39.93
S	C2P1	3/16/16	2.90	0.16	6.16	6.08	15.66	1.52	0.27	0.08	1.35	46.25
GW	C1P2	3/16/16	9.25	0.94	1.30	9.48	16.95	0.77	0.58	0.06		53.22
S	C1P1	3/8/16	2.24	0.07	6.37	3.81	11.04	1.44	0.83	0.08		39.34
GW	C1P3	3/16/16	15.95	0.84	3.19	4.75	12.09	16.65	5.01	0.28	0.04	
S	C1P1	2/17/16	14.52	1.55	2.48	12.03	35.45	3.95	0.24	0.08	0.13	
S	C2P3	3/16/16	2.90	0.11	4.92	4.72	18.42	1.30	0.16	0.06		44.53
S	C1P2	3/16/16	3.46	0.14	5.59	4.36	14.07	1.33	0.41	0.06		56.13
S	C1P1	3/8/16	3.57	0.09	5.45	3.23	11.00	1.62	1.47	0.06	0.01	44.66
GW	C1P1	3/8/16	8.09	1.18	2.12	4.13	11.88	3.72	2.79	0.03	0.06	46.1
S	C2P3	3/8/16	2.80	0.12	5.21	2.39	9.55	1.60	0.73	0.09	0.03	37.29
S	C2P2	2/4/16	3.30	0.23	6.12	2.58	13.41	2.55	0.66	0.13	0.28	45.22
GW	C1P3	2/4/16	20.82	1.88	3.10	5.62	22.51	12.14	1.48	0.04	0.06	63.46
S	C2P2	1/27/16	3.63	0.50	7.84	2.55	13.51	3.61	1.04	0.02		41.78
S	C2P3	2/24/16	8.19	0.34	7.33	6.45	34.69	3.72	0.14	0.15	0.11	89.24
GW	C1P2	3/8/16	8.20	0.67	0.84	2.50	8.14	1.60	3.41	0.32	0.06	34
GW	C1P1	2/24/16	11.56	1.71	2.70	6.28	28.13	7.13	0.43	0.12	0.07	90.68
S	C2P1	2/4/16	4.31	0.25	5.52	3.72	18.93	2.60	0.30	0.21	0.15	56.98
S	C2P1	1/27/16	3.25		6.18	3.01	16.81	2.35	0.67	0.06		48.29
S	C2P2	2/11/16	3.11	0.23	5.10	2.41	12.86	1.65	0.18		0.03	43.9
S	C2P2	3/8/16	2.53	0.13	6.17	1.72	9.66	2.13	0.83	0.11	0.03	35.1
S	C2P2	2/24/16	3.45		4.80	2.33	13.24	0.77	0.38	0.05	0.02	44.13
S	C2P3	2/11/16	8.09		7.04	4.64	35.59	4.37	0.09	0.09		84.59
S	C1P2	2/4/16	4.56	0.18	5.17	2.23	13.56	1.89	0.21			55.24
S	C1P1	2/4/16	7.80	0.46	5.10	3.56	22.00	3.14	0.60	0.22	0.27	76.16
S	C1P3	1/27/16	10.68		30.63	2.75	21.35	16.21	1.29	0.63	0.02	79.44
GW	C1P1	2/11/16	14.86	1.45	2.36	5.19	32.84	4.78	1.19	0.05	0.24	82.85
S	C1P2	3/8/16	2.95	0.20	4.51	1.54	9.35	1.61	0.74	0.14	0.06	41.46
S	C2P3	2/17/16	7.39		7.39	3.54	29.48	3.17	0.16	0.03	0.21	72.68
S	C2P3	2/4/16	5.69	0.30	4.88	2.52	21.44	3.09	1.04	0.08	0.06	59.62
S	C1P2	1/27/16	4.95		6.47	2.05	15.50	3.05	1.27	0.11		70.56
S	C2P2	2/17/16	3.18		4.82	1.52	12.61	1.04	0.19		0.04	44.98
S	C2P2	3/31/16	2.93	0.56	8.71	8.68	17.30	1.85	0.33			59.01
S	C2P2	4/28/16	6.84	0.74	28.42	8.16	12.89	20.49	13.91			72.02
S	C2P2	4/20/16	5.89	0.17	23.88	9.79	16.38	10.40	4.79			70.97

Table 9 Charge balance.

Source	Vernal Pool	Date	Na^+	NH_4^+	K^+	Mg^+	Ca^{2+}	Cl^-	SO_4^{2-}	Br^-	NO_3^-	Δ Charge Balance (m eq/L)
S	C1P1	2/4/2016	0.34	0.03	0.13	0.29	1.10	–0.09	–0.01	0.00	0.00	1.78
S	C1P1	2/17/2016	0.63	0.09	0.06	0.99	1.77	–0.11	–0.01	0.00	0.00	3.42
S	C1P1	3/8/2016	0.10	0.00	0.16	0.31	0.55	–0.04	–0.02	0.00	0.00	1.07
G	C1P1	3/8/2016	0.16	0.00	0.14	0.27	0.55	–0.05	–0.03	0.00	0.00	1.04
G	C1P1	2/11/2016	0.65	0.08	0.06	0.43	1.64	–0.13	–0.02	0.00	0.00	2.69
G	C1P1	2/24/2016	0.50	0.09	0.07	0.52	1.40	–0.20	–0.01	0.00	0.00	2.37
G	C1P1	3/8/2016	0.35	0.07	0.05	0.34	0.59	–0.11	–0.06	0.00	0.00	1.24
G	C1P1	3/16/2016	0.34	0.09	0.07	0.77	0.93	–0.07	–0.02	0.00	0.00	2.12
S	C1P2	1/27/2016	0.22	0.00	0.17	0.17	0.77	–0.09	–0.03	0.00	0.00	1.21
S	C1P2	2/4/2016	0.20	0.01	0.13	0.18	0.68	–0.05	0.00	0.00	0.00	1.14
S	C1P2	3/8/2016	0.13	0.01	0.12	0.13	0.47	–0.05	–0.02	0.00	0.00	0.78
S	C1P2	3/16/2016	0.15	0.01	0.14	0.36	0.70	–0.04	–0.01	0.00	0.00	1.32
G	C1P2	3/8/2016	0.36	0.04	0.02	0.21	0.41	–0.05	–0.07	0.00	0.00	0.91
G	C1P2	3/16/2016	0.40	0.05	0.03	0.78	0.85	–0.02	–0.01	0.00	0.00	2.08
S	C1P3	1/27/2016	0.46	0.00	0.78	0.23	1.07	–0.46	–0.03	–0.01	0.00	2.05
G	C1P3	2/4/2016	0.91	0.10	0.08	0.46	1.12	–0.34	–0.03	0.00	0.00	2.30
G	C1P3	3/16/2016	0.63	0.05	0.07	0.59	0.63	–0.37	–0.12	0.00	0.00	1.47
G	C1P3	3/16/2016	0.69	0.05	0.08	0.39	0.60	–0.47	–0.10	0.00	0.00	1.24
S	C2P1	1/27/2016	0.14	0.00	0.16	0.25	0.84	–0.07	–0.01	0.00	0.00	1.30
S	C2P1	2/4/2016	0.19	0.01	0.14	0.31	0.94	–0.07	–0.01	0.00	0.00	1.51
S	C2P1	3/16/2016	0.13	0.01	0.16	0.50	0.78	–0.04	–0.01	0.00	–0.02	1.50
S	C2P2	1/27/2016	0.16	0.03	0.20	0.21	0.67	–0.10	–0.02	0.00	0.00	1.15
S	C2P2	2/4/2016	0.14	0.01	0.16	0.21	0.67	–0.07	–0.01	0.00	0.00	1.10
S	C2P2	2/11/2016	0.14	0.01	0.13	0.20	0.64	–0.05	0.00	0.00	0.00	1.07
S	C2P2	2/17/2016	0.14	0.00	0.12	0.13	0.63	–0.03	0.00	0.00	0.00	0.98
S	C2P2	2/24/2016	0.15	0.00	0.12	0.19	0.66	–0.02	–0.01	0.00	0.00	1.09
S	C2P2	3/8/2016	0.11	0.01	0.16	0.14	0.48	–0.06	–0.02	0.00	0.00	0.82
S	C2P2	3/16/2016	0.09	0.00	0.15	0.38	0.67	–0.05	–0.01	0.00	0.00	1.23
S	C2P2	3/31/2016	0.13	0.03	0.22	0.71	0.86	–0.05	–0.01	0.00	0.00	1.90
S	C2P2	4/20/2016	0.26	0.01	0.61	0.81	0.82	–0.29	–0.10	0.00	0.00	2.11
S	C2P2	4/28/2016	0.30	0.04	0.73	0.67	0.64	–0.58	–0.29	0.00	0.00	1.51
S	C2P3	2/4/2016	0.25	0.02	0.12	0.21	1.07	–0.09	–0.02	0.00	0.00	1.55
S	C2P3	2/11/2016	0.35	0.00	0.18	0.38	1.78	–0.12	0.00	0.00	0.00	2.56
S	C2P3	2/17/2016	0.32	0.00	0.19	0.29	1.47	–0.09	0.00	0.00	0.00	2.18
S	C2P3	2/24/2016	0.36	0.02	0.19	0.53	1.73	–0.10	0.00	0.00	0.00	2.71
S	C2P3	3/8/2016	0.12	0.01	0.13	0.20	0.48	–0.05	–0.02	0.00	0.00	0.87

Table 10 Distance between vernal pools.

	Distance (m)
Catchment 1	
P1–P2	14.83
P2–P3	12.85
Catchment 2	
P1–P2	10.08
P2–P3	44.26